

2111 **Chapter 2** Observed Changes of Weather and Climate
2112 Extremes

2113

2114 **Convening Lead Author:** Kenneth Kunkel, Univ. Ill. Urbana-Champaign, Ill. State
2115 Water Survey

2116

2117 **Lead Authors:** Peter Bromirski, Scripps Inst. Oceanography, UCSD; Harold Brooks,
2118 NOAA; Tereza Cavazos, Centro de Investigación Científica y de Educación Superior de
2119 Ensenada, Mexico; Arthur Douglas, Creighton Univ.; David Easterling, NOAA; Kerry
2120 Emanuel, Mass. Inst. Tech.; Pavel Groisman, UCAR/NCDC; Greg Holland, NCAR;
2121 Thomas Knutson, NOAA; James Kossin, Univ. Wis.-Madison, CIMSS; Paul Komar,
2122 Oreg. State Univ.; David Levinson, NOAA; Richard Smith, Univ. N.C., Chapel Hill

2123

2124 **Contributing Authors:** Jonathan Allan, Oreg. Dept. Geology and Mineral Industries;
2125 Raymond Assel, NOAA; Stanley Changnon, Univ. Ill. Urbana-Champaign, Ill. State
2126 Water Survey; Jay Lawrimore, NOAA; Kam-biu Liu, La. State Univ., Baton Rouge;
2127 Thomas Peterson, NOAA

2128

2129 **KEY FINDINGS**

2130

2131 **Observed Changes**

2132 Upward trends in the frequency of unusually warm nights, extreme precipitation
2133 episodes, the frequency of North Atlantic tropical cyclones (hurricanes), the length of the
2134 frost-free season, and extreme wave heights along the west coast are notable changes in
2135 the North American climate record.

- 2136 • Most of North America is experiencing more unusually hot days. The number of
2137 warm spells has been increasing since 1950. However, the heat waves of the 1930s
2138 remain the most severe in the U.S. historical record back to 1895.

- 2139 • There are fewer unusually cold days during the last few decades. The last 10 years
2140 have seen a lower number of severe cold waves than for any other 10-yr period in the
2141 historical record which dates back to 1895. There has been a decrease in the number
2142 of frost days and a lengthening of the frost-free season, particularly in the western
2143 part of North America.
- 2144 • Extreme precipitation episodes (heavy downpours) have become more frequent and
2145 more intense in recent decades than at any other time in the historical record dating
2146 back to the late 19th Century and account for a larger percentage of total precipitation.
2147 The most significant changes have occurred in most of the U.S., northern Mexico,
2148 southeastern, northern and western Canada, and southern Alaska.
- 2149 • There are recent regional tendencies toward more severe droughts in the southwestern
2150 U.S., parts of Canada and Alaska, and Mexico.
- 2151 • For the continental U.S. and southern Canada, the most severe droughts occurred in
2152 the 1930s and there is no indication of an overall trend since 1895; in Mexico, the
2153 1950s and 1994-present were the driest period.
- 2154 • Atlantic tropical cyclone (hurricane) activity, as measured by both frequency and the
2155 Power Dissipation Index (which combines storm intensity, duration and frequency)
2156 has increased.
- 2157 – The increases are substantial since about 1970, and are likely substantial since
2158 the 1950s and 60s, in association with warming Atlantic sea surface temperatures.
2159 There is less confidence in data prior to 1900.
- 2160 – It is likely that there has been an increase in tropical cyclone *frequency* in the
2161 North Atlantic over the past 100 years, which has closely followed warming

- 2162 tropical Atlantic sea surface temperatures. There is increasing uncertainty in the
2163 data as one proceeds further back in time.
- 2164 – The frequency of major hurricanes has increased coincident with overall
2165 tropical cyclone numbers.
- 2166 • There is no observational evidence for an increase in North American mainland land-
2167 falling hurricanes since the late 1800s.
 - 2168 • The hurricane Power Dissipation Index in the eastern Pacific, affecting the Mexican
2169 west coast and shipping lanes, has decreased since 1980, but rainfall from near-
2170 coastal hurricanes has increased since 1949.
 - 2171 • The balance of evidence suggests that there has been a northward shift in the tracks of
2172 strong low pressure systems (storms) in both the N. Atlantic and N. Pacific basins.
2173 There is a trend toward stronger intense low pressure systems in the North Pacific.
 - 2174 • Increases in extreme wave height characteristics have been observed along the
2175 Atlantic and Pacific coasts of North America during recent decades based on 3
2176 decades of buoy data.
 - 2177 – Increases along the West coast have been greatest in the Pacific Northwest, and are
2178 likely a reflection of changes in storm tracks.
 - 2179 – Increases along the U.S. east coast are evident during the hurricane season.
 - 2180 • Although snow cover extent has decreased over North America, there is no indication
2181 of continental-scale trends in snowstorms and episodes of freezing rain during the
2182 20th Century.
 - 2183 • There is no trend in the frequency of tornadoes and other severe convective storms
2184 when the data are adjusted for changes in observing practices.

2185 2.1 Background

2186 Weather and climate extremes exhibit substantial spatial variability. It is not unusual for
2187 severe drought and flooding to occur simultaneously in different parts of North America
2188 (e.g. catastrophic flooding in the Mississippi River basin and severe drought in the
2189 southeast U.S. during summer 1993). These reflect temporary shifts in large-scale
2190 circulation patterns that are an integral part of the climate system (Chapter 2, Box 2.3).
2191 The central goal of this chapter is to identify long-term shifts/trends in extremes and to
2192 characterize the continental-scale patterns of such shifts. Such characterization requires
2193 data that is homogeneous, of adequate length, and with continental-scale coverage. Many
2194 datasets meet these requirements for limited periods only. For temperature and
2195 precipitation, rather high quality data are available for the conterminous U.S. back to the
2196 late 19th Century. However, shorter data records are available for parts of Canada,
2197 Alaska, Hawaii, Mexico, the Caribbean, and U.S. territories. In practice, this limits true
2198 continental-scale analyses of temperature and precipitation extremes to the middle part of
2199 the 20th Century onward. Other phenomena have similar limitations and continental-scale
2200 characterizations are generally limited to the last 50-60 years or less, or must confront
2201 data homogeneity issues which add uncertainty to the analysis. We consider all studies
2202 that are available, but in many cases these studies have to be interpreted carefully because
2203 of these limitations. A variety of statistical techniques are used in the studies cited here.
2204 General information about statistical methods along with several illustrative examples are
2205 given in the Appendix.

2206

2207

2208 2.2 Observed Changes and Variations in Weather and Climate Extremes

2209 2.2.1 Temperature Extremes

2210 Extreme temperatures do not always correlate with average temperature, but they often
2211 change in tandem; thus, average temperature changes provide a context for discussion of
2212 extremes. In 2005, virtually all of North America was above to much above average¹¹
2213 (Shein et al. 2006) and 2006 was one of the warmest years on record in the conterminous
2214 United States (Arguez et al., 2007). The areas experiencing the largest temperature
2215 anomalies included the higher latitudes of Canada and Alaska. Annual average
2216 temperature time series for Canada, Mexico and the United States all show substantial
2217 warming since the middle of the 20th century (Shein et al. 2006). Since 1998 over half of
2218 the U.S. annual average temperatures have been extremely high, including the hottest two
2219 years on record (1998 and 2006).

2220

2221 Since 1950, the annual percent of days exceeding the 90th, 95th, and 97.5th percentile
2222 thresholds¹² for both maximum (daytime highs) and minimum (nighttime lows)
2223 temperature has increased when averaged over all the land area (Figure 2.1; Peterson et
2224 al. 2007). Although the changes are greatest in the 90th percentile (increasing from about
2225 10% of the days to about 13% for maximum and almost 15% for minimum) and decrease
2226 as the threshold temperatures increase indicating more rare events (the 97.5th percentage
2227 increases from about 3% of the days to 4% for maximum and 5% for minimum), the

¹¹ NOAA's National Climatic Data Center uses the following terminology for classifying its monthly/seasonal/annual U.S. temperature and precipitation rankings: "near-normal" is defined as within the *mid-tercile*, "above/below normal" is within the *top-tercile*, and "much-above/much-below normal" is within the *top-decile* of all such periods on record.

¹² An advantage of the use of percentile, rather than absolute, thresholds is that they account for regional climate differences

2228 relative changes are similar. There are important regional differences in the changes. For
2229 example, the largest increases in the 90th percentile threshold temperature occur in the
2230 western part of the continent from northern Mexico through the western U.S. and Canada
2231 and across Alaska, while some areas, such as eastern Canada, show declines of as many
2232 as 10 days per year from 1950 to 2004 (Fig. 2.2).

2233

2234 Other regional studies have shown similar patterns of change. For the U.S., the number of
2235 days exceeding the 90th, 95th and 99th percentile thresholds (defined monthly) have
2236 increased in recent years¹³, but are also dominated earlier in the 20th century by the
2237 extreme heat and drought of the 1930s¹⁴ (DeGaetano and Allen 2002). Changes in cold
2238 extremes (days falling below the 10th, 5th, and 1st percentile threshold temperatures) show
2239 decreases, particularly since 1960¹⁵. For the 1900-1998 period in Canada, there are fewer
2240 cold extremes in winter, spring and summer in most of southern Canada and more high
2241 temperature extremes in winter and spring, but little change in warm extremes in
2242 summer¹⁶ (Bonsal et al. 2001). However, for the more recent (1950-1998) period there
2243 are significant increases in warm extremes over western Canada, but decreases in eastern
2244 Canada. Similar results averaged across all of Canada are found for the longer 1900-2003
2245 period, with 28 fewer cold nights, 10 fewer cold days, 21 more extreme warm nights and
2246 8 more warm days per year now than in 1900¹⁷ (Vincent and Mekis 2006). For the U.S.
2247 and Canada, the largest increases in daily maximum and minimum temperature are

¹³ The number of stations with statistically significant positive trends for 1960-1996 passed tests for field significance based on resampling.

¹⁴ The number of stations with statistically significant negative trends for 1930-1996 was greater than the number with positive trends.

¹⁵ The number of stations with statistically significant downward trends for 1960-1996 passed tests for field significance based on resampling, but not for 1930-1996.

¹⁶ Statistical significance of trends was assessed using Kendall's tau test

¹⁷ These trends were statistically significant at more than 20% of the stations based on Kendall's tau test

2248 occurring in the colder days of each month (Robeson 2004). For the Caribbean region,
2249 there is an 8% increase in the number of very warm nights and 6% increase in the number
2250 of very warm days for the 1958-1999 period. There also has been a corresponding
2251 decrease of 7% in the number of cold days and 4% in the number of cold nights (Peterson
2252 et al. 2002). The number of warm nights has increased by 10 or more per year for Hawaii
2253 and 15 or more per year for Puerto Rico from 1950 to 2004 (Fig. 2.2).

2254

2255 Analysis of multi-day very extreme heat and cold episodes¹⁸ in the U.S. were updated¹⁹
2256 from Kunkel et al. (1999) for the period 1895-2005. The most notable feature of the
2257 pattern of the annual number of the extreme heat waves (Fig. 2.3a) through time is the
2258 high frequency in the 1930s compared to the rest of the years in the 1895-2005 period.
2259 This was followed by a decrease to a minimum in the 1960s and 1970s and then an
2260 increasing trend since then. There is no trend over the entire period, but a highly
2261 statistically significant upward trend since 1960. The heat waves during the 1930s were
2262 characterized by extremely high daytime temperatures while nighttime temperatures were
2263 not as unusual (Fig. 2.3b,c). An extended multi-year period of intense drought
2264 undoubtedly played a large role in the extreme heat of this period, particularly the
2265 daytime temperatures, by depleting soil moisture and reducing the moderating effects of
2266 evaporation. By contrast, the recent period of increasing heat wave index is distinguished
2267 by the dominant contribution of a rise in extremely high nighttime temperatures (Fig.
2268 2.3c). Cold waves show a decline in the first half of the 20th century, then a large spike of

¹⁸ The threshold is approximately the 99.9 percentile.

¹⁹ The data were first transformed to create near-normal distributions using a log transformation for the heat wave index and a cube root transformation for the cold wave index. The transformed data were then subjected to least squares regression. Details are given in the Appendix, Example 2.

2269 events during the mid-1980s, then a decline²⁰. The last 10 years have seen a lower
2270 number of severe cold waves in the U.S. than in any other 10-yr period since 1895,
2271 consistent with observed impacts such as insect populations (Chapter 1, Box 1.2).
2272 Decreases in the frequency of extremely low nighttime temperatures have made a
2273 somewhat greater contribution than extremely low daytime temperatures to this recent
2274 low period of cold waves. Over the entire period there is a downward trend but it is not
2275 statistically significant at the $p=0.05$ level.

2276

2277 The annual number of warm spells²¹ averaged over North America has increased since
2278 1950 (Peterson et al. 2007). In the U.S. the annual number of warm spells²² has increased
2279 by about 1 ½ per year, and the duration has increased by about 1 day since 1950
2280 (Easterling et al. 2007a). Regionally the largest increases, up to about 2 ½ per year, were
2281 found in the western U.S., with many parts of the south and southeast showing little
2282 change. Seasonal results show the largest increases in the spring and winter, with little
2283 change in the number of events for the fall or summer. These results for warm spells are
2284 roughly consistent with those for the much more extreme heat waves illustrated in Fig.
2285 2.3a for the common period of analysis (1950-present); the warm spell analyses do not
2286 extend back to the 1930s when very extreme heat was frequent. The frequency and extent
2287 of hot summers²³ was highest in the 1930s, 1950s, and 1995-2003; the geographic pattern

²⁰ Details of this analysis are given in the Appendix, Example 1.

²¹ Defined as at least 3 consecutive days above the 90th percentile threshold done separately for maximum and minimum temperature.

²² Defined as at least 3 consecutive days with both the daily maximum and succeeding daily minimum temperature above the 80th percentile.

²³ Based on percentage of North American grid points with summer temperatures above the 90th or below the 10th percentiles of the 1950-1999 summer climatology.

2288 of hot summers during 1995-2003 was similar to that of the 1930s (Gershunov and
2289 Douville 2007).

2290

2291 The occurrence of temperatures below the biologically- and societally-important freezing
2292 threshold (0°C, 32°F) is an important aspect of the cold season climatology. Studies have
2293 typically characterized this either in terms of the number of frost days (days with the
2294 minimum temperature below freezing) or the length of the frost-free season²⁴. The
2295 number of frost days decreased by 4 days per year in the U.S. during the 1948-1999
2296 period, with the largest decreases, as many as 13 days per year, occurring in the Western
2297 U.S.²⁵ (Easterling 2002). In Canada, there have been significant decreases in frost day
2298 occurrence over the entire country from 1950 to 2003, with the largest decreases in
2299 extreme western Canada where there have been decreases of up to 40 or more frost days
2300 per year, and slightly smaller decreases in eastern Canada (Vincent and Mekis 2006). The
2301 start of the frost-free season in the Northeastern U.S. occurred 11 days earlier in the
2302 1990s than in the 1950s (Cooter and LeDuc 1995). For the entire U.S., the average length
2303 of the frost-free season over the 1895-2000 period for the U.S. increased by almost 2
2304 weeks²⁶ (Figure 2.4; Kunkel et al. 2004). The change is characterized by 4 distinct
2305 regimes, with decreasing frost-free season length from 1895 to 1910, an increase in length
2306 of about 1 week from 1910 to 1930, little change during 1930-1980, and large increases
2307 since 1980. The frost-free season length has increased more in the western U.S. than in
2308 the eastern U.S. (Easterling 2002; Kunkel et al. 2004), which is consistent with the

²⁴ The difference between the date of the last spring frost and the first fall frost

²⁵ Trends in the western half of the U.S. were statistically significant based on simple linear regression

²⁶ Statistically significant based on least-squares linear regression

2309 finding that the spring pulse of snow melt water in the Western U.S. now comes as much
2310 as 7-10 days earlier than in the late 1950s (Cayan et al. 2001).

2311

2312 Ice cover on lakes and the oceans is a direct reflection of the number and intensity of
2313 cold, below freezing days. Ice cover on the Laurentian Great Lakes of North American
2314 usually forms along the shore and in shallow areas in December and January, and in
2315 deeper mid-lake areas in February due to their large depth and heat storage capacity. Ice
2316 loss usually starts in early to-mid-March and lasts through mid-to-late April (Assel 2003).

2317

2318 Annual maximum ice cover on the Great Lakes has been monitored since 1963. The
2319 maximum extent of ice cover over the past 4 decades varied from less than 10% to over
2320 90%. The winters of 1977-1982 were characterized by a higher ice cover regime relative
2321 to the prior 14 winters (1963-1976) and the following 24 winters (1983-2006) (Assel et
2322 al. 2003, Assel 2005a, Assel personal communication for winter 2006). A majority of the
2323 mildest (lowest) seasonal average ice cover winters (Assel 2005b) over the past 4 decades
2324 occurred during the most recent 10-year period (1997-2006). Analysis of ice breakup
2325 dates on other smaller lakes in North America with at least 100 years of data (Magnuson
2326 et al. 2000) show a uniform trend toward earlier breakup dates (up to 13 days earlier per
2327 100 years)²⁷.

2328

2329 Reductions in Arctic sea ice, especially near-shore sea ice, allow strong storm and wave
2330 activity to produce extensive coastal erosion resulting in extreme impacts. Observations
2331 from satellites starting in 1978 show that there has been a substantial decline in Arctic sea

²⁷ Statistically significant trends were found for 16 of 24 lakes

2332 ice, with a statistically significant decreasing trend in annual Arctic sea ice extent of -33
2333 $\pm 8.8 \times 10^3 \text{ km}^2$ per year (equivalent to approximately $-2.7\% \pm 0.7\%$ per decade).

2334 Seasonally the largest changes in Arctic sea ice have been observed in the ice that
2335 survives the summer, where the trend in the minimum Arctic sea ice extent, between
2336 1979 and 2005, was $-60 \pm 24 \times 10^3 \text{ km}^2$ per year ($-7.4 \pm 2.9\%$ per decade) (Lemke et al.
2337 2007).

2338

2339 Rising sea surface temperatures have led to an increase in the frequency of extreme high
2340 SST events causing coral bleaching (see Box 1.1, Chapter 1). Mass bleaching events were
2341 not observed prior to 1980. However, since the 1970s, there have been 6 major global
2342 cycles of mass bleaching, with increasing frequency and intensity (Hoegh-Guldberg
2343 2005). Almost 30% of the world's coral reefs have disappeared in that time.

2344

2345 Less scrutiny has been focused on Mexico temperature extremes, in part, because much
2346 of the country can be classified as a 'tropical climate' where temperature changes are
2347 presumed fairly small, or semi-arid to arid climate where moisture availability exerts a far
2348 greater influence on human activities than does temperature.

2349

2350 Most of the sites in Mexico's oldest temperature observing network are located in major
2351 metropolitan areas and there is considerable evidence to indicate that trend behaviors at
2352 least partly reflect urbanization and urban heat island influences (Englehart and Douglas,
2353 2003). To avoid such issues in analysis, a monthly rural temperature dataset has recently

2354 been developed²⁸. Examined in broad terms as a national aggregate, a couple of basic
2355 behaviors emerge. First, long period temperature trends over Mexico are generally
2356 compatible with continental-scale trends which indicate a cooling trend over North
2357 America from about the mid-1940s to the mid-1970s, with a warming trend thereafter.
2358
2359 The rural gridded data set indicates that much of Mexico experienced decreases in both
2360 T_{\max} and T_{\min} during 1941-1970 ($-0.27^{\circ}\text{C}/\text{decade}$ for T_{\max} and $-0.19^{\circ}\text{C}/\text{decade}$ for T_{\min})
2361 while the later period of 1971-2001 is dominated by positive trends that are most strongly
2362 evident in T_{\max} ($0.35^{\circ}\text{C}/\text{decade}$ for T_{\max} and $0.10^{\circ}\text{C}/\text{decade}$ for T_{\min}). Based on these
2363 results it appears very likely that much of Mexico has experienced an increase in average
2364 temperature driven in large measure by increases in T_{\max} . The diurnal temperature range
2365 (T_{\max} minus T_{\min}) for the warm season (June-September) averaged over all of Mexico has
2366 increased by $0.26^{\circ}\text{C}/\text{decade}$ since 1970 with particularly rapid rises since 1990 (Fig. 2.5)
2367 reflecting a comparatively rapid rise in T_{\max} with respect to T_{\min} (Englehart and Douglas
2368 2005)²⁹. This behavior departs from the general picture for many regions of the world,
2369 where warming is attributable mainly to a faster rise in T_{\min} than in T_{\max} (e.g. Easterling
2370 et al., 1997).
2371
2372 Given Mexico's largely tropical/sub-tropical climate and the influence of nearby oceans,
2373 a reasonable expectation would be that changes in the behavior of temperature extremes

²⁸ It consists of monthly historical surface air temperature observations (1940-2001) compiled from stations (n=103) located in places with population <10,000 (2000 Census). To accommodate variable station record lengths and missing monthly observations, the dataset is formatted as a grid-type ($2.5^{\circ} \times 2.5^{\circ}$ lat.-long.) based on the climate anomaly method (Jones and Moberg, 2003)

²⁹ Statistically significant trends were found in the northwest, central, and south, but not the northeast regions

2374 could be small and difficult to detect as compared to at many mid-and high latitude
2375 locations. However, the cold surge³⁰ phenomena – the equatorward penetration of
2376 modified cold air, known as *nortes* in Mexico – is an integral part of the country’s cool
2377 season climatology. The frequency of both cold surge days and cold surge events tends to
2378 vary depending in part on Pacific Decadal Oscillation (PDO) phase: under negative PDO
2379 phase cold surge activity tends to be more prevalent. However, the intensity of cold surge
2380 events as indicated by the maximum daily drop in T_{\min} tends to be greater under positive
2381 PDO phase. Analysis of linear trends indicates that from the early 1950s onward, it is
2382 very likely that southern Mexico has experienced a trend toward decreasing frequency of
2383 both cold surge days by 2.4 cold days/decade and cold surge events by 0.88
2384 events/decade (Englehart and Douglas 2007).

2385

2386 **2.2.2 Precipitation Extremes**

2387 **2.2.2.1 Drought**

2388 Droughts are one of the most costly natural disasters (Chapter 1, Box 1.4), with estimated
2389 annual U.S. losses of \$6 – 8 billion (Federal Emergency Management Agency, 1995). An
2390 extended period of deficient precipitation is the root cause of a drought episode, but the
2391 intensity can be exacerbated by high evaporation rates arising from excessive
2392 temperatures, high winds, lack of cloudiness, and/or low humidity. Drought can be
2393 defined in many ways, from acute short-term to chronic long-term hydrological drought,
2394 agricultural drought, meteorological drought, and so on. The assessment in this report
2395 focuses mainly on meteorological droughts based on the Palmer (1965) Drought Severity
2396 Index (PDSI), though other indices are also documented in the report (Chapter 2, Box
2397 2.1).

³⁰ Cold surges are defined for the period 1925-2002 based on daily station observations of T_{\min} from two locations – stations in south Texas and near coastal stations from the southern Mexican state of Veracruz. Cold surge days have T_{\min} below its climatological values by 1 standard deviation. Cold surge events are runs of 1 or more consecutive cold surge days.

2398

2399 Individual droughts can occur on a range of spatial scales, but they often affect rather
2400 large areas and can persist for many months and even years. Thus, the aggregate impacts
2401 can be very large. For the U.S., the percentage area affected by severe to extreme drought
2402 (Fig. 2.6) highlights some major episodes of extended drought. The most widespread and
2403 severe drought conditions occurred in the 1930s and 1950s (Andreadis et al. 2005). The
2404 early 2000s were also characterized by severe droughts in some areas, notably in the
2405 western U.S. When averaged across the entire U.S. (Fig. 2.6), there is no clear tendency
2406 for a trend based on the PDSI. Similarly, long-term trends (1925-2003) of hydrologic
2407 droughts based on model derived soil moisture and runoff show that droughts have, for
2408 the most part, become shorter, less frequent, and cover a smaller portion of the U. S. over
2409 the last century (Andreadis and Lettenmaier, 2006). The main exception is the Southwest
2410 and parts of the interior of the West, where increased temperature has led to positive
2411 drought trends (Andreadis and Lettenmaier, 2006). The trends averaged over all of North
2412 America since 1950 (Fig. 2.6) are similar to U.S. trends for the same period, indicating no
2413 overall trend.

2414

2415 Since the contiguous United States has experienced an increase in both temperature and
2416 precipitation during the 20th century, one question is whether these increases are
2417 impacting the occurrence of drought. Easterling et al (2007b) examined this possibility by
2418 looking at drought, as defined by the PDSI, for the United States using detrended
2419 temperature and precipitation. Results indicate that without the upward trend in

2420 precipitation the increase in temperatures would have lead to an increase in the area of
2421 the U.S. in severe-extreme drought of up to 30% in some months.

2422

2423 Summer conditions, which relate to fire danger, have trended toward lesser drought in the
2424 upper Mississippi, Midwest, and Northwest, but the fire danger has increased in the
2425 Southwest, in California in the spring season (not shown), and, surprisingly, over the
2426 Northeast, despite the fact that annual precipitation here has increased. A century-long
2427 warming in this region is quite significant in summer, which reverses the tendencies of
2428 the precipitation contribution to soil wetness (Groisman et al. 2004). Westerling *et al.*
2429 (2006) document that large wildfire activity in the Western U.S. increased suddenly and
2430 markedly in the mid-1980s, with higher large-wildfire frequency, longer wildfire
2431 durations, and longer wildfire seasons. The greatest increases occurred in mid-elevation,
2432 Northern Rockies forests, where land-use histories have relatively little effect on fire risks
2433 and are strongly associated with increased spring and summer temperatures and an earlier
2434 spring snowmelt.

2435

2436 For the entire North American continent, there is a north-south pattern in drought trends
2437 (Dai et al. 2004). Since 1950, there is a trend toward wetter conditions over much of the
2438 conterminous U.S., but a trend toward drier conditions over southern and western
2439 Canada, Alaska, and Mexico. The summer PDSI averaged for Canada indicates dry
2440 conditions during the 1940s and 1950s, generally wet conditions from the 1960s to 1995,
2441 but much drier after 1995 (Shabbar and Skinner, 2004). In Alaska and Canada, the
2442 upward trend in temperature, resulting in increased evaporation rates, has made a

2443 substantial contribution to the upward trend in drought (Dai et al. 2004). In agreement
2444 with this drought index analysis, the area of forest fires in Canada has been quite high
2445 since 1980 compared to the previous 30 years and Alaska experienced a record high year
2446 for forest fires in 2004 followed by the third highest in 2005 (Soja et al. 2007). During
2447 the mid-1990s and early 2000s, central (Stahle *et al.* 2007) and western Mexico (Kim *et*
2448 *al.* 2002; Nicholas and Battisti, 2006; Hallack and Watkins, 2007) experienced
2449 continuous cool-season droughts having major impacts in agriculture, forestry, and
2450 ranching, especially during the warm summer season. In 1998, “El Niño” caused one of
2451 the most severe droughts in Mexico since the 1950s (Ropelewski, 1999), creating the
2452 most difficult wildfire season in Mexico’s history. Mexico had 14,445 wildfires affecting
2453 849,632 hectares - the largest area ever burned in Mexico in a single season
2454 (SEMARNAP, 2000).

2455

2456 Reconstructions of drought prior to the instrumental record based on tree-ring
2457 chronologies indicate that the 1930s may have been the worst drought since 1700 (Cook
2458 et al. 1999). There were three major multiyear droughts in the U.S. during the latter half
2459 of the 1800s: 1856-1865, 1870-1877 and 1890-1896 (Herweijer et al. 2006). Similar
2460 droughts have been reconstructed for northern Mexico (Therrell et al. 2002). There is
2461 evidence of earlier, even more intense drought episodes (Woodhouse and Overpeck
2462 1998). A period in the mid to late 1500s has been termed a “mega-drought” and was
2463 longer-lasting and more widespread than the 1930s Dust Bowl (Stahle et al. 2000).
2464 Several additional mega-droughts occurred during 1000-1470 (Herweijer et al. 2007).
2465 These droughts were about as severe as the 1930s Dust Bowl episode but much longer,

2466 lasting 20-40 years. In the western U.S., the period of 900-1300 was characterized by
2467 widespread drought conditions (Fig. 2.7; Cook et al. 2004). In Mexico, reconstructions of
2468 seasonal precipitation (Stahle et al. 2000, Acuña-Soto et al. 2002, Cleaveland et al. 2004)
2469 indicate that there have been droughts more severe than the 1950s drought, e.g., the
2470 mega-drought in the mid- to late- 16th century, which appears as a continental-scale
2471 drought.

2472

2473 During the summer months, excessive heat and drought often occur simultaneously
2474 because the meteorological conditions typically causing drought are also conducive to
2475 high temperatures. The impacts of the Dust Bowl droughts and the 1988 drought were
2476 compounded by episodes of extremely high temperatures. The month of July 1936 in the
2477 central U.S. is a notable example. To illustrate, Lincoln, NE received only 0.05” of
2478 precipitation that month (after receiving less than 1 inch the previous month) while
2479 experiencing temperatures reaching or exceeding 110°F on 10 days, including 117°F on
2480 July 24. Although no studies of trends in such “compound” extreme events have been
2481 performed, they represent a significant societal risk.

2482

2483 **BOX 2.1: Drought Indicators and Resources**

- 2484 • **Palmer Drought Severity Index (PDSI; Palmer, 1965)** – meteorological drought.

2485 The PDSI is a commonly-used drought index that measures intensity, duration, and
2486 spatial extent of drought. It is derived from measurements of precipitation, air
2487 temperature, and local estimated soil moisture content. Categories range from less
2488 than -4 (extreme drought) to more than +4 (extreme wet conditions), and have been

2489 standardized to facilitate comparisons from region to region. Alley (1984) identified
2490 some positive characteristics of the PDSI that contribute to its popularity: (1) it is an
2491 internationally recognized index; (2) it provides decision makers with a measurement
2492 of the abnormality of recent weather for a region; (3) it provides an opportunity to
2493 place current conditions in historical perspective; and (4) it provides spatial and
2494 temporal representations of historical droughts. However, the PDSI has some
2495 limitations (1) it may lag emerging droughts by several months; (2) it is less well
2496 suited for mountainous land or areas of frequent climatic extremes; (3) it does not
2497 take into account streamflow, lake and reservoir levels, and other long-term
2498 hydrologic impacts (Karl and Knight, 1985), such as snowfall and snow cover; (4) the
2499 use of temperature alone to estimate potential evapotranspiration (PET) can introduce
2500 biases in trend estimates because humidity, wind and radiation also affect PET and
2501 changes in these elements are not accounted for. In fact, Hobbins et al. (2007) show
2502 that the PDSI trends in Australia and New Zealand are exaggerated compared to
2503 trends using more realistic methods to estimate evapotranspiration. The use of
2504 temperature alone is a practical consideration since measurements of these other
2505 elements are often not available.

- 2506 • **Crop Moisture Index (CMI; Palmer, 1968)** – short-term meteorological drought.
2507 Whereas the PDSI monitors long-term meteorological wet and dry spells, the CMI
2508 was designed to evaluate short-term moisture conditions across major crop-producing
2509 regions. It is based on the mean temperature and total precipitation for each week, as
2510 well as the CMI value from the previous week. Categories range from less than -3
2511 (severely dry) to more than +3 (excessively wet). The CMI responds rapidly to

2512 changing conditions, and it is weighted by location and time so that maps, which
2513 commonly display the weekly CMI across the United States, can be used to compare
2514 moisture conditions at different locations. Weekly maps of the CMI are available as
2515 part of the USDA/JAWF Weekly Weather and Crop Bulletin.

2516 • **Standardized Precipitation Index (SPI; McKee *et al.*, 1993)** – precipitation-based
2517 drought. The SPI was developed to categorize rainfall as a standardized departure
2518 with respect to a rainfall probability distribution function; categories range from less
2519 than -3 (extremely dry) to more than +3 (extremely wet). The SPI is calculated on the
2520 basis of selected periods of time (typically from 1 to 48 months of total precipitation)
2521 and it indicates how the precipitation for a specific period compares with the long-
2522 term record at a given location (Edwards and McKee, 1997). The index correlates
2523 well with other drought indices. Sims *et al.* (2002) suggested that the SPI was more
2524 representative of short-term precipitation and a better indicator of soil wetness than
2525 the PDSI. The 9-month SPI corresponds closely to the PDSI (Heim 2002; Guttman
2526 1998).

2527 • **Keetch-Byram Index (KBDI; Keetch and Byram, 1968)** – meteorological drought
2528 and wildfire potential index. This was developed to characterize the level of potential
2529 fire danger. It uses daily temperature and precipitation information and estimates soil
2530 moisture deficiency. High values of KBDI are indicative of favorable conditions for
2531 wildfires. However, the index needs to be regionalized, as values are not comparable
2532 among regions (Groisman *et al.* 2004, 2007a).

2533 • **No-rain episodes** – meteorological drought. Groisman and Knight (2007) proposed
2534 to directly monitor frequency and intensity of prolonged no-rain episodes (greater

2535 than 20, 30, 60, etc. days) during the warm season, when evaporation and
2536 transpiration are highest and the absence of rain may affect natural ecosystems and
2537 agriculture. They found that during the past four decades the duration of prolonged
2538 dry episodes has significantly increased over the Eastern and Southwestern United
2539 States and adjacent areas of Northern Mexico and Southeastern Canada.

- 2540 • **Soil Moisture and Runoff Index (SMRI; Andreadis and Lettenmaier, 2006)** –
2541 hydrologic and agricultural droughts. The SMRI is based on model-derived soil
2542 moisture and runoff as drought indicators; it uses percentiles and the values are
2543 normalized from 0 (dry) to 1 (wet conditions). The limitation of this index is that it is
2544 based on land-surface model-derived soil moisture. However, long-term records of
2545 soil moisture – a key variable related to drought – are essentially non-existent
2546 (Andreadis and Lettenmaier, 2006). Thus, the advantage of the SMRI is that it is
2547 physically based and with the current sophisticated land-surface models it is easy to
2548 produce multimodel average climatologies and century-long reconstructions of land
2549 surface conditions, which could be compared under drought conditions.

2550 *Resources:* A list of these and other drought indicators, data availability, and current
2551 drought conditions based on observational data can be found at the National Climatic
2552 Data Center (NCDC, <http://www.ncdc.noaa.gov>). The North American Drought Monitor
2553 at NCDC monitors current drought conditions in Canada, the United States, and Mexico.
2554 Tree-ring reconstruction of PDSI across North America over the last 2000 years can be
2555 also found at NCDC
2556
2557

2558 **2.2.2.2 Short Duration Heavy Precipitation**

2559 **2.2.2.2.1 Data Considerations and Terms**

2560 Intense precipitation often exhibits higher spatial variability than many other extreme
2561 phenomena. This poses challenges for the analysis of observed data since the heaviest
2562 area of precipitation in many events may fall between stations. This adds uncertainty to
2563 estimates of regional trends based on the climate network. The uncertainty issue is
2564 explicitly addressed in some recent studies.

2565

2566 Precipitation extremes are typically defined based on the frequency of occurrence [by
2567 percentile (e.g., upper 5%, 1%, 0.1%, etc) or by return period (e.g. an average occurrence
2568 of once every 5 years, once every 20 years, etc.)] of rain events and/or their absolute
2569 values (e.g., above 50 mm, 100 mm, 150 mm, or more). Values of percentile or return
2570 period thresholds vary considerably across North America. For example, in the U.S.,
2571 regional average values of the 99.9 percentile threshold for daily precipitation are lowest
2572 in the Northwest and Southwest (average of 55 mm) and highest in the South (average of
2573 130mm)³¹.

2574

2575 As noted above, spatial patterns of precipitation have smaller spatial correlation scales
2576 (for example, compared to temperature and atmospheric pressure) which means that a
2577 denser network is required in order to achieve a given uncertainty level. While monthly
2578 precipitation time series for flat terrain have typical radii of correlation³² (ρ) of ~300 km

³¹ The large magnitude of these differences is a major motivation for the use of regionally-varying thresholds based on percentiles.

³² Spatial correlation decay with distance, r , for many meteorological variables, X , can be approximated by

2579 or even more, daily precipitation may have ρ less than 100 km with typical values for
2580 convective rainfall in isolated thunderstorms of ~15 to 30 km (Gandin and Kagan 1976).
2581 Values of ρ can be very small for extreme rainfall events and sparse networks may not be
2582 adequate to detect a desired minimum magnitude of change that can result in societally-
2583 important impacts and can indicate important changes in the climate system.

2584

2585 **2.2.2.2.2 United States**

2586 One of the clearest trends in the U.S. observational record is that of an increasing
2587 frequency and intensity of heavy precipitation events (Karl and Knight 1998; Groisman et
2588 al. 1999, 2001, 2004; Kunkel et al. 1999; Easterling et al. 2000; IPCC 2001; Semenov
2589 and Bengtsson 2002, Kunkel 2003). For example, the area of the United States affected
2590 by a much above normal contribution to total annual precipitation of daily precipitation
2591 events exceeding 50.8 mm (2 inches) increased by a statistically significant amount from
2592 about 9% in the 1910s to about 11% in the 1980s and 1990s (Karl and Knight 1998).
2593 Total precipitation also increased during this time, due in large part to increases in the
2594 intensity of heavy precipitation events (Karl and Knight 1998). In fact, there has been
2595 little change or decreases in the frequency of light and average precipitation days
2596 (Easterling et al. 2000; Groisman et al. 2004, 2005) during the last 30 years while heavy
2597 precipitation frequencies have increased (Sun and Groisman 2004). For example, the
2598 amount of precipitation falling in the heaviest 1% of rain events has increased by 20%
2599 during the 20th Century while total precipitation has increased by only 7% (Groisman et
2600 al. 2004). Although the exact character of those changes has been questioned (e.g.

an exponential function of distance: $\text{Corr}(X(A), X(B)) \sim e^{-r/\rho}$ where r is a distance between point A and B and ρ is a radius of correlation, which is a distance where the correlation between the points is reduced to $1/e$ compared to an initial “zero” distance.

2601 Michaels et al. 2004), it is highly likely that in recent decades extreme precipitation
2602 events have increased more than light to medium events.

2603

2604 A statistically significant 50% increase during the 1900s in the frequency of days with
2605 precipitation exceeding 101.6 mm (4 inches) was found in the upper Midwest U.S.
2606 (Groisman et al. 2001). Upward trends in the amount of precipitation occurring in the
2607 upper 0.3% of daily precipitation events are statistically significant for the period of
2608 1908-2002 within three major regions (the South, Midwest, and Upper Mississippi; see
2609 Fig. 2.8) of the central United States (Groisman et al. 2004). The upward trends are
2610 primarily a warm season phenomenon when the most intense rainfall events typically
2611 occur. A time series of the frequency of events in the upper 0.3% averaged for these 3
2612 regions (Fig 2.8) shows a 20% increase over the period of 1893-2002 with all of this
2613 increase occurring over the last third of the 1900s (Groisman et al. 2005).

2614

2615 Examination of intense precipitation events defined by return period, covering the period
2616 of 1895-2000, indicates that the frequencies of extreme precipitation events before 1920
2617 were generally above the long-term averages for durations of 1 to 30 days and return
2618 periods 1 to 20 years and only slightly lower than values during the 1980s and 1990s
2619 (Kunkel et al. 2003). The highest values occur after about 1980, but the elevated levels
2620 prior to about 1920 are an interesting feature suggesting that there is considerable
2621 variability in the occurrence of extreme precipitation on multi-decadal time scales

2622

2623 There is a seeming discrepancy between the results for the 99.7th percentile (which do not
2624 show high values early in the record in the analysis of Groisman et al. 2004) and for 1 to
2625 20-yr return periods (which do in the analysis of Kunkel et al. 2003). The number of
2626 stations with available data is only about half (about 400) in the late 1800s of what is
2627 available in most of the 1900s (800-900). Furthermore, the spatial distribution of stations
2628 throughout the record is not uniform; the density in the western U.S. is relatively lower
2629 than in the central and eastern U.S. It is possible that the resulting uncertainties in heavy
2630 precipitation estimates are too large to make unambiguous statements about the recent
2631 high frequencies.

2632

2633 Recently, this question was addressed (Kunkel et al. 2007a) by analyzing the modern
2634 dense network to determine how the density of stations affects the uncertainty and then to
2635 estimate the level of uncertainty in the estimates of frequencies in the actual (sparse)
2636 network used in the long-term studies. The results were unambiguous. For all
2637 combinations of three durations (1-day, 5-days and 10-days) and 3 return periods (1-yr,
2638 5-yr, and 20-yr), the frequencies for 1983-2004 were significantly higher than those for
2639 1895-1916 at a high level of confidence. In addition, the observed linear trends were all
2640 found to be upward, again with a high level of confidence. Based on these results, it is
2641 highly likely that the recent elevated frequencies in the U.S. are the highest since 1895.

2642

2643 **2.2.2.2.3 Alaska and Canada**

2644 The sparse network of long-term stations in Canada increases the uncertainty in estimates
2645 of extremes. Changes in the frequency of heavy events exhibit considerable multi-decadal

2646 variability since 1900, but no long-term trend for the entire century (Zhang et al. 2001).
2647 However, according to Zhang et al. (2001), there are not sufficient instrumental data to
2648 discuss the nationwide trends in precipitation extremes over Canada prior to 1950.
2649 Nevertheless, there are changes that are noteworthy. For example, the frequency of
2650 99.7% events exhibits a statistically significant upward trend of 19%/50yr in British
2651 Columbia since 1910 (Fig. 2.8; Groisman et al. 2005). For Canada, increases in
2652 precipitation intensity during the second half of the 1900s are concentrated in heavy and
2653 intermediate events, with the largest changes occurring in Arctic areas (Stone et al. 2000).
2654 The tendency for increases in the frequency of intense precipitation while the frequency
2655 of days with average and light precipitation does not change or decreases has also been
2656 observed in Canada over the last 30 years (Stone et al. 2000), mirroring U.S. changes.
2657 Recently, Vincent and Mekis (2006) repeated analyses of precipitation extremes for the
2658 second half of 1900s (1950-2003 period). They reported a statistically significant increase
2659 of 1.8 days per 54 years in heavy precipitation days (defined as the days with
2660 precipitation above 10 mm) and statistically insignificant increases in the maximum 5-
2661 day precipitation (by ~5%) and in the number of “very wet days” defined as days with
2662 precipitation above the upper 5th percentiles of local daily precipitation (by 0.4 days).
2663
2664 There is an upward trend of 37%/50yr in southern Alaska since 1950 although this trend
2665 is not statistically significant (Fig. 2.8; Groisman et al. 2005).
2666
2667
2668

2669 **2.2.2.2.4 Mexico**

2670 On an annual basis, the number of heavy precipitation ($P > 10$ mm) days has increased in
2671 northern Mexico and the Sierra Madre Occidental and decreased in the south-central part
2672 of the country (Alexander et al. 2006). The percent contribution to total precipitation
2673 from heavy precipitation events exceeding the 95th percentile threshold has increased in
2674 the monsoon region (Alexander et al., 2006) and along the southern Pacific coast
2675 (Aguilar et al. 2005), while some decreases are documented for south-central Mexico
2676 (Aguilar et al. 2005).

2677

2678 On a seasonal basis, the maximum precipitation reported in 5 consecutive days during
2679 winter and spring has increased in Northern Mexico and decreased in south-central
2680 Mexico (Alexander et al. 2006). Northern Baja California, the only region in Mexico
2681 characterized by a Mediterranean climate, has experienced an increasing trend in winter
2682 precipitation exceeding the 90th percentile, especially after 1977 (Cavazos and Rivas,
2683 2004). Heavy winter precipitation in this region is significantly correlated with El Niño
2684 events (Pavia and Badan, 1998; Cavazos and Rivas, 2004); similar results have been
2685 documented for California (e.g., Gershunov and Cayan, 2003). During the summer there
2686 has been a general increase of 2.5 mm in the maximum 5-consecutive-day precipitation in
2687 most of the country and an upward trend in the intensity of events exceeding the 99th and
2688 99.7th percentiles in the high plains of Northern Mexico during the summer season
2689 (Groisman et al. 2005).

2690

2691 During the monsoon season (June-September) in northwestern Mexico, the intensity and
2692 seasonal contribution of rainfall events exceeding the 95th percentiles significantly
2693 increased ($p < 0.05$) in the core monsoon region and at mountain sites (Fig. 2.8; Cavazos et
2694 al. 2007). The mean intensity of 95th percentile events in the monsoon region increased
2695 significantly by 0.6 mm dec^{-1} during 1950-2003. It went from 17.9 mm d^{-1} in the 1950-
2696 1976 period to 19.6 mm d^{-1} in 1977-2003 while at mountain sites the increase was from
2697 40.8 mm d^{-1} to 43.9 mm d^{-1} , respectively. These increases are mainly due to an increase
2698 in tropical cyclone-derived rainfall after 1980. The frequency of heavy events does not
2699 show a significant trend (Englehart and Douglas 2001; Neelin et al. 2006; Cavazos *et al.*,
2700 2007). Similarly, Groisman et al. (2005) report that the frequency of very heavy summer
2701 precipitation events (above the 99th percentile) in the high plains of Northern Mexico
2702 (east of the core monsoon) has not increased, whereas their intensity has increased
2703 significantly.

2704

2705 The increase in the mean intensity of heavy summer precipitation events in the core
2706 monsoon region during the 1977-2003 period are significantly correlated with the
2707 Oceanic El Niño Index (ONI³³) conditions during the cool season. El Niño SST
2708 anomalies antecedent to the monsoon season are associated with less frequent, but more
2709 intense, heavy precipitation events³⁴ (exceeding the 95th percentile threshold), and vice
2710 versa.

³³ ONI INDEX:

http://www.cpc.ncep.noaa.gov/products/analysis_monitoring/ensostuff/ensoyears.shtml

Warm and cold episodes based on a threshold of $\pm 0.5^\circ\text{C}$ for the Oceanic Niño Index (ONI) [3 month running mean of ERSST.v2 SST anomalies in the Niño 3.4 region (5°N - 5°S , 120° - 170°W)], based on the 1971-2000 base period.

³⁴ The correlation coefficient between ONI and heavy precipitation frequency (intensity) is -0.37 ($+0.46$)

2711 There has been an insignificant decrease in the number of consecutive dry days in
2712 northern Mexico, while an increase is reported for south-central Mexico (Alexander et
2713 al., 2006), and the southern Pacific coast (Aguilar et al. 2005).

2714

2715 **2.2.2.2.5 Summary**

2716 All studies indicate that changes in heavy precipitation frequencies are *always* higher
2717 than changes in precipitation totals and, in some regions, an *increase* in heavy and/or
2718 very heavy precipitation occurred while no change or even a decrease in precipitation
2719 totals was observed (e.g., in the summer season in central Mexico). There are regional
2720 variations in where these changes are statistically significant (Fig. 2.8). The most
2721 significant changes occur in the central U.S., central Mexico, southeastern, northern and
2722 western Canada, and southern Alaska. These changes have resulted in a wide range of
2723 impacts, including human health impacts (Chapter 1, Box 1.3).

2724

2725 **2.2.2.3 Monthly to Seasonal Heavy Precipitation**

2726 On the main stems of large river basins, significant flooding will not occur from short
2727 duration extreme precipitation episodes alone. Rather, excessive precipitation must be
2728 sustained for weeks to months. The 1993 Mississippi River flood, which resulted in an
2729 estimated \$17 billion in damages, was caused by several months of anomalously high
2730 precipitation (Kunkel et al. 1994).

2731

2732 A time series of the frequency of 90-day precipitation totals exceeding the 20-year return
2733 period (a simple extension of the approach of Kunkel et al. 2003) indicates a statistically

2734 significant upward trend (Fig. 2.9). The frequency of such events during the last 25 years
2735 is 20% higher than during any earlier 25-year period. Even though the causes of multi-
2736 month excessive precipitation are not necessarily the same as for short duration extremes,
2737 both show moderately high frequencies in the early 20th Century, low values in the 1920s
2738 and 1930s, and the highest values in the past 2-3 decades. The trend³⁵ over the entire
2739 period is highly statistically significant.

2740

2741 **2.2.2.4 North American Monsoon**

2742 Much of Mexico is dominated by a monsoon type climate with a pronounced peak in
2743 rainfall during the summer (June through September) when up to 60% to 80% of the
2744 annual rainfall is received (Douglas et al., 1993; Higgins et al., 1999 and Cavazos et al.,
2745 2002). Monsoon rainfall in southwest Mexico is often supplemented by tropical cyclones
2746 moving along the coast. Farther removed from the tracks of Pacific tropical cyclones,
2747 interior and northwest sections of Mexico receive less than 10% of the summer rainfall
2748 from passing tropical cyclones (Fig. 2.10; Englehart and Douglas 2001). The main
2749 influences on total monsoon rainfall in these regions rests in the behavior of the monsoon
2750 as defined by its start and end date, rainfall intensity and duration of wet and dry spells
2751 (Englehart and Douglas 2006). Extremes in any one of these parameters can have a
2752 strong effect on the total monsoon rainfall.

2753

2754 The monsoon in northwest Mexico has been studied in detail because of its singular
2755 importance to that region and because summer rainfall from this core monsoon region

³⁵ The data were first subjected to a square root transformation to produce a data set with an approximate normal distribution; then least squares regression was applied. Details can be found in the Appendix, Example 4.

2756 spills over into the U.S. Desert Southwest (Douglas et al., 1993; Higgins et al. 1999,
2757 Cavazos et al. 2002). Based on long term data from 8 stations in southern Sonora, the
2758 summer rains have become increasingly late in arriving (Englehart and Douglas 2006)
2759 and this has had strong hydrologic and ecologic repercussions for this northwest core
2760 region of the monsoon. Based on linear trend, the mean start date for the monsoon has
2761 been delayed almost 10 days (9.89 days with a significant trend of 1.57 days per decade)
2762 over the past 63 years (Figure 2.11a). Because extended periods of intense heat and
2763 desiccation typically precede the arrival of the monsoon, the trend toward later starts to
2764 the monsoon will place additional stress on the water resources and ecology of the region
2765 if continued into the future.

2766

2767 Accompanying the tendency for later monsoon starts, there also has been a notable
2768 change in the “consistency” of the monsoon as indicated by the average duration of wet
2769 spells in southern Sonora (Figure 2.11b). Based on a linear trend, the average wet spell³⁶
2770 has decreased by almost one day (0.88 days with a significant trend of -0.14 days per
2771 decade) from nearly four days in the early 1940s to slightly more than three days in
2772 recent years. The decrease in wet spell length indicates a more erratic monsoon is now
2773 being observed. Extended periods of consecutive days with rainfall are now becoming
2774 less common during the monsoon. These changes can have profound influences on
2775 surface soil moisture levels which affect both plant growth and runoff in the region.

2776

³⁶ For southern Sonora, Mexico, wet spells are defined as the mean number of consecutive days with mean regional precipitation ≥ 1 mm.

2777 A final measure of long term change in monsoon activity is associated with the change in
2778 rainfall intensity over the past 63 years (Figure 2.11c). Based on linear trend, rainfall
2779 intensity³⁷ in the 1940s was roughly 5.6mm per rain day, but in recent years has risen to
2780 nearly 7.5mm per rain day³⁸. Thus, while the summer monsoon has become increasingly
2781 late in arriving and wet spells have become shorter, the average rainfall during rain
2782 events has actually increased very significantly by 17% or 1.89mm over the 63 year
2783 period (0.3 mm per decade) as well as the intensity of heavy precipitation events (Fig.
2784 2.9). Taken together, these statistics indicate that the rainfall in the core region of the
2785 monsoon (i.e., northwest Mexico) has become more erratic with a tendency towards high
2786 intensity rainfall events countering the tendency towards a shorter monsoon with shorter
2787 wet spells.

2788

2789 Variability in Mexican monsoon rainfall shows modulation by large-scale climate modes.
2790 Englehart and Douglas (2002) demonstrate that a well developed inverse relationship
2791 exists between ENSO and total seasonal rainfall (June-September) over much of Mexico,
2792 but the relationship is only operable in the positive phase of the PDO. Evaluating
2793 monsoon rainfall behavior on intraseasonal time scales, Englehart and Douglas (2006)
2794 demonstrate that rainfall intensity (mm/rain day) in the core region of the monsoon is
2795 related to PDO phase with the positive (negative) phase favoring relatively high (low)
2796 intensity rainfall events. Analysis indicates that other rainfall characteristics of the
2797 monsoon respond to ENSO with warm events favoring later starts to the monsoon and

³⁷ Daily rainfall intensity during the monsoon is defined as the regional average rainfall for all days with rainfall ≥ 1 mm.

³⁸ The linear trend in this time series is significant at the $p=0.01$ level

2798 shorter length wet spells (days) with cold events favoring opposite behavior (Englehart
2799 and Douglas 2006).

2800

2801 **2.2.2.5 Tropical Storm Rainfall in Western Mexico**

2802 Across southern Baja California and along the southwest coast of Mexico, 30% to 50% of
2803 warm season rainfall (May-November) is attributed to tropical cyclones (Fig. 2.10) and in
2804 years heavily affected by tropical cyclones (upper 95th percentile) 50% to 100% of the
2805 summer rainfall comes from tropical cyclones. In this region of Mexico, there is a long
2806 term, upward trend in tropical cyclone-derived rainfall at both Manzanillo
2807 (41.8mm/decade; Fig. 2.12a) and Cabo San Lucas (20.5mm/decade)³⁹. This upward trend
2808 in tropical cyclone rainfall has led to an increase in the importance of tropical cyclone
2809 rainfall in the total warm season rainfall for southwest Mexico (Fig. 2.12b) and this has
2810 resulted in a higher ratio of tropical cyclone rainfall to total warm season rainfall. Since
2811 these two stations are separated by more than 700km, these significant trends in tropical
2812 cyclone rainfall imply large scale shifts in the summer climate of Mexico.

2813

2814 This recent shift in emphasis on tropical cyclone warm season rainfall in western Mexico
2815 has strong repercussions as rainfall becomes less reliable from the monsoon and becomes
2816 more dependent on heavy rainfall events associated with passing tropical cyclones. Based
2817 on the large scale and heavy rainfall characteristics associated with tropical cyclones,
2818 dams in the mountainous regions of western Mexico are often recharged by strong

³⁹ The linear trends in tropical cyclone rainfall at these two stations are significant at the $p=0.01$ and $p=0.05$ level, respectively.

2819 tropical cyclone events which therefore have positive benefits for Mexico despite any
2820 attendant damage due to high winds or flooding.

2821

2822 This trend in tropical cyclone-derived rainfall is consistent with a long term analysis of
2823 near-shore tropical storm tracks along the west coast of Mexico (storms passing within 5°
2824 of the coast) which indicates an upward trend in the number of near shore storms over the
2825 past 50 years (Fig. 2.12c). While the number of tropical cyclones occurring in the entire
2826 east Pacific Basin is uncertain prior to the advent of satellite tracking in about 1967, it
2827 should be noted that the long term data sets for near shore storm activity (within 5° of the
2828 coast) are considered to be much more reliable due to coastal observatories and heavy
2829 ship traffic to and from the Panama Canal to Pacific ports in Mexico and the United
2830 States. The number of near shore storm days (storms less than 550km from the station)
2831 has increased by 1.3 days/decade in Manzanillo and about 0.7days/decade in Cabo San
2832 Lucas (1949-2006)⁴⁰. The long term correlation between tropical cyclone days at each
2833 station and total tropical cyclone rainfall is $r = 0.61$ for Manzanillo and $r = 0.37$ for Cabo
2834 San Lucas, illustrating the strong tie between passing tropical cyclones and the rain that
2835 they provide to coastal areas of Mexico.

2836

2837 Interestingly, the correlations between tropical cyclone days and total tropical cyclone
2838 rainfall actually drop slightly when based only on the satellite era, 1967-2006 ($r = 0.54$
2839 for Manzanillo and $r = 0.31$ for Cabo San Lucas). The fact that the longer time series has
2840 the higher set of correlations shows no reason to suggest problems with near shore

⁴⁰ The linear trends in near shore storm days are significant at the $p=0.05$ level and $p=0.10$ level, respectively.

2841 tropical cyclone tracking in the pre-satellite era. The lower correlations in the more recent
2842 period between tropical cyclone days and total tropical cyclone rainfall may be tied to
2843 tropical cyclone derived rainfall rising at a faster pace compared to the rise in tropical
2844 cyclone days. In other words, tropical cyclones are producing more rain per event than in
2845 the earlier 1949-1975 period when SSTs were colder.

2846

2847 **2.2.2.6 Tropical Storm Rainfall in the Southeastern United States**

2848 Tropical cyclone-derived rainfall along the southeastern coast of the United States on a
2849 century time scale has changed insignificantly in summer (when no century-long trends
2850 in precipitation was observed) as well as in autumn (when the total precipitation
2851 increased by more than 20% since the 1900s; Groisman et al. 2004).

2852

2853 **2.2.3 Storm Extremes**

2854 **2.2.3.1 Tropical Cyclones**

2855 **2.2.3.1.1 Introduction**

2856 Each year, about 90 tropical cyclones develop over the world's oceans, and some of these
2857 make landfall in populous regions, exacting heavy tolls in life and property. Their
2858 occurrence is often statistically modeled as a Poisson process. The global number has
2859 been quite stable since 1970, when global satellite coverage began in earnest, having a
2860 standard deviation of 10 and no evidence of any substantial trend (e.g. Webster et al
2861 1995). However,, there is some evidence for trends in storm intensity and/or duration
2862 (e.g. Holland and Webster 2007 and quoted references for the North Atlantic; Chan 2000
2863 for the Western North Pacific), and there is substantial variability in tropical cyclone

2864 frequency within each of the ocean basins they affect. Regional variability occurs on all
2865 resolved time scales, and there is also some evidence of trends in certain measures of
2866 tropical cyclone energy, affecting many of these regions and perhaps the globe as well.

2867

2868 There are at least two reasons to be concerned with such variability. The first and most
2869 obvious is that tropical cyclones rank with flash floods as the most lethal and expensive
2870 natural catastrophes, greatly exceeding other phenomena such as earthquakes. In
2871 developed countries, such as the U.S., they are enormously costly: Hurricane Katrina is
2872 estimated to have caused in excess of \$80 billion 2005 dollars in damage, and killed more
2873 than 1500 people. Death and injury from tropical cyclones is yet higher in developing
2874 nations; for example, Hurricane Mitch of 1998 took more than 11,000 lives in Central
2875 America. Any variation or trend in tropical cyclone activity is thus of concern to coastal
2876 residents in affected areas, compounding trends related to societal factors such as
2877 changing coastal population.

2878

2879 A second, less obvious and more debatable issue is the possible feedback of tropical
2880 cyclone activity on the climate system itself. The inner cores of tropical cyclones have
2881 the highest specific entropy content of any air at sea level, and for this reason such air
2882 penetrates higher into the stratosphere than is the case with other storm systems. Thus
2883 tropical cyclones may play a role in injecting water and trace gases and microscopic
2884 airborne particles into the upper troposphere and lower stratosphere, though this idea
2885 remains largely unexamined. There is also considerable evidence that tropical cyclones
2886 vigorously mix the upper ocean, affecting its circulation and biogeochemistry, perhaps to

2887 the point of having a significant effect on the climate system. Since the current generation
2888 of coupled climate models greatly under-resolves tropical cyclones, such feedbacks are
2889 badly underrepresented, if they are represented at all.

2890 For these reasons, it is important to quantify, understand, and predict variations in
2891 tropical cyclone activity. The following sections review current knowledge of these
2892 variations on various time scales.

2893

2894 **2.2.3.1.2 Data Issues**

2895 Quantifying tropical cyclone variability is limited, sometimes seriously, by a large suite
2896 of problems with the historical record of tropical cyclone activity. In the North Atlantic
2897 and eastern North Pacific regions, responsibility for the tropical cyclone database rests
2898 with NOAA's National Hurricane Center (NHC), while in other regions, archives of
2899 hurricane activity are maintained by several organizations, including the U.S. Navy's
2900 Joint Typhoon Warning Center (JTWC), the Japan Meteorological Agency (JMA), the
2901 Hong Kong Observatory (HKO) and the Australian Bureau of Meteorology (BMRC).
2902 The data, known as ``best track" data (Jarvinen et al. 1984; Chu et al. 2002), comprise a
2903 global historical record of tropical cyclone position and intensity, along with more recent
2904 structural information. Initially completed in real time, the best tracks are finalized by
2905 teams of forecasters update the best track data at the end of the hurricane season in each
2906 ocean basin using data collected during and after each hurricane's lifetime.

2907

2908 It should first be recognized that the primary motivation for collecting data on tropical
2909 cyclones was initially to support real-time forecasts and this remains the case in many

2910 regions today. From the 1970s onwards increasing emphasis has been placed on
2911 improving the archive for climate purposes, and on extending the record back to include
2912 historical systems (e.g. Laurensz 1977; Neumann 1993; Landsea et al 2004).
2913 Unfortunately, improvements in measurement and estimation techniques have often been
2914 implemented with little or no effort to calibrate against existing techniques and with poor
2915 documentation where such calibrations were done. Thus the available tropical cyclone
2916 data contain an inhomogeneous mix of changes in quality of observing systems, reporting
2917 policies, and the methods utilized to analyze the data

2918

2919 It remains a scientific tragedy that insufficient effort is expended in re-examining and
2920 quality controlling the tropical cyclone record on a year to year basis, particularly outside
2921 the Atlantic and eastern North Pacific regions. Efforts are ongoing to reanalyze the
2922 historic best track data, but such a posteriori reanalyses are less than optimal because not
2923 all of the original data that the best track was based on are readily available.

2924

2925 Documentation of the occurrence of tropical cyclones is thought to be reliable back to
2926 about 1945 in the Atlantic and 1970 in the Eastern Pacific (e.g. Holland and Webster
2927 2007 and references therein), and back to about 1975 for the Western and Southern
2928 Pacific basins, thanks to earth-orbiting satellites (e.g. Holland 1981). Until the launch of
2929 MeteoSat-7 in 1998, the Indian Oceans were seen only obliquely, but storm counts may
2930 still be expected to be accurate after 1977. Before those periods, storms could and
2931 undoubtedly remain undetected, especially if they did not pass near ships at sea or land
2932 masses. For the North Atlantic it is likely that up to 3 storms per year were missing

2933 before 1900 dropping to zero by the early 1960s (Holland and Webster 2007; Chang and
2934 Guo 2007). Estimates of the duration of storms are considered to be less reliable prior to
2935 the 1970's due particularly to a lack of good information on their time of genesis. Since
2936 the 1970s storms were more accurately tracked throughout their lifetimes by
2937 geostationary satellites.

2938

2939 Estimates of storm intensity are far less reliable, and this remains true for large portions
2940 of the globe even today. Airborne hurricane reconnaissance flight became increasingly
2941 routine in the North Atlantic and western North Pacific regions after 1945, but was
2942 discontinued in the western North Pacific region in 1987. Some missions are today being
2943 conducted under the auspices of the government of Taiwan. However airborne
2944 reconnaissance only samples a small fraction of storms, and then only over a fraction of
2945 their lifetimes; moreover, good, quantitative estimates of wind speeds from aircraft did
2946 not become available until the late 1950s. Beginning in the mid 1970s, tropical cyclone
2947 intensity has been estimated from satellite imagery. Until relatively recently, techniques
2948 for doing so were largely subjective, and the known lack of homogeneity in both the data
2949 and techniques applied in the post-analyses has resulted in significant skepticism
2950 regarding the consistency of the intensity estimates in the data set. This lack of temporal
2951 consistency renders the data suspect for identifying trends, particularly in metrics related
2952 to intensity.

2953

2954 Recent studies have addressed these known data issues. Kossin et al. (2007a) constructed
2955 a more homogeneous record of hurricane activity and found remarkably good agreement

2956 in both variability and trends between their new record and the best track data in the N.
2957 Atlantic and Eastern Pacific basins during the period 1983–2005. They concluded that the
2958 best track maintained by the NHC does not appear to suffer from data quality issues
2959 during this period. On the other hand, they were not able to corroborate the presence of
2960 upward intensity trends in any of the remaining tropical cyclone-prone ocean basins. This
2961 could be due to inaccuracies in the satellite best tracks, or could be due to the training of
2962 the Kossin et al technique on North Atlantic data. This is supported by Wu et al. (2006),
2963 who considered Western Pacific best track data constructed by other agencies (HKMO
2964 and JMA) who construct best track data for the western North Pacific. Harper and
2965 Callaghan (2006) report on reanalyzed data from the Southeastern Indian Ocean and
2966 showed some biases, but a remaining upward intensity trend. These studies underscores
2967 the need for improved care in analyzing tropical cyclones and in obtaining better
2968 understanding of the climatic controls of tropical cyclone activity beyond SST-based
2969 arguments alone.

2970

2971 The standard tropical cyclone databases do not usually contain information pertaining to
2972 the geometric size of tropical cyclones. Exceptions include the Australian region and the
2973 enhanced database for the North Atlantic over the last few decades. A measure of size of
2974 a tropical cyclone is a crucial complement to estimates of intensity as it relates directly to
2975 storm surge and damage area associated with landfalling storms. Such size measures can
2976 be inferred from aircraft measurements and surface pressure distributions, and can now
2977 be estimated from satellite imagery (e.g. Mueller et al. 2006; Kossin et al. 2007b).

2978

2979

2980 **2.2.3.1.3 Low-frequency Variability and Trends of Tropical cyclone Activity Indices**

2981 “Low frequency” variability is here defined as variations on time scales greater than
2982 those associated with ENSO (i.e. more than 3-4 years). Several papers in recent years
2983 have quantified interdecadal variability of tropical cyclones in the Atlantic (Goldenberg
2984 et al., 2001; Bell and Chelliah, 2006) and the western North Pacific (Chan and Shi, 1996),
2985 attributing most of the variability to natural interdecadal variability of regional climates
2986 in the Atlantic and Pacific, respectively. In the last few years, however, several papers
2987 have attributed both low frequency variability and trends in tropical cyclone activity to
2988 changing radiative forcing owing to anthropogenic sulfate aerosols and greenhouse gases.
2989 Emanuel (2005a) developed a “Power Dissipation Index” (PDI) of tropical cyclones,
2990 defined as the sum of the cubed estimated maximum sustained surface wind speeds at 6-
2991 hour intervals accumulated over each Atlantic tropical cyclone from the late 1940s to
2992 2003. Landsea (2005) commented on the quality of data comprising the index. An
2993 updated version of this analysis (Emanuel 2007), shown in Fig. 2.13, confirms that there
2994 has been a substantial increase in tropical cyclone activity since about 1970, and indicates
2995 that the low-frequency Atlantic PDI variations are strongly correlated with low-frequency
2996 variations in tropical Atlantic SSTs. Based on this analysis, it is likely that hurricane
2997 activity, as measured by the Power Dissipation Index (PDI), has increased substantially
2998 since the 1950s and 60s in association with warmer Atlantic SSTs. The magnitude of this
2999 increase depends on the adjustment to the wind speed data from the 1950s and 60s
3000 (Landsea 2005; Emanuel 2007). It is very likely that PDI has generally tracked SST
3001 variations on decadal time scales in the tropical Atlantic since 1950 and likely that it also

3002 generally tracked the secular increase of SST. Confidence in these statistics prior to the
3003 late 1940s is low, due mainly to the decreasing confidence in hurricane duration and
3004 intensity observations. The PDI in the eastern Pacific has decreased since 1980 (Kossin et
3005 al. 2007).

3006

3007 The Power Dissipation Index for U.S. landfalling tropical cyclones has not increased
3008 since the late 1800s (Landsea 2005). Pielke (2005) noted that there are no evident trends
3009 in observed damage in the North Atlantic region, after accounting for population
3010 increases and coastal development. However, Emanuel (2005b) notes that a PDI series
3011 such as Landsea's (2005) based on only U.S. landfalling data, contains only about 1
3012 percent of the data that Emanuel's (2005a) basin-wide PDI contains, which is based on all
3013 storms over their entire lifetimes. Thus a trend in basin-wide PDI may not be detectable
3014 in U.S. landfalling PDI since the former index has a factor of 10 advantage in signal to
3015 noise ratio.

3016

3017 Figure 2.14 (from Holland and Webster 2007), indicates that there has been no distinct
3018 trend in the mean intensity of all Atlantic storms, hurricanes, and major hurricanes. A
3019 distinct increase in the most intense storms occurred around the time of onset of aircraft
3020 reconnaissance, but this is considered to be largely due to better observing methods.

3021 Holland and Webster also found that the overall proportion of hurricanes has remained
3022 remarkably constant during the 20th century at around 50%, and there has been a marked
3023 oscillation in major hurricane proportions, which has no observable trend.

3024 Webster et al. (2005) reported that the number of category 4 and 5 hurricanes has almost

3025 doubled globally over the past three decades. The recent reanalysis of satellite data
3026 beginning in the early 1980s by Kossin et al. (2007a) support these results in the Atlantic
3027 although the results in the remaining basins were not corroborated.

3028

3029 The recent Emanuel and Webster et al. studies have generated much debate in the
3030 hurricane research community, particularly with regard to homogeneity of the tropical
3031 cyclone data over time and the required adjustments (e.g. Landsea 2005; Knaff and
3032 Sampson 2006; Chan 2006; Hoyos et al. 2006; Landsea et al. 2006; Srivier and Huber
3033 2006; Klotzbach 2006; Elsner et al. 2006; Maue and Hart 2007; Manning and Hart 2007;
3034 Holland and Webster 2007, Landsea 2007, Mann et al 2007, Holland 2007). Several of
3035 these studies argue that data problems preclude determination of significant trends in
3036 various tropical cyclone measures, while others provide further evidence in support of
3037 reported trends. In some cases, differences between existing historical data sets
3038 maintained by different nations can yield strongly contrasting results (e.g., Kamahori et
3039 al. 2006).

3040

3041 Several studies have examined past regional variability in tropical cyclone tracks (Wu et
3042 al. 2005; Xie et al. 2005; Vimont and Kossin 2007; Kossin and Vimont 2007). Thus far,
3043 no clear long-term trends in this metric have been reported, but there is evidence that
3044 Atlantic tropical cyclone formation regions have undergone systematic long-term shifts to
3045 more eastward developments (Holland 2007). These shifts affect track and duration,
3046 which subsequently affects intensity. The modulation of the Atlantic tropical cyclone
3047 genesis region occurs through systematic changes of the regional SST and circulation

3048 patterns. Thus SST affects intensity not just through thermodynamic pathways that are
3049 local to the storms, but also through changes in basinwide circulation patterns (Kossin
3050 and Vimont 2007).

3051

3052 In summary, we conclude that Atlantic tropical storm and hurricane destructive potential
3053 as measured by the Power Dissipation Index (which combines storm intensity, duration,
3054 and frequency) has increased. This increase is substantial since about 1970, and is likely
3055 substantial since the 1950s and 60s, in association with warming Atlantic sea surface
3056 temperatures.

3057

3058 **2.2.3.1.4 Low-frequency Variability and Trends of Tropical Cyclone Counts**

3059 Mann and Emanuel (2006) reported that Atlantic tropical cyclone counts closely track
3060 low-frequency variations in tropical Atlantic SSTs, including a long-term increase since
3061 the late 1800s and early 1900s (see also Fig. 2.15 from Holland and Webster 2007).

3062 There is currently debate on the relative roles of internal climate variability (e.g.,
3063 Goldenberg et al. 2001) versus radiative forcing, including greenhouse gases, and sulfate
3064 aerosols (Mann and Emanuel 2006; Santer et al 2006) in producing the multi-decadal
3065 cooling of the tropical North Atlantic. This SST variation is correlated with reduced
3066 hurricane activity during the 1970s and 80s relative to the 1950s and 60s or to the period
3067 since 1995 (see also Zhang et al. 2007).

3068

3069 On a century time scale, time series of tropical storm frequency in the Atlantic (Fig. 2.15)
3070 show substantial interannual variability and a marked increase (of over 100%) since

3071 about 1900. This increase occurred in two sharp jumps of around 50%, one in the 1930s
3072 and another that commenced in 1995 and has not yet stabilized. Holland and Webster
3073 (2007) have suggested that these sharp jumps are transition periods between relatively
3074 stable climatic periods of tropical cyclone frequency (Fig. 2.15). Figure 2.15 uses
3075 unadjusted storm—an issue which will be addressed further below.

3076

3077 For tropical cyclone frequency, the finding that the largest recorded increases over the
3078 past century have been in the eastern North Atlantic (e.g., see recent analysis in Vecchi
3079 and Knutson 2007; Holland 2007), which historically has been the least well observed,
3080 has led to questions of whether this may be due to data issues (Landsea et al. 2004;
3081 Landsea 2007). The major observing system change points over the past century have
3082 been:

- 3083 • The implementation of routine aircraft reconnaissance in 1944-45;
- 3084 • The use of satellite observations and related analysis procedures from the late
3085 1960s onwards; and,
- 3086 • A change in analysis practice by the National Hurricane Center from 1970 to
3087 include more mid-latitude systems.

3088 In addition, there have steady improvements in techniques and instrumentation, which
3089 may also introduce some spurious trends.

3090

3091 Landsea (2007) has used the fraction of storms striking land in the satellite and pre-
3092 satellite era to estimate the number of missing storms per year in the pre-satellite era
3093 (1900 to 1965) to be about 3.2 storms per year. This assumes that the fraction of all

3094 storms that strike land in the real world has been relatively constant over time, which has
3095 been shown to be incorrect by Holland (2007). Holland also shows that the smaller
3096 fraction of storms that made landfall during the past fifty years (1956-2005) compared to
3097 the previous fifty years (1906-1955) is directly related to changes in the main formation
3098 location regions, with a decrease in western Caribbean and Gulf of Mexico developments
3099 and an increase in the eastern Atlantic.

3100

3101 Alternative approaches to estimating the earlier data deficiencies have been used by
3102 Chang and Guo (2007), Vecchi and Knutson (2007) and Mann et al (2007). The first two
3103 studies use historical ship tracks from the pre-satellite era, combined with storm track
3104 information from the satellite era, to infer an estimated adjustment for missing storms in
3105 the pre-satellite era (assumed as all years prior to 1965). Mann et al used statistical
3106 climate relationships to estimate potential errors. Vecchi and Knutson found 2.5 storms
3107 per year were missing prior to 1900, decreasing to zero by 1960. Chang and Guo found
3108 1.2 storms missing around 1910 also decreasing to zero by 1960. Mann et al, estimated a
3109 more modest undercount bias of 1 per year back to 1970. The adjusted time series by
3110 Vecchi and Knutson (Fig. 2.16) suggest a statistically significant ($p=0.003$ or less)
3111 positive linear trend in adjusted storm counts of 55%/century since 1900. However,
3112 beginning the trend from 1878, the trend through 2006 is smaller (+15%/century) and not
3113 statistically significant at the $p=0.05$ level (p -value of about 0.3)⁴¹. It is notable that the
3114 degree of increase over the past century depends on the analysis methodology. When
3115 using a linear trend, as above, the increase from 1900 to 2005 is around 55% in the
3116 adjusted storm counts. However, using the essentially non-linear approach by Holland

⁴¹ Details of the statistical analysis are given in the Appendix, Example 5.

3117 and Webster (2007) of separate climatic regimes, the increase in adjusted storm counts
3118 from the 1900-1920 regime to the 1995-2006 regime is 85%. The trend from 1900 begins
3119 near a local minimum in the time series and ends with the recent high activity, perhaps
3120 exaggerating the significance of the trend due to multidecadal variability. On the other
3121 hand high levels of activity during the late 1800s, which lead to the insignificant trend
3122 result, are indirectly inferred in large part from lack of ship track data, and the uncertainty
3123 in the late 1800s storm counts is greater than that during the 1900s.

3124

3125 Hurricane frequency closely follows the tropical cyclone variability, with a stable 50% of
3126 all cyclones developing to hurricane strength over much of the past century (Holland and
3127 Webster 2007). However, there has been a concomitant increase in both overall storm
3128 frequency and the proportion of major hurricanes since 1995. Taken together, these result
3129 in a very sharp increase in major hurricane numbers, which can be associated with
3130 changes of SST (Holland and Webster 2007, Webster et al 2005). The PDI trend reported
3131 by Emanuel (2007) is largely due to this increase in major hurricane numbers.

3132

3133 Atlantic basin total hurricane counts, major hurricane counts, and U.S. landfalling
3134 hurricane counts as recorded in the HURDAT data base for the period 1851-2006 are
3135 shown in Fig. 2.17. These have not been adjusted for missing storms, as there was likely
3136 less of a tendency to miss both hurricanes and major hurricanes in earlier years compared
3137 to tropical storms, largely because of their intensity and damage potential. There is a
3138 slight negative trend in U.S. landfalling hurricane frequency. The basin-wide major
3139 hurricane counts increase over the long-term. For total hurricanes, trends to 2005

3140 beginning in 1881 through 1921 are positive and statistically significant ($p=0.05$)
3141 whereas trends beginning in 1851 through 1871 are positive but not statistically
3142 significant, owing to the prolonged active period in the late 1800s. For major hurricanes,
3143 trends beginning in 1851 through 1911 were positive and statistically significant, whereas
3144 the trend beginning from 1921 was positive but not statistically significant⁴².

3145

3146 Regional storm track reconstructions for the basin (Vecchi and Knutson 2007; Holland
3147 and Webster 2007b(?)) indicate a decrease in tropical storm occurrence in the western
3148 part of the basin, consistent with the minimal change or slight decrease in U.S.
3149 landfalling tropical storm or hurricane counts. These analyses further suggest that—after
3150 adjustment for missing storms-- a century-scale increase in basin-wide Atlantic tropical
3151 storm occurrence has occurred, with increases mainly in the central and eastern parts of
3152 the basin (also consistent with Chang and Guo 2007). From a climate variability
3153 perspective, Kossin and Vimont (2007) have shown that a positive phases of the Atlantic
3154 Meridional Mode is correlated to an systematic eastward extension of the genesis region
3155 in the Atlantic. Elsner (1996) and Holland and Webster (2007) have shown that the
3156 increasing frequency over the past 30 years is associated with a changeover to equatorial
3157 developments and particularly to developments in the eastern equatorial region.

3158

3159 In summary, we conclude that there have been fluctuations from decade to decade in
3160 tropical cyclone numbers, and data uncertainty is larger in the earlier parts of the record,
3161 particularly prior to aircraft reconnaissance beginning in the mid-1940s. While there are
3162 undoubtedly data deficiencies and missing storms in the early record, they appear

⁴² Further details of the statistical analysis are given in the Appendix, Example 6.

3163 insufficient to remove the observed positive trends in basin-wide tropical storm counts. It
3164 is likely that that the annual numbers of tropical storms/hurricanes and major hurricanes
3165 in the North Atlantic basin have increased significantly over the past 100 years in close
3166 relationship with warming equatorial Atlantic sea surface temperatures. The positive
3167 linear trend in all storm categories extends back to the 1800s, but is generally not
3168 significant prior to 1890. The increasingly decreased confidence in the data before 1900
3169 precludes any definitive conclusions from this era. The increases in basin-wide storm
3170 counts has occurred primarily from an eastward shift in the formation and occurrence
3171 regions and there has been a distinct decrease in western Caribbean and Gulf of Mexico
3172 developments. As a result, North American mainland land-falling hurricanes have
3173 remained quasi-static over the past century.

3174

3175 **2.2.3.1.5 Paleoclimate Proxy Studies of Past Tropical Cyclone Activity**

3176 Paleotempestology is an emerging field of science that attempts to reconstruct past
3177 tropical cyclone activity using geological proxy evidence or historical documents. This
3178 work attempts to expand knowledge about hurricane occurrence back in time beyond the
3179 limits of conventional instrumental records, which cover roughly the last 150 years. A
3180 broader goal of paleotempestology is to help researchers explore physically based
3181 linkages between prehistoric tropical cyclone activity and other aspects of past climate.

3182

3183 Among the geologically based proxies, overwash sand layers deposited in coastal lakes
3184 and marshes have proven to be quite useful (Liu and Fearn, 1993, 2000; Liu 2004;
3185 Donnelly and Webb 2004). Similar methods have been used to produce proxy records of

3186 hurricane strikes from back-barrier marshes in Rhode Island and New Jersey extending
3187 back about 700 years (Donnelly et al. 2001a, 2001b; Donnelly et al. 2004; Donnelly and
3188 Webb 2004), and more recently in the Caribbean (Donnelly 2005). Stable isotope signals
3189 in tree rings (Miller et al. 2006), cave deposits (Frappier et al. 2007) and coral reef
3190 materials are also being actively explored for their utility in providing paleoclimate
3191 information on tropical cyclone activity. Historical documents apart from traditional
3192 weather service records (newspapers, plantation diaries, Spanish and British historical
3193 archives, etc.) can also be used to reconstruct some aspects of past tropical cyclone
3194 activity (Ludlam, 1963; Millas, 1968; Fernandez-Partagas and Diaz, 1996; Chenoweth,
3195 2003; Mock 2004; Garcia Herrera et al. 2004; 2005; Liu et al. 2001; Louie and Liu 2003;
3196 Louie and Liu 2004).

3197

3198 Donnelly and Woodruff's (2007) proxy reconstruction the past 5,000 years of intense
3199 hurricane activity in the western North Atlantic suggests that hurricane variability has
3200 been strongly modulated by El Nino during this time and that the past 250 years has been
3201 relatively active in the context of the past 5,000 years. Nyberg et al. (2007) suggest that
3202 major hurricane activity in the Atlantic was anomalously low in the 1970s and 1980s
3203 relative to the past 270 years. As with Donnelly and Woodruff, their proxy measures
3204 were located in the western part of the basin (near Puerto Rico), and in their study,
3205 hurricane activity was inferred indirectly through statistical associations with proxies for
3206 vertical wind shear and SSTs.

3207

3208

3209

3210 **2.2.3.2 Strong Extratropical Cyclones Overview**

3211 Extra-tropical cyclone (ETC)⁴³ is a generic term for any non-tropical, large-scale low
3212 pressure storm system that develops along a boundary between warm and cold air
3213 masses. These types of cyclonic⁴⁴ disturbances are the dominant weather phenomenon
3214 occurring in the mid- and high-latitudes during the cold season because they are typically
3215 large and often have associated severe weather. The mid-latitude North Pacific and North
3216 Atlantic basins, between ~30°N-60°N, are regions where large-numbers of ETC's
3217 develop and propagate across the ocean basins each year. Over land or near populous
3218 coastlines, strong or extreme ETC events generate some of the most devastating impacts
3219 associated with extreme weather and climate, and have the potential to affect large areas
3220 and dense population centers. A notable example was the blizzard of 12-14 March 1993
3221 along the East Coast of the U.S. that is often referred to as the “super-storm” or “storm of
3222 the century”⁴⁵ (e.g., Kocin et al.1995;). Over the ocean, strong ETCs generate high waves
3223 that can cause extensive coastal erosion when combined with storm surge as they reach
3224 the shore, resulting in significant economic impact. Rising sea level extends the zone of
3225 impact from storm surge and waves farther inland, and will likely result in increasingly
3226 greater coastal erosion and damage from storms of equal intensity.

3227

3228

⁴³ The fundamental difference between the characteristics of extra-tropical and tropical cyclones is that ETC's have a cold core and their energy is derived from baroclinic instability, while tropical cyclones have a warm core and derive their energy from barotropic instability (Holton 1979).

⁴⁴ A term applied to systems rotating in the counter-clockwise direction in the Northern Hemisphere.

⁴⁵ The phrase “Storm of the Century” is also frequently used to refer to the 1991 Halloween ETC along the Northeast US coast, immortalized in the movie *The Perfect Storm*

3229

3230 Studies of changes in strong ETC's and associated frontal systems have focused on
3231 locations where ETCs form and the resulting storm tracks, frequencies, and intensities⁴⁶.
3232 The primary constraint on these studies has been the limited period of record available
3233 that has the best observation coverage for analysis and verification of results, with most
3234 research focused on the latter half of the 20th century. Model reanalysis data is used in the
3235 majority of studies, either NCEP-NCAR (Kalnay et al. 1996) or ERA-40 (Upalla et al.
3236 2005) datasets, although prior to 1965 data quality have been shown to be less reliable
3237

3238 It is important to stress that any observed changes in ETC storm tracks, frequencies or
3239 intensities are highly dependent on broad-scale atmospheric modes of variability, and the
3240 noise associated with this variability is large in relation to any observed linear trend.
3241 Therefore, detection and attribution of long-term (decadal- to century-scale) changes in
3242 ETC activity is extremely difficult.

3243

3244 **2.2.3.2.1 Variability of Extra-Tropical Cyclone Activity**

3245 Inter-annual and inter-decadal variability of ETC's is primarily driven by the location and
3246 other characteristics associated with the Polar jet stream. The mean location of the Polar
3247 jet is often referred to as the "storm track". The large-scale circulation is governed by the
3248 equator-to-pole temperature gradient, which is strongly modulated by SST's over the
3249 oceans. The magnitude of the equator-to-pole temperature gradient is of utmost

⁴⁶ These studies use *in situ* observations (both surface and upper-air), re-analysis fields, and Atmospheric-Ocean Global Climate Model (GCM) hind-casts

3250 importance in determining the intensity of storms: the smaller (larger) the gradient in
3251 temperature, the weaker (stronger) the potential energy available for extra-tropical
3252 cyclone formation. The observed intensity of ETC's at the surface is related to the
3253 amplitude of the large-scale circulation pattern, with high-amplitude, negatively tilted
3254 troughs favoring stronger development of ETC's at the surface (Sanders and Gyakum
3255 1980).

3256

3257 From a seasonal perspective, the strongest ETC's are temporally out of phase in the
3258 Pacific and Atlantic basins, since the baroclinic wave energy climatologically reaches a
3259 peak in late fall in the North Pacific and in January in the North Atlantic (Nakamura
3260 1992; Eichler and Higgins 2006). While it remains unclear what the physical basis is for
3261 the offset in peak storm activity between the two basins, Nakamura (1992) showed
3262 statistically that when the Pacific jet exceeds 45 m s^{-1} there is a suppression of baroclinic
3263 wave energy, even though the low-level regional baroclinicity and strength of the Pacific
3264 jet are at a maximum (this effect is not evident in the Atlantic basin, since the peak
3265 strength of the jet across the basin rarely exceeds 45 m s^{-1}). Despite the observed
3266 seasonal difference in the peak of ETC activity, Chang and Fu (2002) found a strong
3267 positive correlation between the Pacific and Atlantic storm tracks using monthly mean
3268 reanalysis data covering 51 winters (1949 to 1999). They found the correlations between
3269 the two basins remained positive and robust over individual months during winter (DJF)
3270 or over the entire season (Chang and Fu 2002).

3271

3272 It has been widely documented that the track position, intensity and frequency of ETC's

3273 is strongly modulated on inter-annual time-scales by different modes of variability, such
3274 as the El Niño/Southern Oscillation (ENSO) phenomenon (Gershunov and Barnett 1998;
3275 An et al. 2007). In a recent study, Eichler and Higgins (2006) used both NCEP-NCAR
3276 and ERA-40 reanalysis data to diagnose the behavior of ETC activity during different
3277 ENSO phases. Their results showed that during El Niño events there is an equator-ward
3278 shift in storm tracks in the North Pacific basin, as well as an enhancement of the storm
3279 track along the U.S. East Coast. However, they found significant variability related to the
3280 magnitude of the El Niño event. During strong El Niños, ETC frequencies peak over the
3281 North Pacific and along the eastern U.S., from the southeast coast to the Maritime
3282 Provinces of Canada (Eichler and Higgins 2006), with a weaker track across the Midwest
3283 from the lee of the Rocky Mountains to the Great Lakes. During weak to moderate El
3284 Niños, the storm tracks are similar to the strong El Niños, except there is a slight increase
3285 in the number of ETC's over the northern Plains and the frequency of ETC activity
3286 decreases over the mid-Atlantic region. Similar to other previous studies (e. g. Hirsch et
3287 al. 2001; Noel and Changnon 1998), an inverse relationship typically exists during La
3288 Niñas; as the strength of La Niña increases, the frequency maxima of East Coast storms
3289 shifts poleward, the North Pacific storm track extends eastward toward the Pacific
3290 Northwest, and the frequency of cyclones increases across the Great Lakes region
3291 (Eichler and Higgins (2006).

3292

3293 In addition to ENSO, studies have shown that the Arctic Oscillation (AO) can strongly
3294 influence the position of storm tracks and the intensity of ETC's. Previous studies have
3295 shown that during positive AO conditions Northern Hemisphere cyclone activity shifts

3296 poleward (Serreze et al. 1997; Clark et al. 1999). Inversely, during negative AO
3297 conditions the polar vortex is weaker and cyclone activity shifts southward. Since the
3298 North Atlantic Oscillation (NAO) represents the primary component of the AO, it has a
3299 similar affect on storm tracks position, especially over the eastern North Atlantic basin
3300 (McCabe et al. 2001). For futher information on the different atmospheric modes of
3301 variability (Chapter 2, Box 2.3).

3302

3303 **2.2.3.2.2 Changes in Storm Tracks and Extra-Tropical Cyclone Characteristics**

3304 Many studies have documented changes in storm track activity. Specifically, a significant
3305 pole-ward shift of the storm track in both the Pacific and Atlantic ocean basins has been
3306 verified by a number of recent studies that have shown a decrease in ETC frequency in
3307 mid-latitudes, and a corresponding increase in ETC activity in high-latitudes (Wang et al.
3308 2006a; Simmons and Key 2002; Paciorek et al. 2002; Graham and Diaz 2001; Geng and
3309 Sugi 2001; McCabe et al. 2001; Key and Chan 1999; Serreze et al. 1997). Several of
3310 these studies have examined changes in storm tracks over the entire Northern Hemisphere
3311 (i.e. McCabe et al. 2001; Paciorek et al. 2002; Key and Chan 1999), while several others
3312 have focused on the storm track changes over the Pacific (i.e., Graham and Diaz 2001)
3313 and Atlantic basins (i.e., Geng and Sugi 2001), or both (i.e., Wang and Swail 2001). Most
3314 of these studies focused on changes in frequency and intensity observed during winter
3315 (DJF) or the entire cold season (Oct-Mar). However, for spring, summer and autumn,
3316 Key and Chan (1999) found opposite trends in 1000-hPa and 500-hPa cyclone
3317 frequencies for both the mid- and high latitudes of the Northern Hemisphere.

3318 The standardized annual departures⁴⁷ of ETC frequency for the entire Northern
3319 Hemisphere over the period 1959-1997 (Fig. 2.18a,b; McCabe et al. 2001) shows that
3320 cyclone frequency has decreased for the mid-latitudes (30⁰-60⁰N) and increased for the
3321 high latitudes (60⁰-90⁰N). For the 55-year period of 1948-2002, a metric called the
3322 Cyclone Activity Index (CAI)⁴⁸ was developed by Zhang et al. (2004) to document the
3323 variability of Northern Hemisphere cyclone activity. The CAI has increased in the Arctic
3324 Ocean (70⁰-90⁰N) during the latter half of the 20th century, while it has decreased in mid-
3325 latitudes (30⁰-60⁰N) from 1960 to 1993, which is evidence of a pole-ward shift in the
3326 average storm track position. Interestingly, the number and intensity of cyclones entering
3327 the Arctic from the mid-latitudes has increased, particularly during summer (Zhang et al.
3328 2004). The increasing activity in the Arctic was more recently verified by Wang et al.
3329 (2006a), who analyzed ETC counts by applying two separate cyclone detection
3330 thresholds to ERA-40 reanalysis of mean sea level pressure data. Their results showed an
3331 increase in high latitude storm counts, and a decrease in ETC counts in the mid-latitudes
3332 during the latter half of the 20th century.

3333

3334 Northern Hemisphere ETC intensity has increased over the period 1959-1997 across both
3335 mid- and high-latitudes cyclone intensity (McCabe et al. 2001; Fig. 2.18c,d), with the
3336 upward trend more significant for the high latitudes (0.01 level) than for the mid-latitudes

⁴⁷ Standardized departures (z scores) were computed for each 5⁰ latitudinal band by subtracting the respective 1959-1997 mean from each value and dividing by the respective 1959-1997 standard deviation (McCabe et al. 2001).

⁴⁸ The CAI integrates information on cyclone intensity, frequency, and duration into a comprehensive index of cyclone activity. The CAI is defined as the sum over all cyclone centers, at a 6-hourly resolution, of the differences between the cyclone central SLP and the climatological monthly mean SLP at corresponding grid points in a particular region during the month (Zhang et al. 2004).

3337 (0.10 level). From an ocean basin perspective, the observed increase in intense ETC's
3338 appears to be more robust across the Pacific than the Atlantic. Using reanalysis data
3339 covering the period 1949-1999, Paciorek et al. (2002) found that extreme wind speeds
3340 have increased significantly in both basins (Fig. 2.19a,d). Their results also showed that
3341 the observed upward trend in the frequency of intense cyclones has been more
3342 pronounced in the Pacific basin (Fig. 2.19c), although the inter-annual variability is much
3343 less in the Atlantic (Fig. 2.19f). Surprisingly, they found that the overall counts of ETC's
3344 showed either no long-term change, or a decrease in the total number of cyclones (Fig.
3345 2.19b,e). However, this may be a result of the large latitudinal domain used in their study
3346 (20° - 70° N), which included parts of the tropics, sub-tropics, mid- and high latitudes.

3347

3348 On a regional scale, ETC activity has increased in frequency, duration and intensity in the
3349 lower Canadian Arctic during 1953-2002 with the most statistically significant trends
3350 during winter⁴⁹ ($p=0.05$ level; Wang et al. 2006b). In contrast to the Arctic region,
3351 cyclone activity was less frequent and weaker along the southeast and southwest coasts of
3352 Canada. Winter cyclone deepening rates (i.e. rates of intensification) have increased in
3353 the zone around 60° N, but decreased further south in the Great Lakes area and southern
3354 Prairies-British Columbia region of Canada. This is also indicative of a pole-ward shift in
3355 ETC activity, and corresponding weakening of ETC's in the mid-latitudes and an
3356 increase in observed intensities in the high latitudes. For the period of 1949-1999, the
3357 intensity of Atlantic ETC's increased from the 1960's to the 1990's during the winter

⁴⁹ Results based on hourly average sea level pressure data observed at 83 stations

3358 season⁵⁰ (Harnik and Chang 2003). Their results showed no significant trend in the
3359 Pacific region but this is a limited finding because of a lack of upper-air (i.e. radiosonde)
3360 data over the central North Pacific⁵¹ in the region of the storm track peak (Harnik and
3361 Chang 2003).

3362

3363 There have been very few studies that have analyzed the climatological frequencies and
3364 intensities of ETC's across the central U.S., specifically in the Great Lakes region (e.g.,
3365 Lewis 1987; Harmon et al. 1980; Garriott 1903). Over the period 1900 to 1990 the
3366 number of strong cyclones (≤ 992 mb) increased significantly across the Great Lakes
3367 (Angel and Isard 1998). This increasing trend was evident (at the $p=0.05$ level) both
3368 annually and during the cold season,. In fact, over the 91-yr period analyzed, they found
3369 that the number of strong cyclones per year more than doubled during both November
3370 and December.

3371

3372 In addition to studies using reanalysis data, which have limited record lengths, other
3373 longer-term studies of the variability of *storminess* typically use wave or water level
3374 measurements as proxies for storm frequency and intensity. Along the U.S. West Coast,
3375 one of the longest continuous climate-related instrumental time series in existence is the
3376 hourly tide gauge record at San Francisco that dates back to 1858. A derived metric
3377 called non-tide residuals (NTR)⁵², which are related to broad-scale atmospheric

⁵⁰ Results based on gridded rawinsonde observations covering the Northern Hemisphere

⁵¹ Besides the few radiosonde sites located on islands (i.e., Midway or the Azores), most upper-air observations over the vast expanses of the North Pacific and Atlantic are from automated pilot reports (pireps) that measure temperature, wind speed, and barometric pressure onboard commercial aircraft traveling at or near jet stream level (between 200-300 hPa).

⁵² Non-tide residuals are obtained by first removing the known tidal component from the water level variations using a spectral method; then, variations longer than 30 days and shorter than 2.5 days are

3378 circulation patterns across the eastern North Pacific that affect storm track location,
3379 provides a measure of *storminess* variability along the California coast (Bromirski et al.
3380 2003). Average monthly variations in NTR, which are associated with the numbers and
3381 intensities of all ETCs over the eastern North Pacific, did not change substantially over
3382 the period 1858-2000 or over the period covered by most ETC reanalysis studies, 1951-
3383 2000. However, the highest 2% of extreme winter NTR (Fig. 2.20), which are related to
3384 the intensity of the most extreme ETCs, had a significant upward trend since ~1950, with
3385 a pronounced quasi-periodic decadal-scale variability that is relatively consistent over the
3386 last 140 yr. Changes in storm intensity from the mid-1970s to early 1980s are also
3387 suggested by a substantial pressure decreases at an elevation above sea level of about
3388 3000 m over the eastern North Pacific and North America (Graham 1994), indicating that
3389 the pattern of variability of extreme storm conditions observed at San Francisco (as
3390 shown in Fig. 2.20) likely extends over much of the North Pacific basin and the U.S. The
3391 oscillatory pattern of variability is thought to be influenced by teleconnections from the
3392 tropics, predominately during ENSO events (Trenberth and Hurrell 1994), resulting in a
3393 deepened Aleutian low shifted to the east that causes both ETC intensification and a shift
3394 in storm track. It is interesting to note that peaks in the 5-year moving average in Fig.
3395 2.20 generally correspond to peaks in extreme rainfall in Fig. 2.10 suggesting that the
3396 influence of El Niño and broad-scale atmospheric circulation patterns across the Pacific
3397 that affect sea level variability along the West Coast are associated with storm systems
3398 that affect rainfall variability across the U.S..

3399

3400 The amplitude and distribution of ocean wave energy measured by ocean buoys is

removed with a bandpass filter.

3401 determined by ETC intensity and track location. Changes in long period (>12 sec),
3402 intermediate period, and short period (<6 sec) components in the wave-energy spectra
3403 permit inferences regarding the changes over time of the paths of the storms, as well as
3404 their intensities and resulting wave energies (Bromirski et al. 2005). Analysis of the
3405 combination of observations from several buoys in the eastern North Pacific supports a
3406 progressive northward shift of the dominant Pacific storm tracks to the central latitudes
3407 (section 2.2.3.3).

3408

3409 **2.2.3.2.3 Nor'easters**

3410 Those ETCs that develop and propagate along the East Coast of the U.S. and southeast
3411 Canada are often termed colloquially as *Nor'easters*⁵³. In terms of their climatology and
3412 any long-term changes associated with this subclass of ETCs, there are only a handful of
3413 studies in the scientific literature that have analyzed their climatological frequency and
3414 intensity (Jones and Davis 1995), likely due to a lack of any formal objective definition
3415 of this important atmospheric phenomenon (Hirsch et al. 2001).

3416

3417 Because waves generated by ETCs are a function of storm size and the duration and area
3418 over which high winds persist, changes in significant wave heights can also be used as a
3419 proxy for changes in Nor'easters. Using hindcast wave heights and assigning a minimum
3420 criterion of open ocean waves greater than 1.6 m in height (a commonly used threshold
3421 for storms that caused some degree of beach erosion along the mid-Atlantic coast) to
3422 qualify as a nor'easter, the frequency of nor'easters along the Atlantic coast peaked in the

⁵³ According to the *Glossary of Meteorology* (Huschke 1959), a *nor'easter* is any cyclone forming within 167 km of the East Coast between 30^o-40^oN and tracking to the north-northeast

3423 1950's, declined to a minimum in the 1970's, and then increased again to the mid-1980's
3424 (Dolan et al. 1988; Davis et al. 1993).

3425

3426 An alternate approach utilized by Hirsch et al. (2001) uses pressure, direction of
3427 movement and wind speed to identify such systems and generically names them as East
3428 Coast Winter Storms (ECWS)⁵⁴. Hirsch et al. (2001) defined an ECWS as "strong" if the
3429 maximum wind speed is greater than 23.2 m s^{-1} (45 kt). During the period of 1951-1997,
3430 their analysis showed that there were an average of 12 ECWS events occurring each
3431 winter (October-April), with a maximum in January, and an average of 3 strong events
3432 (Fig. 2.21a). They found a general tendency toward weaker systems over the past few
3433 decades, based on a marginally significant (at the 90% confidence level) increase in
3434 average storm minimum pressure (not shown). However, their analysis found no
3435 statistically significant trends in ECWS frequency for all nor'easters identified in their
3436 analysis, for those storms that occurred over the northern portion of the domain ($>35^{\circ}\text{N}$),
3437 or those that traversed full coast (Fig. 2.21b,c) during the 46-year period of record used in
3438 this study.

3439

3440 Because strong storms over the open ocean generate high amplitude waves, buoy
3441 measurements of wave height and wave period can be used to infer characteristics of
3442 ETC variability. The wave power index (WPI) of strong storm-forced wave events

⁵⁴ According to Hirsch et al. (2001), in order to be classified as an ECWS, an area of low pressure is required to (1) have a closed circulation; (2) be located along the east coast of the United States, within the quadrilateral bounded at 45°N by 65° and 70°W and at 30°N by 75° and 85°W ; (3) show general movement from the south-southwest to the north-northeast; and (4) contain winds greater than 10.3 m s^{-1} (20 kt) during at least one 6-h period.

3443 (significant wave heights > 3 m) measured at deep-water open-ocean NOAA buoys
3444 44004, 41001, 41002 along the U.S. Atlantic coast (see Figure 2.25 for locations) during
3445 winter months (October-March, excluding tropical cyclone wave events) shows a
3446 decreasing trend that is significant at the $p=0.05$ level amounting to a decrease in ETC-
3447 forced wave power of about 1%/yr (Bromirski 2007). Coupled with no statistically
3448 significant change in either mean wave height or the number of measurements exceeding
3449 3 m (implying no change in storm duration and/or the number of strong storms), the
3450 downward trend in the WPI suggests that winter ETC intensity has decreased since 1980,
3451 in general agreement with Hirsch et al. (2001).

3452

3453 **BOX 2.2: Extreme Coastal Storm Impacts: “The Perfect Storm” as a True**

3454 **Nor’easter:** From a coastal impacts perspective, damage is greatest when large storms
3455 are propagating *towards* the coast, which generally results in both a larger storm surge
3456 and more long period wave energy (resulting in greater run-up causing more
3457 beach/coastal erosion/damage). Storm intensity (winds) is usually greatest in the right-
3458 front quadrant of the storm (based on the cyclone’s forward movement), so the typical
3459 track of east coast winter storms propagating parallel to the coast leaves the most intense
3460 part of the storm out to sea. In contrast to storms propagating parallel to the coast,
3461 Nor’easters (such as “the Perfect Storm”) that propagate from east-to-west in a retrograde
3462 track at some point in their lifetime (Fig. 2.22) can generate much greater surge and
3463 greater long period wave energy, and also potentially have the most intense associated
3464 winds making landfall along the coast.

3465

3466 2.2.3.3 Coastal Waves: Trends of Increasing Heights and Their Extremes

3467 The high wind speeds of hurricanes and extratropical cyclones over bodies of water cause
3468 extremes in the heights and energies of the waves they generate. Seasonal and long-term changes
3469 in storm intensities and their tracks produce corresponding variations in wave heights and
3470 periods along coasts, defining their wave climates. Waves generated by extratropical storms
3471 dominate the oceans at higher latitudes, including the Northeast Pacific along the shores of
3472 Canada and the west coast of the United States, and along the Atlantic coast of North America
3473 where they originate from destructive Nor'easters. Tropical cyclones dominate the wave climates
3474 at lower latitudes during the warm season (June-September), including the southeast Atlantic
3475 coast of the United States, Gulf of Mexico, and the Caribbean, while hurricanes in the East
3476 Pacific generate waves along the western shores of Mexico and Central America . The
3477 magnitude of associated damage from storm waves depends to a large extent on whether the
3478 storms make landfall, when storm surge, high winds, and heavy rainfall combined with high
3479 waves cause severe impacts. However, high waves from strong tropical cyclones that reach
3480 hurricane strength and then track northward along the East Coast as they weaken, can combine
3481 with extratropical systems, such as the 1991 Halloween Storm (Bromirski 2001; Chapter 2, Box
3482 2.2), and cause severe coastal erosion and have significant economic impacts (Davis et al. 1993;
3483 Dolan et al. 1988; Mather et al. 1967).

3484

3485 2.2.3.3.1 The Waves of Extratropical Storms and Hurricanes

3486 The heights and periods of waves generated by a storm depend on the speed of its winds, the area
3487 over which the winds blow (the storm's fetch), and on the duration of the storm, factors that
3488 determine the amount of energy transferred to the waves. Wave climate variability has been

3489 estimated from: (1) direct measurements by buoys; (2) visual observations from ships; (3) wave
3490 hindcast analyses where wave heights and periods are assessed using forecast models that are run
3491 retrospectively using observed meteorological data; and (4) in recent years from satellite
3492 altimetry. The reliability of the wave records ranges widely for these different sources, and
3493 changes in data-collection methodologies and processing techniques can affect the data
3494 consistency. However, long records from these sources make it possible to identify long-term
3495 trends, and to investigate underlying climate controls.

3496

3497 In the Northern Hemisphere the hurricane winds are strongest on the right-hand side of the storm
3498 relative to its track, where its cyclonic winds coincide with the direction of the storm's
3499 propagation, in turn producing the highest waves on that side of the storm. They achieve their
3500 greatest heights in proximity to the wall of the storm's eye where the winds reach their
3501 maximum, and systematically decrease outward as the wind speeds are reduced. Extreme heights
3502 are closely associated with the Saffir-Simpson hurricane classification system, where the central
3503 atmospheric pressures are lower and the associated wind speeds are higher for the higher
3504 hurricane categories. A correlation between the measured wave heights and the central
3505 atmospheric pressure (Hsu et al. 2000) allows the magnitude of the significant wave height⁵⁵,
3506 H_s , to be related to the hurricane categories⁵⁶. Estimates of the maximum H_s generated close to
3507 the wall of the hurricane's eye on the storm's leading right quadrant where the wind speeds are
3508 greatest, range from 6 to 7 m for Category 1 storms to about 20 m and greater for Category 5
3509 storms. The decrease in observed H_s outward from the hurricane's eye in response to the

⁵⁵ The "significant wave height" is a commonly used statistical measure for the waves generated by a storm, defined as the average of the highest one-third of the measured wave heights

⁵⁶ Hsu et al. (2000) have developed the empirical formula $H_{smax}=0.2(P_n-P_c)$ where P_c and $P_n \sim 1013$ mbar are respectively the atmospheric pressures at the center and edge of the tropical cyclone, and H_{smax} is the maximum value of the significant wave height

3510 outward decrease in wind speeds, demonstrates that H_S is reduced by 50% at approximately a
3511 distance of 5 times the radius of the eye, typically occurring about 250 km outward from the
3512 storm's center (Hsu, et al. 2000).

3513

3514 The impression has been, however, that such models under-predict the highest waves of
3515 Category 4 and 5 storms, and this has led to recent investigations that included the direct
3516 measurement of waves generated by hurricanes. For example, measurements obtained by six
3517 wave gauges deployed by the Naval Research Laboratory (NRL) at depths of 60 to 90 m in the
3518 Gulf of Mexico, when the Category 4 Hurricane Ivan passed directly over the array on 15
3519 September 2004, recorded significant wave heights ranging from 16.1 to 17.9 m; the largest
3520 individual wave height reached 27.7 m (Wang et al. 2005). The simple model of Hsu et al.
3521 (2000) yields a maximum significant wave height of 15.6 m for Ivan's 935-mbar central
3522 pressure, seemingly in agreement with the 16-m measured waves. However, the NRL gauges
3523 were about 30 km outward from the zone of strongest winds and were positioned toward the
3524 forward face of Ivan rather than in its right-hand quadrant, so Wang et al. (2005) concluded it is
3525 likely that the maximum significant wave height was greater than 21 m, with the largest
3526 individual wave heights having been greater than 40 m, indicating that the Hsu et al. (2000)
3527 empirical formula somewhat under predicts the waves generated by high-category hurricanes. On
3528 the other hand, hurricane waves from more complex models that use spatially distributed surface
3529 wind measurements (Tolman et al. 2002) compare well with satellite and buoy observations both
3530 in deep water and in shallow water as hurricanes make landfall (Moon et al. 2003).

3531

3532 Any trend over the years of increasing intensities of hurricanes or of extratropical storms should
3533 on average be reflected in similar upward trends in associated wave heights. Analyses of wave-
3534 buoy data along both the Atlantic and Pacific coasts of the United States document that wave-
3535 height increases have occurred at some locations since the late 1970s.

3536

3537 **2.2.3.3.2 Atlantic Coast Waves**

3538 Two analyses have recently been undertaken of the hourly measurements of the significant wave
3539 heights collected by the buoys of NOAA's National Data Buoy Center (NDBC) along the U.S.
3540 Atlantic shore. These analyses, while differing in some important methodological aspects that
3541 affect some of the results, both show changes in waves generated by hurricanes while the ranges
3542 of wave heights created by extratropical storms appear to have undergone little change.

3543

3544 Komar and Allan (2007a) analyzed the data from three buoys located in deep water to the east of
3545 Cape May, New Jersey, Cape Hatteras, North Carolina, and offshore from Charleston, South
3546 Carolina. These buoys were selected due to their long record lengths and because the sites
3547 represent a range of latitudes where the wave climate is expected to be affected by both tropical
3548 hurricanes and extratropical storms (Nor'easters). Separate analyses were undertaken for the
3549 winter season dominated by extratropical storms and the summer season of hurricanes⁵⁷. There
3550 was not a statistically significant change over the decades in the heights of waves generated by
3551 extratropical storms, but statistically significant increases have occurred for the hurricane-
3552 generated waves. The increases in annual-averaged significant wave heights measured by the

⁵⁷ The hurricane waves were analyzed for the months of July through September, expected to be dominated by tropical cyclones, while the waves of extratropical storms were based on the records from November through March; transitional months such as October were not included, when both types of storms could be expected to be important in wave generation. Also, strict missing data criteria eliminated some years from the analysis.

3553 three Atlantic buoys for the summer hurricane seasons are graphed in Figure 2.23. These annual
3554 averages have included only occurrences when the significant wave heights were greater than 3
3555 m, it having been found that those higher waves can be directly attributed to specific hurricanes,
3556 whereas the lower waves represent the calmer periods between storms. It is seen in Figure 2.23
3557 that there has been a dependence on the latitude, with the highest rate of increase having
3558 occurred in the south; 0.059 m/yr (1.8 m in 30 years) for the Charleston buoy, 0.024 m/yr for the
3559 Hatteras buoy, and 0.017 m/yr for Cape May⁵⁸.

3560

3561 Figure 2.24 provides a comparison of histograms for the numbers of significant wave heights
3562 measured during the hurricane season by the Cape Hatteras buoy, one histogram for data from
3563 early in its record (1977-1990) and the second from 1996-2005, this comparison further
3564 documenting the decadal increase seen in Figure 2.23, especially of the more-extreme waves⁵⁹.
3565 The histogram for the early decade in the wave record shows that the maximum significant wave
3566 height measured was 7.8 m, providing an approximate estimate for the height expected to have a
3567 10-year recurrence interval. From this, we could expect that the 100-year extreme (1%
3568 probability) would have been on the order of 9.5 m significant wave height. In contrast, during
3569 1996-2005 there has been a considerably larger number of occurrences having significant wave
3570 heights greater than 4 m, with the most extreme heights measured ranging up to 10.3 m. The
3571 100-year extreme is now on the order of 12 m, about 3 m higher than in the 1980s. Similar

⁵⁸ The regressions in Figure 2.38 for the Charleston and Cape Hatteras buoy data are statistically significant at the $p=0.05$ level according to the Wilcoxon Test, whereas the value of the trend for the Cape May does not pass that test.

⁵⁹ Traditionally a wave histogram is graphed as the percentages of occurrences, but here the actual numbers of occurrences for the range of wave heights have been plotted, using a log scale that emphasizes the most-extreme heights.

3572 results have been found in analyses of the wave-height histograms for the Cape May and
3573 Charleston buoys (Komar and Allan, 2007a).
3574
3575 This analysis of the three U.S. East Coast buoys (Figures 2.23 and 2.24) demonstrate that there
3576 has been a 30-year increase in wave heights measured during the hurricane season. This increase
3577 could depend on several factors, including changes from year to year in the numbers and
3578 intensities of storms, their tracks that determine whether they traveled northward through the
3579 Atlantic where their generated waves could be recorded by these buoys, and how distant the
3580 hurricanes were from the buoys, whether they passed far offshore within the central Atlantic, or
3581 approached the east coast and possibly made landfall. Analyses by Komar and Allan (2007b)
3582 indicate that all of these factors have been important to the observed wave-height increases, but
3583 the increased hurricane intensities found by Emanuel (2005) based on the measured wind speeds
3584 provide the best explanation for the progressive increase in wave heights seen in Figure 2.23,
3585 since the numbers and tracks of the storms show considerable variability from year to year.
3586
3587 In the second study (Bromirski and Kossin, 2007)⁶⁰, extreme tropical cyclone-associated H_S
3588 events (deep water H_S exceeding 3 m) measured at buoys in both the Atlantic and Gulf regions
3589 (Figure 2.25a) show a general tendency for more significant tropical cyclone-associated wave
3590 events since 1995 (Figure 2.25b), consistent with increasing overall counts of named storms
3591 during recent years [Webster et al. 2005; Klotzbach 2006]. As would be expected, the intense
3592 2005 hurricane season had the highest incidence of significant H_S events over the data record in

⁶⁰ In this study, the entire hurricane season (June-November) was analyzed. Hurricane track data were used to restrict the analysis to time periods when hurricanes were likely the cause of extreme waves, the goal being to minimize the effects of ETCs during the transition months of October and November. Less stringent missing data were applied, resulting in the inclusion of more years than in Komar and Allan (2007).

3593 the Gulf when Hurricanes Katrina, Rita, and Wilma occurred. Since 1978, there were
3594 substantially more significant H_S events along the Atlantic coast than in the Gulf, with almost
3595 three times as many events during September (Figure 2.25c). The monthly distribution along
3596 both coasts peaks in September, with an equally likely chance of a significant tropical cyclone
3597 wave event occurring during October as during August over the 1978-2006 data record. About 3
3598 times as many extreme events occurred in September in the Atlantic compared with the Gulf
3599 from 1978-2006. However, inclusion of all tropical cyclone generated wave events (listed in
3600 <http://www.nhc.noaa.gov/pastall.shtml>) for the entire June through November hurricane season
3601 indicates that there is no significant trend in mean tropical cyclone associated H_S at either the
3602 western North Atlantic or Gulf buoys (Bromirski and Kossin, 2007; Figure 2.25b).

3603

3604 A tropical cyclone wave power index, WPI^{61} , shows an increase in the Atlantic during
3605 the mid-1990s (Bromirski and Kossin, 2007; Figure 2.26), associated with an increase in
3606 the number of significant tropical cyclone forced wave events, that is proportionally
3607 consistent with the increase observed for the tropical cyclone power dissipation index
3608 (PDI, Emanuel 2005]). The Gulf WPI indicates that only the 2005 hurricane season was
3609 exceptional in the Gulf, but is highly correlated with the Atlantic multidecadal oscillation
3610 (AMO, Goldenberg et al. 2001) over the 1980-2006 period. In contrast, the Atlantic WPI
3611 is not well correlated with the AMO, suggesting that tropical sea surface temperature
3612 variability has a greater influence on the characteristics of tropical cyclones that reach the
3613 Gulf.

3614

⁶¹ The WPI for the Atlantic and Gulf regions is obtained as the average of the total wave power for all tropical cyclone associated wave events during the June – November hurricane season at the three southernmost Atlantic buoys and the three Gulf buoys in Figure 2.waves.1a (Bromirski, 2007).

3615 To summarize, these 2 studies both detect changes in tropical cyclone-related waves, but
3616 in different aspects. Komar and Allan (2007a) show statistically significant increases in
3617 extreme wave heights during July-September, while Bromirski and Kossin (2007) do not
3618 find the trends over the entire hurricane season to be statistically significant. However,
3619 Bromirski and Kossin (2007) do find a statistically significant increase in tropical
3620 cyclone-caused wave power, a trend that is attributed to an increase in numbers of events
3621 rather than intensity.

3622

3623 In contrast to the changes in the hurricane waves, analyses of the winter wave heights
3624 generated by extratropical storms and recorded since the mid-1970s by the three buoys
3625 along the central U.S. Atlantic shore have shown little change (Komar and Allan, 2007a).
3626 The records from the Cape Hatteras and Charleston NDBC buoys yield regressions
3627 indicating that they have actually experienced a slight decrease over the decades (-0.005
3628 m/yr), while the Cape May buoy shows a lower rate of reduction (-0.001 m/yr). These
3629 trends are not statistically significant, but may a reflection in the changes in storm tracks
3630 over the decades, with the storms having shifted to the north.

3631

3632 Analyses of the winter waves generated by extratropical storms demonstrate that the highest
3633 measured occurrences are on the order of 10.5-m significant wave heights, with the extreme-
3634 value assessments placing the 100-year event at on the order of 11.5 m, effectively the same as
3635 seen in the histogram of Figure 2.24 for the summer hurricane waves recorded by the Hatteras
3636 buoy during the 1996-2005 decade, so the wave climates of the two seasons are now quite
3637 similar. However, thirty-years ago when these buoys first became operational, the significant

3638 wave heights generated in the summer by hurricanes were much lower than those of the
3639 extratropical storms during the winter; while the heights of hurricane-generated waves have
3640 progressively increased since the 1970s, the wave heights due to extratropical storms have not.
3641

3642 Although minimal change in the heights of waves generated by extratropical storms have been
3643 measured by buoys along the U.S. shore in the Western Atlantic, progressive increases have
3644 occurred in the Northeast Atlantic extending back to at least the 1960s, documented by the Seven
3645 Stones ship-borne wave recorder located in deep water off the southwest coast of England
3646 (Carter and Draper, 1988; Bacon and Carter, 1991). Of interest, the rate of increase (0.022 m/yr)
3647 in the annual averages are closely similar to those measured by buoys along the northwest coast
3648 of the United States in the Pacific Ocean, discussed below.
3649

3650 The documentation by buoys of trends in wave heights in the North Atlantic are limited by
3651 their relatively short records, hindering a determination of the longevity of the identified trends
3652 and the possible presence of any decadal cycles in climate-determined variability. To
3653 supplement the buoy data, visual observations from ships in transit provide longer time series
3654 of estimated ocean wave-heights; although the quality of the data may be questionable, its
3655 availability extends back through the entire 20th century, and in general appears to yield
3656 reasonably consistent trends when compared with the buoy data and with wave hindcasts.
3657 Gulev and Grigorieva (2004) have undertaken detailed analyses of the visual assessments of
3658 wave heights from ships, covering the years 1895-2002 except for a gap in the data during
3659 World War II. The observations for the northeast Atlantic showed a distinct increase in wave
3660 heights after about 1955, corresponding to the wave-sensor measurements since the 1960s

3661 collected southwest of England. Earlier in the 20th century, however, there were distinct cycles
3662 in the visual wave heights observed from ships, with years during which the average wave
3663 heights were some 0.2 m higher than at present. These cycles correlate with the North Atlantic
3664 Oscillation (NAO), with the higher wave heights having been associated with high NAO
3665 indices.

3666

3667 Hindcasts by Wang and Swail (2001) of the wave climates based on the meteorological records
3668 of extratropical storms have been analyzed with respect to changes in the 90th and 99th
3669 percentiles of the significant wave heights, thereby representing the trends for the more
3670 extreme wave conditions. The results indicate a lack of change along the east coast of North
3671 America, in agreement with the buoy data for waves generated by extratropical storms.

3672

3673 **2.2.3.3.3 Pacific Coast Waves**

3674 Analyses of the wave data from NDBC buoys have also been undertaken along the U.S. Pacific
3675 coast, similar to those discussed above for the Atlantic but with the focus having been on the
3676 waves generated by extratropical storms in the Northeast Pacific. The principal investigations of
3677 the trends of changing wave heights and their potential climate controls are those of Allan and
3678 Komar (2000, 2006), who analyzed the records from 6 buoys along the coast from Washington
3679 to south-central California (Point Conception). The analyses were limited to the “winter” waves,
3680 October through the following March, the season with the most intense storms and highest waves.
3681 Trends of increasing wave heights spanning the past 30 years were found, with the greatest rate
3682 of increase having occurred off the coast of Washington where the regression yielded an average
3683 rate of 0.032 m/yr for the winter, with a regular pattern of lesser rates of increase for the latitudes

3684 to the south, such that off the coast of south-central California there has not been a statistically
3685 significant trend⁶².
3686
3687 Analyses of the more extreme wave heights measured off the Washington coast were undertaken
3688 due to their importance to coastal-erosion occurrences (Allan and Komar, 2006). Figure 2.27
3689 contains graphs of the annual averages of the winter wave heights, and the averages of the five
3690 largest significant wave heights measured each winter, the latter showing a higher rate of
3691 increase (0.095 m/yr, a 2.85-m increase in the significant wave heights in 30 years). The full
3692 series of analyses are listed in Table 2.1, demonstrating that there is an orderly progression with
3693 the more extreme the assessment the greater the rate of increase, up to a rate of 0.108 m/yr for
3694 the single highest measured significant wave height each year. While the data in Figure 2.27 for
3695 the averages of the largest five storm-wave occurrences each year are statistically significant at
3696 the $p=0.05$ level, the trends for the more extreme waves do not meet this criterion (Table 2.1).
3697 However, for applications to engineering design of coastal structures and in coastal management
3698 assessments of hazards, these extremes for the measured wave heights are of greatest relevance,
3699 and therefore are sometimes used in applications as is the trend for the assessment of the 100-
3700 year projected extreme, which has increased at a still greater rate over the decades, from about 11
3701 m in 1975 to 16 m at present. This use in applications is further supported by the fact that much
3702 of the scatter in the diagrams, as seen in Figure 2.27, can be accounted for by considering the
3703 range of climate events from El Niños to La Niñas (Allan and Komar, 2000, 2006).
3704

⁶² Where trends of increasing wave heights do exist, they have again been verified by application of the Wilcoxon test, a statistical analysis that basically compares the first half the record with the second half to establish that there has been a meaningful change.

3705 The intensities of North Pacific extratropical storms and their associated tracks are strongly
3706 affected by the depth and position of the Aleutian Low, which tends to intensify and shift
3707 southward and eastward during strong El Nino events (Mo and Livezey, 1986). This southward
3708 shift results in increased occurrences of extreme waves throughout the eastern North Pacific,
3709 particularly along the south-central California coast (Seymour et al. 1984; Allan and Komar
3710 2000, 2006; Bromirski et al. 2005). Correlations between the measured wave heights and the
3711 Multivariate ENSO Index show that increased wave heights occur at all latitudes along the U.S.
3712 Pacific coast during major El Niños, but with the greatest increases along the shore of southern
3713 California (Allan and Komar, 2006). Along the coast of California where the trends of decadal
3714 increases are small to non-existent, it is this cycle between El Niños and La Niñas that exerts the
3715 primary climate control on the storm-wave heights and their extremes (and also on the monthly-
3716 mean winter water levels, which are elevated by 20 to 50 cm during a major El Niño above the
3717 long-term mean sea levels).

3718

3719 The documentation of increasing wave heights in the North Pacific is given limited by the
3720 relatively short records from buoys, extending back only to the 1970s. Similar to discussed for
3721 the Atlantic, visual observations from ships in transit provide longer time series of ocean wave
3722 height estimates, but of questionable quality. Gulev and Grigorieva (2004) examined this source
3723 of wave data for the North Pacific, finding that there has been a general increase in the
3724 significant wave heights throughout the 20th century, with a rapid increase from 1900 to about
3725 1925, and a leveling off from 1925 to about 1950-60 but with an apparent maximum during the
3726 1940s (there being a gap in the data during World War II). There was a renewed increase
3727 beginning in about 1960, corresponding to that documented by the wave buoy measurements

3728 (Fig. 2.27). The wave hindcasts⁶³ by Wang and Swail (2001), representing the more extreme
3729 significant wave-height occurrences (the 90th and 99th percentiles), largely also confirm the
3730 general increase in wave heights throughout the central to eastern North Pacific.

3731

3732 There is the potential for the use of proxy evidence to examine the changes in wave heights
3733 back beyond that provided by the wave data, the proxy having the clearest potential being
3734 measurements by seismometers installed to monitor earthquake activity. During the “quiet”
3735 intervals between earthquakes it has been noted that there is a consistent level of "noise" in the
3736 recorded ground motions, termed "microseisms". It has been shown that much of this energy is
3737 derived from surf on the coast, with the microseisms increasing at times of storms. Analyses
3738 have been undertaken by Bromirski et al. (1999) correlating buoy measurements of ocean
3739 waves along the coast of central California and the microseisms measured by the seismometer
3740 at the University of California, Berkeley. The results of that study yielded a calibration
3741 between the ocean wave heights and the microseism energy, demonstrating the potential use of
3742 the archived seismic data that dates back to 1930, to investigate changes in the U.S. West Coast
3743 wave climate.

3744

3745 **2.2.3.4 Winter Storms**

3746 **2.2.3.4.1 Snowstorms**

3747 The amount of snow that causes serious impacts varies depending on a given location's
3748 usual snow conditions. A snowstorm is defined here as an event in which more than 15
3749 cm of snow falls in 24 hours or less at some location in the U.S. This is an amount

⁶³ Hindcasts are model estimates of waves using forecast models that are run retrospectively using observed meteorological data

3750 sufficient to cause societally-important impacts in most locations. During the 1901-2001
3751 period, 2,257 snowstorms occurred (Changnon et al. 2006). Temporal assessment of the
3752 snowstorm incidences during 1901-2000 revealed major regional differences.
3753 Comparison of the storm occurrences in 1901-1950 against those in 1951-2000 revealed
3754 that much of the eastern U.S. had more storms in the early half of the 20th Century,
3755 whereas in the West and New England, the last half of the century had more storms.
3756 Nationally, 53% of the weather stations had their peaks in 1901-1950 and 47% peaked in
3757 1951-2000.
3758
3759 The South and lower Midwest had distinct statistically significant downward trends in
3760 snowstorm frequency from 1901 to 2000. In direct contrast, the Northeast and upper
3761 Midwest had statistically significant upward linear trends. These contrasting regional
3762 trends suggest a northward shift in snowstorm occurrence. Nationally, the regionally
3763 varying up and down trends resulted in a national storm trend that was slightly upward
3764 for 1901-2000, but not statistically significant. The long-term increases in the upper
3765 Midwest and Northeast occurred where snowstorms are most frequent, and thus had an
3766 influence on the upward trend in national snowstorm activity. Research has shown that
3767 cyclonic activity was low during 1931-1950, a period of few snowstorms in the U.S.
3768
3769 Nationally, 39 of 231 stations with long-term records had their lowest frequencies of
3770 storms during 1931-1940, whereas 29 others had their peak of incidences then. The
3771 second ranked decade with numerous stations having low snowstorm frequencies was
3772 1981-1990. Very few low storm occurrences were found during 1911-1920 and in the

3773 1961-1980 period, times when storms were quite frequent. The 1911-1920 decade had the
3774 greatest number of high station values with 38 stations. The fewest peak values occurred
3775 in the next decade, 1921-1930. Comparison of the decades of high and low frequencies of
3776 snowstorms reveals, as expected, an inverse relationship. That is, when many high storm
3777 values occurred, there are few low storm frequencies.

3778

3779 Generally, the decades with high snowstorm frequencies were characterized by cold
3780 winters. The three highest decades for snowstorms (1911-1920, 1961-1970, and 1971-
3781 1980) were ranked 1st, 4th, and 3rd coldest, respectively while the two lowest decades
3782 (1921-1930 and 1931-1940) were ranked as 3rd and 4th warmest. One exception to this
3783 general relationship is the warmest decade (1991-2000), which experienced a moderately
3784 high number of snowstorms.

3785

3786 Very snowy seasons (those with seasonal snowfall totals exceeding the 90th percentile
3787 threshold) were infrequent in the 1920s and 1930s and have also been rare since the mid-
3788 1980s (Kunkel et al. 2007b). There is a high correlation with average winter temperature.
3789 Warm winters tend to have few stations with high snowfall totals and most of the snowy
3790 seasons have also been cold.

3791

3792 Some of the snowiest regions in North America are the southern and eastern shores of the
3793 Great Lakes where cold northwesterly winds flowing over the warmer lakes pick up
3794 moisture and deposit on the shoreline areas. There is evidence of upward trends in
3795 snowfall since 1951 in these regions even while locations away from the snowy shoreline

3796 areas have not experienced increases (Burnett et al. 2003). An analysis of historical heavy
3797 lake-effect snowstorms identified several weather conditions to be closely related to
3798 heavy lake-effect snowstorm occurrence including moderately high surface wind speed,
3799 wind direction promoting a long fetch over the lakes, surface air temperature in the range
3800 of -10 to 0°C, lake surface to air temperature difference of at least 7°C, and an unstable
3801 lower troposphere (Kunkel et al. 2002). It is also necessary that the lakes be mostly ice-
3802 free.

3803

3804 Snow cover extent for North America based on satellite data (Robinson et al. 1993)
3805 abruptly decreased in the mid-1980s and generally has remained low since then
3806 ([http://climate.rutgers.edu/snowcover/chart_anom.php?ui_set=0&ui_region=nam&ui_mo](http://climate.rutgers.edu/snowcover/chart_anom.php?ui_set=0&ui_region=nam&ui_month=6)
3807 [nth=6](http://climate.rutgers.edu/snowcover/chart_anom.php?ui_set=0&ui_region=nam&ui_month=6)).

3808

3809 **2.2.3.4.2 Ice Storms**

3810 Freezing rain is a phenomenon where even light amounts can have substantial impacts.
3811 All days with freezing rain (ZR) were determined during the 1948-2000 period based on
3812 data from 988 stations across the U.S. (Changnon and Karl 2003). The national frequency
3813 of freezing rain days (FZRA) exhibited a downward trend, being higher during 1948-
3814 1964 than in any subsequent period.

3815

3816 The temporal distributions of FZRA for three climate regions (Northeast, Southeast, and
3817 South) reveal substantial variability. They all were high in 1977-1980, low in 1985-1988,
3818 and lowest in 1973-1976. The 52-year linear trends for all three regions were downward

3819 over time. The time distributions for the Central, West North Central, and East North
3820 Central regions are alike, all showing that high values occurred early, 1949-1956. All
3821 climate regions had their lowest FZRA during 1965-1976. The East north central,
3822 Central, Northwest, and Northeast regions, which embrace the northern half of the
3823 conterminous U.S., all had statistically significant downward linear trends. This is in
3824 contrast to trends in snowstorm incidences.

3825

3826 Both snowstorms and ice storms are often accompanied or followed by extreme cold
3827 because a strong ETC (which is the meteorological cause of the snow and ice) is one of
3828 the meteorological components of the flow of extreme cold air from the Arctic. This
3829 compounds the impacts of such events in a variety of ways, including increasing the risks
3830 to human health and adversely affecting the working environment for snow removal and
3831 repair activities. While there have been no systematic studies of trends in such compound
3832 events, observed variations in these events appear to be correlated. For example, the late
3833 1970s were characterized both by a high frequency of extreme cold (Kunkel et al. 1999)
3834 and a high frequency of high snowfall years (Kunkel et al. 2007b).

3835

3836 **2.2.3.5 Convective Storms**

3837 Thunderstorms in the United States are defined to be severe by the National Weather
3838 Service (NWS) if they produce hail of at least 1.9 cm (3/4 inch) in diameter, wind gusts
3839 of at least 25.5 m s^{-1} (50 kt) or a tornado. Currently, reports come from a variety of
3840 sources to the local NWS forecast offices that produce a final listing of events for their
3841 area. Over the years, procedures and efforts to produce that listing have changed. Official

3842 data collection in near real-time began in 1953 for tornadoes and 1955 for hail and wind.
3843 Prior to 1973, tornado reports were verified by state climatologists (Changnon 1982). In
3844 addition, efforts to improve verification of severe thunderstorm and tornado warnings, the
3845 introduction of Doppler radars, changes in population, and increases in public awareness,
3846 have led to increases in reports over the years. Changes in reporting practices have also
3847 led to inconsistencies in many aspects of the records (e.g., Brooks 2004). Changnon and
3848 Changnon (2000) identified regional changes in hail frequency from reports made at
3849 official surface observing sites. With the change to automated surface observing sites in
3850 the 1990s, the number of hail reports at those locations dropped dramatically because of
3851 the loss of human observers at the sites. As a result, comparisons to the Changnon and
3852 Changnon work cannot be continued, although Changnon et al. (2001) have attempted to
3853 use insurance loss records as a proxy for hail occurrence.

3854

3855 The raw reports of annual tornado occurrences show an approximately doubling from
3856 1954-2003 (Brooks and Dotzek 2007), a reflection of the changes in observing and
3857 reporting. When detrended to remove this artificial trend, the data show large interannual
3858 variability, but a persistent minimum in the late 1980s (Fig. 2.28). There were changes in
3859 assigning intensity estimates in the mid-1970s that resulted in tornadoes prior to 1975
3860 being rated more strongly than those in the later part of the record (Verbout et al. 2006).
3861 More recently, there have been no tornadoes rated F5, the highest rating, since 3 May
3862 1999, the longest gap on record. Coupled with a large decrease in the number of F4
3863 tornadoes (McCarthy et al. 2006), it has been suggested that the strongest tornadoes are
3864 now being rated lower than practice prior to 2000.

3865

3866 A dataset of F2 and stronger tornadoes extending back before the official record
3867 (Grazulis 1993) provides an opportunity to examine longer trends. This examination⁶⁴ of
3868 the record from 1921-1995 indicates that the variability between periods was large,
3869 without significant long-term trends (Concannon et al. 2000).

3870

3871 The fraction of strong tornadoes (F2 and greater) that have been rated as violent (F4 and
3872 greater) has been relatively consistent in the US from the 1950s through the 1990s⁶⁵
3873 (Brooks and Doswell 2001)⁶⁶. There were no significant changes in the high-intensity
3874 end of these distributions from 1950s through the 1990s, although the distribution from
3875 2000 and later may differ.

3876

3877 Nontornadic reports have increased even more rapidly than tornadic reports (Doswell et
3878 al. 2005, 2006). Over the period 1955-2004, this increase was approximately exponential,
3879 resulting in an almost 20-fold increase over the period. The increase is mostly in
3880 marginally severe thunderstorm reports (Brooks 2007). An overall increase is seen, but the
3881 distribution by intensity is similar in the 1970s and post-2000 eras for the strongest 10%
3882 of reports of hail and wind. Thus, there is no evidence for a change in the severity of
3883 events, and the large changes in the overall number of reports make it impossible to
3884 detect if meteorological changes have occurred.

⁶⁴ This analysis used the technique described in Brooks et al. (2003a) to estimate the spatial distribution over different periods

⁶⁵ Note that consistent overrating will not change this ratio.

⁶⁶ Feuerstein et al. (2005) showed that the distribution in the US and other countries could be fit to Weibull distributions with the parameters in the distribution converging as time goes along, which they associated with more complete reporting of events.

3885
3886 Environmental conditions that are most likely associated with severe and tornadic
3887 thunderstorms have been derived from reanalysis data (Brooks et al. 2003b) and counts of
3888 the frequency of favorable environments for significant severe thunderstorms⁶⁷ have been
3889 determined for the area east of the Rocky Mountains in the US for the period 1958-1999
3890 (Brooks and Dotzek 2007). The count of favorable environments decreased from the late
3891 1950s into the early 1970s and increased after that through the 1990s, so that the
3892 frequency was approximately the same at both ends of the analyzed period. Given the
3893 high values seen at the beginning of the reanalysis era, it is likely that the record is long
3894 enough to sample natural variability, so that it is possible that even though the 1973-1999
3895 increase is statistically significant, it does not represent a departure from natural
3896 variability. The time series of the count of reports of very large hail (7 cm diameter and
3897 larger) shows an inflection at about the same time as the inflection in the counts of
3898 favorable environments. A comparison of the rate of increase of the two series suggested
3899 that the change in environments could account for approximately 7% of the change in
3900 reports from the mid-1970s through 1999, with the rest coming from non-meteorological
3901 sources. Changes in tornado reports do not correspond to the changes in overall favorable
3902 severe thunderstorm environment, in part because the discrimination of tornadic
3903 environments in the reanalysis data is not as good as the discrimination of severe
3904 thunderstorm environments (Brooks et al. 2003a).

3905

3906

3907

⁶⁷ Hail of at least 5 cm diameter, wind gusts of at least 33 m s⁻¹, and/or a tornado of F2 or greater intensity

3908 BOX 2.3: Changes in Modes of Variability

3909 The atmosphere-ocean system has a wide variety of circulation patterns, or modes, of
3910 climate variability that pulse on time scales ranging from days, to many decades, or
3911 longer. For example, the well-known winter weather pattern of a storm followed by clear
3912 skies and then another storm a week later is, part of an atmospheric wave (wind) pattern
3913 that circles the Earth. As these waves move over the ocean, heat from the ocean is given
3914 up to the air, which impacts both the intensity and the movement of the atmospheric
3915 waves (weather) as well as ocean circulations. Weather and climate extremes are often
3916 linked to one or more of these modes of climate variability, and following is a brief
3917 description of the most important circulation regimes. However, it is important to keep in
3918 mind that these modes of variability are not independent of each other.

3919

3920 *El Niño-Southern Oscillation (ENSO)*

3921 The ENSO phenomenon is the result of coupled ocean-atmosphere dynamics and is the
3922 largest source of interannual variability in global weather and climate. It is characterized
3923 by changes in eastern equatorial Pacific sea surface temperature (SST) and surface air
3924 pressure in the tropical Pacific region. Warm (cold) eastern Pacific SST anomalies are
3925 associated with El Niño (La Niña) events. El Niños occur at irregular intervals of
3926 approximately 2 to 7 years, and generally persists for 12 to 18 months. The Southern
3927 Oscillation component of ENSO is defined by air pressure differences between the
3928 eastern and western tropical Pacific (typically between Darwin and Tahiti) and is
3929 characterized by changes in tropical atmospheric flow patterns which are caused by and
3930 can enhance tropical Pacific SST variations. These tropical atmospheric circulation

3931 changes can alter both the intensity and tracks of North American storms. For example,
3932 El Niño is often associated with heavy winter rains in southern California.

3933

3934 The nature of ENSO has varied considerably through time. Strong ENSO events occurred
3935 with regularity from the late 19th Century through 1925 and again after 1950. Between
3936 1976 and 1977 rapid warming occurred in the Tropical Pacific with concurrent cooling in
3937 the Central Pacific that has been termed the climate shift of 1976/1977 (Trenberth 1990,
3938 Miller et al. 1994). The shift has been associated with increased El Niño activity, changes
3939 in storm tracks, increased storm intensity and is at the start of the period of rapid
3940 warming in global temperatures, and the 1997-1998 El Niño was the strongest on record.

3941

3942 *The North Atlantic Oscillation (NAO)*

3943 The NAO is the most important mode of winter climate variability in the North Atlantic
3944 region and is measured by an index that is based on air pressure differences between
3945 Iceland/Greenland and the Azores in the north Atlantic. As Figure 2.29 illustrates, high
3946 values of the NAO index are associated with intensified westerly winds around the arctic.
3947 Changes in the strength and location of the westerlies produce characteristic shifts in
3948 temperature, rainfall, and winds. Low NAO values correspond with cold extremes in
3949 central North America and high NAO index values increase the chances of warm winter
3950 extremes. Proxy and instrumental data show evidence for intervals of decadal and longer
3951 positive and negative NAO index in the last few centuries (Cook et al., 2002; Jones et al.,
3952 2003). A reversal occurred from minimum winter index values in the late 1960s to

3953 strongly positive NAO index values in the mid-1990s but since have declined to near the
3954 long-term mean.

3955

3956 *Atlantic Multidecadal Oscillation (AMO)*

3957 The Atlantic Ocean meridional overturning circulation carries warm salty surface waters
3958 into far-northern latitudes around Greenland where it cools, sinks, and returns cold deep
3959 waters southward across the equator. An oscillating pattern of SSTs in the northern
3960 Atlantic that is related to this overturning circulation, called the Atlantic Multidecadal
3961 Oscillation (AMO), has been identified by a number of researchers (Delworth and Mann,
3962 2000; Folland *et al.*, 1986; Mann and Park, 1994). The AMO is commonly identified by
3963 subtracting a linear trend from a time series of the North Atlantic SST. This trend
3964 subtraction is intended to remove, or at least reduce, the influence of greenhouse-gas
3965 induced global warming from the AMO so that the bulk of the variability in the
3966 remainder is due to natural causes. The warm phase, the decades when the temperature is
3967 above the trend line, is associated with increased Atlantic hurricane activity, and the cool
3968 phase is associated with reduced Atlantic hurricane activity. Instrumental data has been
3969 used to identify warm phases roughly between 1860-1880, 1930-1960, and one beginning
3970 in the mid-1990s which continues to present. Cool phases were present during 1905-1925
3971 and 1970-1990 (Schlesinger and Ramankutty, 1994).

3972

3973 Some scientists, however, question the validity of subtracting a linear trend from a time
3974 series created by non-linear forcings and wonder if the AMO as commonly calculated is
3975 primarily an artifact of this creation process rather than a real change in the ocean

3976 circulation. Some suggest that subtracting the global SST time series from the North
3977 Atlantic SST time series removes a global climate change signal better than subtracting a
3978 linear trend and produces a very different historical AMO record (Trenberth and Shea,
3979 2006). Proxy and modeling studies have identified an AMO-like signal and found that
3980 multidecadal eras in hurricane activity in the North Atlantic are correlated with the AMO
3981 (Bell and Chelliah, 2006). No matter how it is calculated, the AMO has such a long
3982 period that the observational SST data only records about 1.5 cycles which makes it
3983 difficult to determine whether the AMO is truly a natural oscillation or caused in whole
3984 or at least in part by greenhouse-gas induced climate change.

3985

3986 *Pacific Decadal Oscillation (PDO)*

3987 The Pacific Decadal Oscillation (PDO) is a multidecadal pattern of monthly SST
3988 anomalies in the North Pacific Ocean poleward of 20°N. Two full PDO cycles occurred
3989 through the twentieth century with each phase persisting for 20 to 30 years. The typical
3990 spatial pattern of the “warm” phase of the PDO has negative SST anomalies in the central
3991 and eastern North Pacific and positive SST anomalies along the coast of North America.
3992 Sea level pressure (SLP) anomalies during the warm phase tend to have a basin-scale low
3993 centered over the Aleutian Islands and high sea-level pressure over western North
3994 America. The cool phase of the PDO has SST and SLP patterns that are essentially the
3995 opposite of the warm phase. Because the PDO influences various weather systems it can
3996 affect the chances of, for example, winter temperatures cold enough to cause mountain
3997 pine beetle mortality in British Columbia (Stahl *et al.*, 2006). When an El Niño event
3998 occurs during a warm phase of the PDO, the characteristic El Niño-related temperature

3999 and precipitation anomalies in North America tend to be accentuated. The PDO had
4000 extended periods of negative values indicative of weakened circulation from 1900 to
4001 1924 and 1947 to 1976, and positive values indicative of strengthened circulation from
4002 1925 to 1946 and 1977 to 2005. The 1976-1977 climate shift in the Pacific described
4003 above was associated with a phase change in the PDO from negative to positive
4004 (Trenberth et al., 2002; Deser et al., 2004).

4005

4006 *Pacific North American Pattern (PNA)*

4007 The PNA can be defined as a secondary pattern in the variability of monthly atmospheric
4008 pressure anomalies for the latitude range 20-90°N. When the PNA is positive, the mid-
4009 tropospheric winds over North America and the North Pacific have a strong meridional
4010 (north-south) wave pattern while the negative PNA has more zonal (west to east) flow.
4011 Strong wave patterns tend to bring extreme weather; whether the extremes are warm,
4012 cold, wet or dry at a particular location depends on the shape of the wave. A positive
4013 PNA is associated with El Niños and negative PNA is associated with La Niña.

4014

4015 *The Madden-Julian Oscillation (MJO)*

4016 The atmospheric response to convection on the equator, which heats the atmosphere, is
4017 the creation of circulation cells, which then move eastward. These cells have a period of
4018 about 50 days and either enhance tropical convection or help suppress it. Referred to as
4019 the Madden-Julian Oscillation (MJO), after the two scientists who discovered it (Madden
4020 and Julian, 1971 and 1972), it is the dominant source of tropical atmospheric variability
4021 on intraseasonal time scales. The MJO is related to North American extremes through its

4022 influence on the dynamics of tropical cyclone formation (Hartmann and Maloney, 2001;
4023 Maloney and Hartmann, 2000a; 2000b, 2001) as well as western North American winter
4024 rainfall variability. The MJO can enhance or suppress either depending on which part of
4025 the circulation cell is active in the region.

4026

4027 As the climate changes, some of the atmospheric circulation patterns or modes of
4028 atmospheric variability described above have changed as well. However, only one
4029 circulation pattern, the MJO, would not be expected to have long-term changes since it is
4030 a localized circulation response to convection on the equator.

4031

4032 **2.3 Key Uncertainties Related to Measuring Specific Variations and Change**

4033 In this section we review the statistical methods that have been used to assess
4034 uncertainties in studies of changing extremes. The focus of the discussion is on
4035 precipitation events, though similar methods have also been used for temperature.

4036

4037 **2.3.1 Methods Based on Counting Exceedances Over a High Threshold**

4038 Most existing methods follow some variant of the following procedure, given by Kunkel
4039 et al. (1999). First, daily data are collected, corrected for biases such as winter
4040 undercatchment. Only stations with nearly complete data are used (typically, “nearly
4041 complete” means no more than 5% missing values). Different event durations (for
4042 example, 1-day or 7-day) and different return periods (such as 1 year or 5 years) are
4043 considered. For each station, a threshold is determined according to the desired return
4044 value – for example, with 100 years of data and a 5-year return value, the threshold is the

4045 20th largest event. The number of exceedances of the threshold is computed for each year,
4046 and then averaged either regionally or nationally. The averaging is a weighted average in
4047 which, first, simple averaging is used over climate divisions (typically there are about 7
4048 climate divisions in each state), and then, an area-weighted average is computed over
4049 climate divisions, either for one of the nine U.S. climate regions or the whole contiguous
4050 U.S. This averaging method ensures that parts of the country with relatively sparse data
4051 coverage are adequately represented in the final average. Sometimes (e.g. Groisman et al.
4052 2005, Kunkel et al. 2007a) the climate divisions are replaced by 1° by 1° grid cells. Two
4053 additional refinements used by Groisman et al. (2005) are (i) to replace the raw
4054 exceedance counts for each year by anomalies from a 30-year reference period, computed
4055 separately for each station, (ii) to assess the standard error of the regional average using
4056 spatial statistics techniques. This calculation is based on an exponentially decreasing
4057 spatial covariance function with a range of the order 100-500 km. and a nugget:sill ratio
4058 (the proportion of the variability that is not spatially correlated) between 0 and 85%,
4059 depending on the region, season and threshold.

4060

4061 Once these spatially averaged annual exceedance counts or anomalies are computed, the
4062 next step is to compute trends. In most studies, the emphasis is on linear trends computed
4063 either by least squares regression or by the Kendall slope method, in which the trend is
4064 estimated as the median of all possible slopes computed from pairs of data points. The
4065 standard errors of the trends should theoretically be corrected for autocorrelation, but in
4066 the case of extreme events the autocorrelation is usually negligible (Groisman et al.,
4067 2004).

4068

4069 One of the concerns about this methodology is the effect of changing spatial coverage of
4070 the data set, especially for comparisons that go back to the late years of the 19th century.
4071 Kunkel et al. (2007a) generated simulations of the 1895-2004 data record by first
4072 randomly sampling complete years of data from a modern network of 6351 stations for
4073 1971-2000, projecting to a random subnetwork equivalent in size and spatial extent to the
4074 historical data network, then using repeat simulations to calculate means and 95%
4075 confidence intervals for five 22-year periods. The confidence intervals were then
4076 superimposed on the actual 22-year means calculated from the observational data record.
4077 The results for 1-year, 5-year and 20-year return values show clearly that the most recent
4078 period (1983-2004) has the highest return values of the five periods, but they also show
4079 the second highest return values in 1895-1916 with a sharp drop thereafter, implying a
4080 still not fully explained role due to natural variability.

4081

4082 Some issues that might justify further research include the following:

- 4083 1. Further exploration of why extreme precipitation apparently decreases
4084 after the 1895-1916 period before the recent (post-1983) rise when they exceeded
4085 that level. For example, if one breaks the data down into finer resolution spatially,
4086 does one still see the same effect?
- 4087 2. What about the effect of large-scale circulation effects such as ENSO
4088 events, AMO, PDO, etc? These could potentially be included as covariates in a
4089 time series regression analysis, thus allowing one to “correct” for circulation
4090 effects in measuring the trend.

4091 3. The spatial analyses of Groisman et al. (2005) allow for spatial correlation
4092 in assessing the significance of trends, but they don't do the logical next step,
4093 which is to use the covariance function to construct optimal interpolations (also
4094 known as kriging) and thereby produce more detailed spatial maps. This is
4095 something that might be explored in the future.

4096

4097 **2.3.2 The GEV Approach**

4098 An alternative approach to extreme value assessment is through the Generalized Extreme
4099 Value (GEV) distribution⁶⁸, and its variants. The GEV combines together three “types”
4100 of extreme value distributions that in earlier treatments were often regarded as separate
4101 families (e.g. Gumbel 1958). The distribution is most frequently applied to the annual
4102 maxima of a meteorological or hydrological variable, though it can also be applied to
4103 maxima over other time periods (e.g. one month or one season). With minor changes in
4104 notation, the distributions are also applicable to minima rather than maxima. The
4105 parameters may be estimated by maximum likelihood, though there are also a number of
4106 more specialized techniques such as L-moments estimation. The methods have been
4107 applied in climate researches by a number of authors including Kharin and Zwiers
4108 (2000), Wehner (2004,2005), Kharin et al. (2007).

4109

⁶⁸ The basic GEV distribution is given by the formula (see, e.g. Zwiers and Kharin (1998))
 $F(x) = \exp\{-[1-k(x-\zeta)/\alpha]^{1/k}\}$ in which ζ plays the role of a centering or location constant, α determines the
scale, and k is a key parameter that determines the shape of the distribution. (Other authors have used
different notations, especially for the shape parameter.) The range of the distribution is
 $x < \zeta + \alpha/k$ when $k < 0$, $x > \zeta + \alpha/k$ when $k > 0$, $-\infty < x < \infty$ when $k = 0$, in which case the formula reduces to $F(x) =$
 $\exp\{-\exp[-(x-\zeta)/\alpha]\}$ and is known as the Gumbel distribution.

4110 The potential advantage of GEV methods over those based on counting threshold
4111 exceedances is that by fitting a probability distribution to the extremes, one obtains more
4112 information that is less sensitive to the choice of threshold, and can also derive other
4113 quantities such as the T -year return value X_T , calculated by solving the equation $F(X_T)=1-$
4114 $1/T$. Trends in the T -year return value (for typical values of T , e.g. 1, 10, 25 or 100 years)
4115 would be particularly valuable as indicators of changing extremes in the climate.

4116 Direct application of GEV methods is often inefficient because they only use very sparse
4117 summaries of the data (typically one value per year), and need reasonably long time
4118 series before they are applicable at all. Alternative methods are based on exceedances
4119 over thresholds, not just counting exceedances but also fitting a distribution to the excess
4120 over the threshold. The most common choice of distribution of excess is the Generalized
4121 Pareto distribution or GPD, which is closely related to the GEV (Pickands 1975, Davison
4122 and Smith 1990). Some recent overviews of extreme value distributions, threshold
4123 methods, and a variety of extensions are by Coles (2001) and Smith (2003).

4124

4125 Much of the recent research (e.g. Wehner 2005, Kharin et al. 2007) has used model
4126 output data, using the GEV to estimate for example a 20-year return value at each grid
4127 cell, then plotting spatial maps of the resulting estimates. Corresponding maps based on
4128 observational data must take into account the irregular spatial distribution of weather
4129 stations, but this is also possible using spatial statistics (or “kriging”) methodology. For
4130 example, Cooley et al. (2007) have applied a hierarchical modeling approach to
4131 precipitation data from the Front Range of Colorado, fitting a GPD to threshold
4132 exceedances at each station and combining results from different stations through a

4133 spatial model to compute a map of 25-year return values. Smith et al. (2007) applied
4134 similar methodology to data from the whole contiguous U.S., producing spatial maps of
4135 return values and also calculating changes in return values over the 1970-1999 period.

4136 **Chapter 2 References**

4137

4138 **Acuña-Soto, R., D. W. Stahle, M. K. Cleaveland, and M. D. Therrel, 2002:** Megadrought
4139 and megadeath in 16th century Mexico. *Historical Review*, **8 (4)**, 360-362.

4140

4141 **Aguilar, E., et al. (2005),** Changes in precipitation and temperature extremes in Central
4142 America and northern South America, 1961–2003, *J. Geophys. Res.*, 110,
4143 D23107, doi:10.1029/2005JD006119.

4144

4145 **Alexander, L. V., et al. (2006),** Global observed changes in daily climate extremes of
4146 temperature and precipitation, *J. Geophys. Res.*, 111, D05109,
4147 doi:10.1029/2005JD006290.

4148

4149 **Allan, J. C., and P. D. Komar, 2000:** Are ocean wave heights increasing in the eastern
4150 North Pacific? *EOS, Transaction of the American Geophysical Union*, **47**, 561-
4151 567.

4152

4153 **Allan, J. C. and P. D. Komer, 2006:** Climate controls on US West Coast erosion
4154 processes. *Journal of Coastal Research*, **22**, 511-529.

4155

4156 **Alley, W.M. 1984.** The Palmer Drought Severity Index: Limitations and assumptions.
4157 *Journal of Climate and Applied Meteorology* 23:1100–1109.

4158

4159 **An, S.I., J.S. Kug, A. Timmermann, I.S. Kang, and O. Timm, 2007:** The influence of
4160 ENSO on the generation of decadal variability in the North Pacific. *J. Climate*,
4161 **20**, 667–680.

4162

4163 **Andreadis, K.M., E. A. Clark, A. W. Wood, A. F. Hamlet, and D. P. Lettenmaier, 2005:**
4164 Twentieth-Century drought in the conterminous United States. *Journal of*
4165 *Hydrometeorology*, 6, 985–1001.

4166

4167 **Andreadis, K. M., and D. P. Lettenmaier, 2006:** Trends in 20th century drought over the
4168 continental United States. *Geophysical Research Letters*, 33, L10403,
4169 doi:10.1029/2006GL025711.

4170

4171 **Angel, J.R., and S.A. Isard, 1998:** The frequency and intensity of Great Lake cyclones. *J.*
4172 *Climate*, **11**, 61–71.

4173

4174 **Arguez, A.(ed.), 2007:** State of the Climate in 2006. *Bull. Amer. Meteor. Soc.*, **88**, s1–
4175 s135.

4176

4177 **Assel, R. A., K. Cronk, and D. C. Norton, 2003:** Recent trends in Laurentian Great Lakes
4178 ice cover. *Climatic Change*, 57, 185-204.

4179

- 4180 **Assel, R. A.**, 2003: Great Lakes ice cover, first ice, last ice, and ice duration. NOAA
4181 Technical Memorandum GLERL-125. NOAA, Great Lakes Environmental
4182 Research Laboratory, Ann Arbor, MI, 49 pp.
4183
- 4184 **Assel, R. A.** Great Lakes ice cover climatology update: Winters 2003, 2004, and 2005.
4185 NOAA Technical Memorandum GLERL-135, 2005a: NOAA, Great Lakes
4186 Environmental Research Laboratory, Ann Arbor, MI, 21 pp.
4187
- 4188 **Assel, R. A.**, 2005b: Classification of annual Great Lakes ice cycles: Winters of 1973-
4189 2002. *Journal of Climate*, 18, 4895-4905.
4190
- 4191 **Bacon, S.** and D.J.T. Carter, 1991: Wave climate changes in the North Atlantic and North
4192 Sea. *International Journal of Climatology*, 11, 545-558.
4193
- 4194 **Bell, D. B.** and M. Chelliah, 2006: Leading tropical modes associated with interannual
4195 and multidecadal fluctuations in North Atlantic hurricane activity. *Journal of*
4196 *Climate*, **17**, 590-612.
4197
- 4198 **Bonsal, B. R.**, X. Zhang, L. Vincent and W. Hogg, 2001: Characteristics of daily and
4199 extreme temperatures over Canada. *Journal of Climate*, **14**, 1959-1976.
4200
- 4201 **Bromirski, P.D.**, 2001, Vibrations from the “Perfect Storm”, *Geochem. Geophys.*
4202 *Geosys.*, **2** (7), doi:10.1029/2000GC000119.
4203
- 4204 **Bromirski, P. D.**, 2007: Extratropical cyclone-forced wave power variability along the
4205 U.S. Atlantic coast. *Nature*, submitted.
4206
- 4207 **Bromirski, P. D.** and J. Kossin, 2007: Hurricane waves along the U.S. east and Gulf
4208 coasts. *Science*, submitted.
4209
- 4210 **Bromirski, P. D.**, R.E. Flick and N. Graham, 1999: Ocean wave height determined from
4211 inland seismometer data: Implications for investigating wave climate changes:
4212 *Journal of Geophysical Research*, 104, 20753-20766.
4213
- 4214 **Bromirski, P.D.**, D.R. Cayan, and R.E. Flick, 2005: Wave spectral energy variability in
4215 the northeast Pacific. *Journal of Geophysical Research*, **110**, C03005,
4216 doi:10.1029/2004JC002398.
4217
- 4218 **Bromirski, P.D.**, R.E. Flick, and D.R. Cayan, 2003: Decadal storminess variability along
4219 the California coast: 1858 – 2000. *Journal of Climate*, **16**, 982-993.
4220
- 4221 **Brooks, H. E.**, 2004: On the relationship of tornado path length and width to intensity.
4222 *Weather and Forecasting*, **19**, 310-319.
4223

- 4224 **Brooks, H. E.**, 2007: Development and use of climatologies of convective weather.
4225 *Atmospheric Convection: Research and Operational Forecasting Aspects*.
4226 Springer-Verlag, in press.
4227
- 4228 **Brooks, H. E.** and C. A. Doswell III, 2001: Some aspects of the international climatology
4229 of tornadoes by damage classification. *Atmospheric Research*, **56**, 191-201.
4230
- 4231 **Brooks, H. E.**, C. A. Doswell III and M. P. Kay, 2003a: Climatological estimates of local
4232 daily tornado probability. *Weather and Forecasting*, **18**, 626-640.
4233
- 4234 **Brooks, H. E.**, J. W. Lee and J. P. Craven, 2003b: The spatial distribution of severe
4235 thunderstorm and tornado environments from global reanalysis data. *Atmospheric*
4236 *Research*, **67-68**, 73-94.
4237
- 4238 **Brooks, H. E.** and N. Dotzek, 2007: The spatial distribution of severe convective storms
4239 and an analysis of their secular changes. *Climate Extremes and Society*. H. F.
4240 Diaz and R. Murnane, Eds., Cambridge University Press, in press.
4241
- 4242 **Burnett, A.W.**, M.E. Kirby, H.T. Mullins, and W.P. Patterson, 2003: Increasing Great
4243 Lake-effect snowfall during the Twentieth Century: A regional response to global
4244 warming? *J. Climate*, 16, 3535-3541.
4245
- 4246 **Carter, D.J.T.** and L. Draper, 1988: Has the north-east Atlantic become rougher? *Nature*,
4247 332, 494.
4248
- 4249 **Cavazos, T.**, A. C. Comrie and D. M. Liverman, 2002: Intraseasonal variability
4250 associated with wet monsoons in southeast Arizona. *J. Climate*, **15**, 2477-2490.
4251
- 4252 **Cavazos, T.** and D. Rivas, 2004: Variability of extreme precipitation events in Tijuana,
4253 Mexico. *Climate Research*, **25**, 229-243.
4254
- 4255 **Cavazos, T.**, C. Turrent., and D. P. Lettenmaier, 2007: Extreme precipitation variability
4256 in the core of the North American monsoon. *Geophysical Research Letters*, to be
4257 submitted.
4258
- 4259 **Cayan, D. R.** .A. Kammerdiener, M.D. Dettinger, J.M. Caprio, and D.H. Peterson, 2001:
4260 Changes in the onset of spring in the Western United States. *Bulletin of the*
4261 *American Meteorological Society*, **82**, 399-415.
4262
- 4263 **Chan, J. C. L.**, 2006: Comment on “Changes in tropical cyclone number, duration, and
4264 intensity in a warming environment. *Science*, **311**, 1713.
4265
- 4266 **Chan, J. C. L.** and J.-E. Shi, 1996: Long-term trends and interannual variability in
4267 tropical cyclone activity over the western North Pacific. *Geophysical Research*
4268 *Letters*, **23**, 2765-2767.
4269

- 4270 **Chang**, E.K.M., and Y. Fu, 2002: Inter-decadal variations in Northern Hemisphere
4271 winter storm track intensity. *J. Climate*, **15**, 642–658.
4272
- 4273 **Chang**, E. K., and Y. Guo, 2007: Is the number of North Atlantic tropical cyclones
4274 significantly underestimated prior to the availability of satellite observations?
4275 *Geophys. Res. Lett.*, **34**, L14801, doi:10.1029/2007GL030169.
4276
- 4277 **Changnon**, D., S.A. Changnon and S. Changnon, 2001: A method for estimating crop
4278 losses from hail in uninsured periods and regions. *Journal of Applied*
4279 *Meteorology*, **40**, 84-91.
4280
- 4281 **Changnon**, S.A., 1982: Trends in tornado frequency: Fact or fallacy? *Preprints*, 12th
4282 conference on severe local storms, San Antonio, TX, American Meteorological
4283 Society, 42-44.
4284
- 4285 **Changnon**, S.A. and D. Changnon, 2000: Long-term fluctuations in hail incidences in
4286 the United States. *Journal of Climate*, **13**, 658-664.
4287
- 4288 **Changnon**, S.A., D. Changnon, and T.R. Karl, 2006: Temporal and spatial characteristics
4289 of snowstorms in the contiguous United States. *Journal of Applied Meteorology*
4290 *and Climatology*, **45**, 1141-1155.
4291
- 4292 **Changnon**, S. and T. Karl, 2003: Temporal and spatial variations in freezing rain in
4293 the contiguous U.S. *Journal of Applied Meteorology*, **42**, 1302-1315.
4294
- 4295 **Chenoweth**, M., 2003: *The 18th century climate of Jamaica*. American Philosophical
4296 Society, 212-219.
4297
- 4298 **Chu**, J. –H., C. R. Sampson, A. S. Levine and E. Fukada, 2002: The joint typhoon
4299 warning center tropical cyclone best tracks, 1945-2000. Naval research
4300 Laboratory Reference Number NRL/MR/7540-02-16.
4301
- 4302 **Clark**, M. P., M. C. Serreze, and D. A. Robinson, 1999: Atmospheric controls on
4303 Eurasian snow cover extent. *Int. J. Climatol.*, **19**, 27-40.
4304
- 4305 **Cleaveland**, M. L., D. W. Stahle, M. D. Therrell, J. Villanueva-Diaz, and B. T. Burnes,
4306 2004: Tree-ring reconstructed winter precipitation and tropical teleconnections in
4307 Durango, Mexico. *Climatic Change*, **59(3)**, 369-388.
4308
- 4309 **Coles**, S.G., 2001: *An Introduction to Statistical Modeling of Extreme Values*. Springer
4310 Verlag, New York.
4311
- 4312 **Concannon**, P. R., H. E. Brooks, and C. A. Doswell III, 2000: Climatological risk of
4313 strong and violent tornadoes in the United States. *Preprints*, 2nd Symposium on
4314 Environmental Applications, Long Beach, California, American Meteorological
4315 Society, 212-219.

- 4316
4317 **Cook**, E.R., D. M. Meko, D. W. Stahle, and M. K. Cleaveland, 1999: Drought
4318 reconstructions for the continental United States. *Journal of Climate*, **12**, 1145–
4319 1162.
- 4320
4321 **Cook**, E.R., R.D. D'Arrigo, and M.E. Mann, 2002: A well-verified, multiproxy
4322 reconstruction of the winter North Atlantic Oscillation index since A.D. 1400. *J.*
4323 *Climate*, **15**, 1754–1764.
- 4324
4325 **Cook** ER, Woodhouse CA, Eakin CM, et al., [Long-term aridity changes in the western](#)
4326 [United States](#) SCIENCE 306 (5698): 1015-1018 NOV 5 2004
- 4327
4328 **Cooley**, D., P. Naveau and D. Nychka, 2007: Bayesian spatial modeling of extreme
4329 precipitation return levels. *Journal of the American Statistical Association*, to
4330 appear.
- 4331
4332 **Cooter**, E. and S. LeDuc, 1995: Recent frost date trends in the northeastern United
4333 States. *International Journal of Climatology*, **15**, 65-75.
- 4334
4335 **Dai** A.G., K.E. Trenberth, and T.T. Qian, 2004: [A global dataset of Palmer Drought](#)
4336 [Severity Index for 1870-2002: Relationship with soil moisture and effects of](#)
4337 [surface warming](#). *Journal of Hydrometeorology*, **5**, 1117-1130.
- 4338
4339 **Davis**, R. E., R. Dolan and G. Demme, 1993: Synoptic climatology of Atlantic coast
4340 north-easters, *International Journal of Climatology*, **13** (2), 171-189.
- 4341
4342 **Davison**, A.C. and R.L. Smith, 1990: Models for exceedances over high thresholds (with
4343 discussion). *Journal of the Royal Statistical Society* **52**, 393-442.
- 4344
4345 **DeGaetano**, A. T. and R. J. Allen, 2002: Trends in the twentieth century temperature
4346 extremes across the United States. *Journal of Climate*, **15**, 3188-3205.
- 4347
4348 **Delworth**, T.L. and M.E. Mann, 2000: Observed and simulated multidecadal variability
4349 in the Northern Hemisphere, *Climate Dynamics*, **16**, 661-676.
- 4350
4351 **Deser**, C., A.S. Phillips, and J.W. Hurrell, 2004: Pacific interdecadal climate variability:
4352 Linkages between the tropics and the north Pacific during boreal winter since
4353 1900. *J. Climate*, **17**, 3109–3124.
- 4354
4355 **Dolan**, R., H. Lins and B. Hayden, 1988: Mid-Atlantic coastal storms. *Journal of Coastal*
4356 *Research*, **4** (3), 417-433.
- 4357
4358 **Donnelly**, J.P., 2005: Evidence of past intense tropical cyclones from backbarrier salt
4359 pond sediments: a case study from Isla de Culebrita, Puerto Rico, U.S.A. *Journal*
4360 *of Coastal Research*, **42**, 201-210.
- 4361

- 4362 **Donnelly, J.P., S. S. Bryant, J. Butler, J. Dowling, L. Fan, N. Hausmann, P. Newby, B.**
4363 **Shuman, J. Stern, K. Westover and T. Webb, III, 2001a: A 700 yr. sedimentary**
4364 **record of intense hurricane landfalls in southern New England. *Geological Society***
4365 ***of America Bulletin*, **113**, 714-727.**
4366
- 4367 **Donnelly, J.P., J. Butler, S. Roll, M. Wengren, and T. Webb, III, 2004: A backbarrier**
4368 **overwash record of intense storms from Brigantine, New Jersey. *Marine Geology*,**
4369 ****210**: 107-121.**
4370
- 4371 **Donnelly, J.P., S. Roll, M. Wengren, J. Butler, R. Lederer and T. Webb, III, 2001b:**
4372 **Sedimentary evidence of intense hurricane strikes from New Jersey. *Geology*, **29**,**
4373 **615-618.**
4374
- 4375 **Donnelly, J.P. and T. Webb, III, 2004: Backbarrier sedimentary records of intense**
4376 **hurricane landfalls in the northeastern United States. In: *Hurricanes and***
4377 ***Typhoons: Past, Present, and Future* (eds. R.J. Murnane, R.J. and K-b. Liu,**
4378 ***Columbia University Press*, pp. 58-95.**
4379
- 4380 **Donnelly, J. P., and J. D. Woodruff, 2007: Intense hurricane activity over the past 5,000**
4381 **years controlled by El Nino and the West African monsoon. *Nature*, **447**, 465-**
4382 **468.**
4383
- 4384 **Doswell, C. A. III, H. E. Brooks and M. P. Kay, 2005: Climatological estimates of daily**
4385 **local nontornadic severe thunderstorm probability for the United States. *Weather***
4386 ***and Forecasting*, **20**, 577-595.**
4387
- 4388 **Doswell, C. A. III, R. Edwards, R. L. Thompson and K. C. Crosbie, 2006: A simple and**
4389 **flexible method for ranking severe weather events. *Weather and Forecasting*, **21**,**
4390 **in press.**
4391
- 4392 **Douglas, M.W., R.A. Maddox, K. Howard, and S. Reyes, 1993: The Mexican monsoon.**
4393 ***J. Climate*, **6**, 1665-1677.**
4394
- 4395 **Easterling, D.R., J.L. Evans, P.Ya. Groisman, T.R. Karl, K.E. Kunkel, and P. Ambenje,**
4396 **2000a: Observed variability and trends in extreme climate events: a brief review.**
4397 ***Bulletin of the American Meteorological Society*, **81**, 417-425.**
4398
- 4399 **Easterling, D. R., 2002: Recent changes in frost days and the frost-free season in the**
4400 **United States. *Bulletin of the American Meteorological Society*, **83**, 1327-1332.**
4401
- 4402 **Easterling, D.R., B. Horton, P.D. Jones, T.C. Peterson, T.R. Karl, D.E. Parker, M.J.**
4403 **Salinger, V. Razuvayev, N. Plummer, P. Jamison, and C.K. Folland, 1997:**
4404 **Maximum and minimum temperature trends for the globe. *Science* **277**: 364-367.**
4405

- 4406 **Easterling**, D.R., T. Wallis, J. Lawrimore, and R. Heim, 2007b: The effects of
4407 temperature and precipitation trends on U.S. drought. *Geophysical. Research*
4408 *Letters*, submitted.
- 4409
4410 **Easterling**, D. R. B. Gleason, K. E. Kunkel and R. J. Stouffer, 2007a: A comparison
4411 between observed and model produced warm spells for the United States, to be
4412 submitted.
- 4413
4414 **Edwards**, D. C. and T. B. McKee, 1997: Characteristics of 20th Century Drought in the
4415 United States at Multiple Time Scales. Fort Collins, Colorado, Department of
4416 Atmospheric Science, Colorado State University.
- 4417
4418 **Eichler**, T., and W. Higgins, 2006: Climatology and ENSO-related variability of North
4419 American extra-tropical cyclone activity. *J. Climate*, **19**, 2076–2093.
- 4420
4421 **Elsner**, J. B., A. A. Tsonis and T. H. Jagger, 2006: High-frequency variability in
4422 hurricane power dissipation and its relationship to global temperature. *Bulletin of*
4423 *the American Meteorological Society*, **87**, 763-768.
- 4424
4425 **Emanuel**, K. A., 2005a: Increasing destructiveness of tropical cyclones over the past 30
4426 years. *Nature*, **436**, 686-688.
- 4427
4428 **Emanuel**, K. A., 2005b: Emanuel replies. *Nature*, **438**, doi:10.1038/nature04427.
- 4429
4430 **Emanuel**, K. A., 2007: Environmental factors affecting tropical cyclone power
4431 dissipation. *J. Climate*, accepted for publication.
- 4432
4433 **Englehart**, P.J. and A.V. Douglas, 2001: The Role of Eastern North Pacific Tropical
4434 Storms in the Rainfall Climatology of Western Mexico. *Int. J. Climatology*, **21**,
4435 1357-1370.
- 4436
4437 **Englehart**, P.J., and A.V. Douglas, 2002: Mexico's summer rainfall patterns: an analysis
4438 of regional modes and changes in their teleconnectivity. *Atmósfera*, 15, pp. 147-
4439 164.
- 4440
4441 **Englehart**, P.J. and A.V. Douglas, 2003: Urbanization and seasonal temperature trends:
4442 observational evidence from a data sparse part of North America. *Int. J. Climatol*
4443 **23**: 1253-1263.
- 4444
4445 **Englehart** P.J. and A.V. Douglas, 2005: Changing behavior in the diurnal range of
4446 surface air temperatures over Mexico. *Geophys. Res. Ltrs.* **32** No. 1: L01701
4447 10.1029/2004GL021139.
- 4448
4449 **Englehart**, P.J. and A.V. Douglas, 2006: Defining intraseasonal variability within the
4450 North American monsoon. *J. Climate*, **19**, 4243-4253.
- 4451

- 4452 **Englehart, P. J., M. D. Lewis, and A. V. Douglas, 2007:** Defining the frequency of near
4453 shore tropical cyclone activity in the eastern North Pacific from historical surface
4454 observations 1921-2005. Submitted to *Geophys. Res. Lett.*.
4455
- 4456 **Federal Emergency management Agency, 1995:** National mitigation strategy:
4457 Partnerships for building safer communities. Report, 40 pp, Washington, D. C.
4458
- 4459 **Fernandez-Partagas, J. and H. F. Diaz, 1996:** Atlantic hurricanes in the second half of
4460 the nineteenth century. *Bulletin of the American Meteorological Society*, **77**,
4461 2899-2906.
4462
- 4463 **Feuerstein, B., N. Dotzek and J. Grieser, 2005:** Assessing a tornado climatology from
4464 global tornado intensity distributions, *Journal of Climate*, **18**, 585-596.
4465
- 4466 **Folland, C.K., et al., 1986:** Sahel rainfall and worldwide sea temperatures, *Nature*, **320**,
4467 686-688.
4468
- 4469 **Frappier, A., Sahagian, D., Carpeter, S.J., Gonzalez, L.A., Frappier, B., 2007:** A
4470 stalagmite record of recent tropical cyclones. *Geology*, **7**, 11114; doi:
4471 10.1130/G23145A.
4472
- 4473 **Gandin L. S., and R. L. Kagan, 1976:** *Statistical Methods of Interpretation of*
4474 *Meteorological Data.* (in Russian). Gidrometeoizdat, 359 pp
4475
- 4476 **Garcia Herrera, R., L. Gimeno, P. Ribera and E. Hernandez, 2005:** New records of
4477 Atlantic hurricanes from Spanish documentary sources, *Journal of Geophysical*
4478 *Research*, **110**:D03109.
4479
- 4480 **Garcia Herrera, R., F. Rubio, D. Wheeler, E. Hernandez, M. R. Prieto and L. Gimero,**
4481 **2004:** The use of Spanish and British documentary sources in the investigation of
4482 Atlantic hurricane incidence in historical times. In: *Hurricanes and Typhoons:*
4483 *Past, Present, and Future* (eds. R.J. Murnane, R. J. and K-b. Liu), p. 149-176.
4484 Columbia University Press.
4485
- 4486 **Garriott, E.B., 1903:** Storms of the Great Lakes. U.S. Department of Agriculture,
4487 Weather Bureau, *Bulletin K*, 486 pp.
4488
- 4489 **Geng, Q., and M. Sugi, 2001:** Variability of the North Atlantic cyclone activity in winter
4490 analyzed from NCEP–NCAR reanalysis data. *J. Climate*, **14**, 3863–3873.
4491
- 4492 **Gershunov, A., and T.P. Barnett, 1998:** Inter-decadal modulation of ENSO
4493 teleconnections. *Bull. Amer. Meteor. Soc.*, **79**, 2715–2725.
4494
- 4495 **Gershunov, A. and D. R. Cayan, 2003:** Heavy daily precipitation frequency over the
4496 contiguous United States: sources of climate variability and seasonal

- 4497 predictability. *J. Climate*, **16**, 2752-2765.
- 4498
- 4499 **Gershunov, A.** and H. Douville, 2007: Extensive summer hot and cold extremes under
4500 current and possible future climatic conditions: Europe and North America. In
4501 Diaz, H.F. and Murnane, R.J. eds., *Climate Extremes and Society*, Cambridge:
4502 Cambridge University Press (in press).
- 4503
- 4504 **Goldenberg, S. B., C. W. Landsea, A.M. Mesta-Nuñez and W. M. Gray**, 2001: The
4505 recent increase in Atlantic hurricane activity: Causes and implications. *Science*,
4506 **293**, 474-479.
- 4507
- 4508
- 4509 **Graham, N.E.**, 1994: Decadal-scale climate variability in the tropical and North Pacific
4510 during the 1970s and 1980s: observations and model results, *Climate Dynamics*,
4511 **10**, 135-162.
- 4512
- 4513 **Graham, N. E. and H. F. Diaz**, 2001: Evidence for intensification of North Pacific winter
4514 cyclones since 1948, *Bulletin of the American Meteorological Society*, **82**, 1869-
4515 1893.
- 4516
- 4517 **Grazulis, T. P.**, 1993: *Significant Tornadoes, 1680-1991*. Environmental Films, St.
4518 Johnsbury, VT, 1326 pp.
- 4519
- 4520 **Groisman, P.Ya., T.R. Karl, D.R. Easterling, R.W. Knight, P.B. Jamason, K.J.**
4521 **Hennessy, R. Suppiah, Ch.M. Page, J. Wibig, K. Fortuniak, V.N. Razuvaev, A.**
4522 **Douglas, E. Førland, and P.-M. Zhai**, 1999: Changes in the probability of heavy
4523 precipitation: Important indicators of climatic change. *Climatic Change*, **42**, 243-
4524 283.
- 4525
- 4526 **Groisman, P.Ya. R.W. Knight , and T.R. Karl**, 2001: Heavy precipitation and high
4527 streamflow in the contiguous United States: Trends in the 20th century. *Bull.*
4528 *Amer. Meteorol. Soc.*, **82**, 219-246.
- 4529
- 4530 **Groisman, P. Ya., R. W. Knight, and T. R. Karl, D. R. Easterling, B. Sun and J.**
4531 **H. Lawrimore**, 2004: Contemporary changes of the hydrological cycle over the
4532 contiguous United States: Trends derived from in situ observations, *Journal of*
4533 *Hydrometeorology*, **5**, 64–85.
- 4534
- 4535 **Groisman, P.Ya, R. W. Knight, D. R. Easterling, T. R. Karl, G. C. Hegerl and V.**
4536 **N. Razuvaev**, 2005: Trends in intense precipitation in the climate record. *Journal*
4537 *of Climate*, **18**, 1326–1350.
- 4538
- 4539 **Groisman, P.Ya. and R.W. Knight**, 2007: Prolonged dry episodes over the conterminous
4540 United States: New tendencies emerged during the last 40 years. *J. Climate*,
4541 submitted.
- 4542

- 4543 **Groisman, P.Ya., B.G. Sherstyukov, V.N. Razuvaev, R.W. Knight, J.G. Enloe, N.S.**
4544 **Stroumentova, P. H. Whitfield, E. Førland, I. Hannsen-Bauer, H. Tuomenvirta, H.**
4545 **Aleksandersson, A. V. Mescherskaya, and T.R. Karl, 2007a: Potential forest fire**
4546 **danger over Northern Eurasia: Changes during the 20th century. *Global and***
4547 ***Planetary Change*, **56**, issue 3-4, 371-386.**
4548
- 4549 **Groisman, P. Ya., R. W. Knight, R. W. Reynolds, A. B. Smith, T.R. Karl, and O. N.**
4550 **Bulygina, 2007b: Tropical Cyclone Related Precipitation over the Southeastern**
4551 **United States. (*to be submitted*)**
4552
- 4553 **Gulev S. K. and V. Grigorieva, 2004: Last century changes in ocean wind wave height**
4554 **from global visual wave data. *Geophys. Res. Lett.*, **31**, L24302,**
4555 **doi:10.1029/2004GL021040.**
4556
- 4557 **Gumbel, E.J., 1958: *Statistics of Extremes*. Columbia University Press.**
4558
- 4559 **Guttman, N.B., 1998: Comparing the Palmer Drought Index and the Standardized**
4560 **Precipitation Index. *Journal of the American Water Resources Association* **34**,**
4561 **113–121, doi:10.1111/j.1752-1688.1998.tb05964.**
4562
- 4563 **Hallack-Alegria, M., and D. W. Watkins Jr., 2007: Annual and warm season drought**
4564 **intensity-duration-frequency analysis for Sonora, Mexico. *Journal of Climate*, **20**,**
4565 **1897-1909.**
4566
- 4567 **Harman, J.R., R. Rosen, and W. Corcoran, 1980: Winter cyclones and circulation**
4568 **patterns on the western Great Lakes. *Phys. Geogr.*, **1**, 28–41.**
4569
- 4570 **Harnik N. and E.K.M. Chang, 2003: [Storm track variations as seen in radiosonde](#)**
4571 **[observations and reanalysis data](#). *Journal of Climate*, **16**, 480-495.**
4572
- 4573 **Harper B. A. and J. Callaghan, 2006: On the importance of reviewing historical tropical**
4574 **cyclone intensities. American Meteorological Society, 27th Conference on**
4575 **Hurricanes and Tropical Meteorology, 2C.1, Monterey, Apr.**
4576
- 4577 **Hartmann, D.L. and E.D. Maloney, 2001: The Madden-Julian Oscillation, barotropic**
4578 **dynamics, and North Pacific tropical cyclone formation. Part II: Stochastic**
4579 **barotropic modeling, *Journal of Atmospheric Sciences*, **58**, 2559-2570.**
4580
- 4581 **Heim Jr., R.R., 2002: A review of Twentieth-Century drought indices used in the United**
4582 **States. *Bulletin of the American Meteorological Society*, **83**, 1149–1165.**
4583
- 4584 **Herweijer, C., R. Seager and E.R. Cook, 2006: North American droughts of the mid-to-**
4585 **late nineteenth century: a history, simulation and implication for mediaeval**
4586 **drought. *The Holocene*, **16**, 159-171.**
4587

- 4588 **Herweijer, C.**, R. Seager, E.R. Cook and J. Emile-Geay, 2007: North American droughts
4589 of the last millennium from a gridded network of tree-ring data. *Journal of*
4590 *Climate*, in press.
- 4591 **Higgins, R.W.**, Y. Chen and A.V. Douglas, 1999: Interannual Variability of the North
4592 American Warm Season Precipitation Regime. *J. Climate*, **12**, 653-680.
- 4593
4594
4595 **Hirsch, M. E.**, A. T. DeGaetano and S. J. Colucci, 2001: An East Coast winter storm
4596 climatology. *Journal of Climate*, **14** (5), 882-899.
- 4597
4598 **Hobbins, M.T.**, A. Dai, M. L. Roderick, and G. D. Farquhar, 2007: Back to basics:
4599 Revisiting potential evapotranspiration as a driver of water balance trends.
4600 Geophysical Research Letters, submitted.
- 4601
4602 **Hoegh-Guldberg, O.**, 2005: Low coral cover in a high-CO₂ world. *Journal of*
4603 *Geophysical Research*, 110, C09S06, doi:10.1029/2004JC002528.
- 4604
4605 **Holland, G.J.**, 2007: Misuse of landfall as a proxy for Atlantic tropical cyclone activity.
4606 *EOS* (in press).
- 4607
4608 **Holland, G. J.**, and P. J. Webster, 2007: Heightened tropical cyclone activity in the North
4609 Atlantic: natural variability or climate trend? *Phil. Trans. R. Soc. A*,
4610 doi:10.1098/rsta.2007.2083.
- 4611
4612 **Hoyos, C. D.**, P. A. Agudelo, P. J. Webster and J. A. Curry, 2006: Deconvolution of the
4613 factors contributing to the increase in global hurricane intensity. *Science*, **312**: 94-
4614 97.
- 4615
4616 **Hsu, S.A.**, Martin, M.F., and Blanchard, B.W., 2000: An evaluation of the USACE's
4617 deepwater wave prediction techniques under hurricane conditions during Georges in
4618 1998. *Journal of Coastal Research*, **16**, 823-829.
- 4619
4620 **Huschke, R. E.** (editor) (1959) Glossary of Meteorology, American Meteorological Society,
4621 Boston, Massachusetts, USA, pgs. 106 and 419.
- 4622
4623 **IPCC**, 2001: Climate Change 2001: The Scientific Basis. Contribution of Working Group I to
4624 the Third Assessment Report of the Intergovernmental Panel on Climate Change
4625 [Houghton, J.T., Y. Ding, D.J. Griggs, M. Noguer, P.J. van der Linden, X. Dai, K.
4626 Maskell, and C.A. Johnson (eds.)]. Cambridge University Press, Cambridge, United
4627 Kingdom and New York, NY, USA, 881pp.
- 4628
4629 **Jarvinen, B. R.**, C. J. Neumann and M. A. S. Davis, 1984: A tropical cyclone data tape
4630 for the North Atlantic Basin, 1886-1983. Contents, limitations and uses. Tech.
4631 Memo. NWS NHC-22, 21pp. NOAA, Washington DC.
- 4632
4633

- 4634 **Jones**, G.V., and R.E. Davis, 1995: Climatology of Nor'easters and the 30 kPa jet. *J.*
4635 *Coastal Res.*, **11** (3), 1210-1220.
- 4636
- 4637 **Jones** P.D. and A. Moberg, 2003: Hemispheric and large-scale surface air temperature
4638 variations: an extensive revision and an update to 2001. *J Climate* **16**: 206-223.
4639
- 4640 **Jones**, P.D., T.J. Osborn, and K.R. Briffa, 2003: Pressure-based measures of the North
4641 Atlantic Oscillation (NAO): A comparison and an assessment of changes in the
4642 strength of the NAO and in its influence on surface climate parameters. In: *The*
4643 *North Atlantic Oscillation: Climatic Significance and Environmental Impact*
4644 [Hurrell, J.W., et al. (eds.)].
4645
- 4646 **Kalnay**, E., M. Kanamitsu, R. Kistler, W. Collins, D. Deaven, L. Gandin, M. Iredell, S.
4647 Saha, G. White, J. Woollen, Y. Zhu, A. Leetmaa, B. Reynolds, M. Chelliah, W.
4648 Ebisuzaki, W. Higgins, J. Janowiak, K. Mo, C. Ropelewski, J. Wang, R. Jenne,
4649 and D. Joseph, 1996: The NCEP/NCAR 40-Year reanalysis project. *Bull. Amer.*
4650 *Meteor. Soc.*, **77**, 437–471.
4651
- 4652 **Kamahori**, H. N. Yamazaki, N. Mannoji, and K. Takahashi, 2006: Variability in intense
4653 tropical cyclone days in the western North Pacific. *SOLA*, **2**, 104-107,
4654 doi:10.2151/sola.2006-027.
4655
- 4656 **Karl**, T.R.; and R.W. Knight. 1985. Atlas of Monthly Palmer Hydrological Drought
4657 Indices (1931–1983) for the Contiguous United States. Historical Climatology
4658 Series 3–7, National Climatic Data Center, Asheville, North Carolina.
4659
- 4660 **Karl**, T.R. and R. W. Knight, 1998: Secular Trends of Precipitation Amount, Frequency,
4661 and Intensity in the United States. *Bulletin of the American Meteorological*
4662 *Society*, **79**, 231–241
4663
- 4664 **Keetch**, J.J. and G.M. Byram, 1968: A drought index for forest fire control. U.S.D.A.
4665 Forest Service Research Paper SE-38. 35 pp. [Available from:
4666 <http://www.srs.fs.fed.us/pubs/>]
4667
- 4668 **Key**, J. R. and A. C. K. Chan, 1999: Multidecadal global and regional trends in 1000 mb
4669 and 500 mb cyclone frequencies. *Geophysical Research Letters*, **26** 2035-2056.
4670
- 4671 **Kharin**, V.V., and F.W. Zwiers, 2000: Changes in the extremes in an ensemble of
4672 transient climate simulation with a coupled atmosphere-ocean GCM. *Journal of*
4673 *Climate*, **13**, 3760-3788.
4674
- 4675 **Kharin**, V. V., F. W. Zwiers, X. Zhang, and G. C. Hegerl, 2007: Changes in temperature
4676 and precipitation extremes in the IPCC ensemble of global coupled model
4677 simulations. *Journal of Climate*, *accepted*.
4678

- 4679 **Kim**, T-W., J. B. Valdes, and J. Aparicio, 2002: Frequency and spatial characteristics of
4680 droughts in the Conchos river basin, Mexico. *International Water Resources*,
4681 27(3), 420-430.
4682
- 4683 **Klotzbach**, P. J., 2006: Trends in global tropical cyclone activity over the past twenty
4684 years (1986-2005). *Geophysical Research Letters*, **33**, L10805,
4685 doi:10.1029/2006GL025881.
4686
- 4687 **Knaff**, J. A and C. R. Sampson, 2006: Reanalysis of West Pacific tropical cyclone
4688 intensity 1966-1987. Proceedings of 27th AMS Conference on Hurricanes and
4689 Tropical Meteorology, #5B.5. Available online at:
4690 <http://ams.confex.com/ams/pdfpapers/108298.pdf>
4691
- 4692 **Kocin**, P. J., P. N. Schnumacher, R. F. Morales Jr. and L.W.Uccellini, 1995: Overview of
4693 the 12-14 March 1993 Superstorm. *Bulletin of the American Meteorological*
4694 *Society*, **76** (2), 165-182.
4695
- 4696 **Komar**, P.D. and J.C. Allan, 2007a: Higher waves along U.S. East Coast linked to
4697 hurricanes. *EOS, Transactions, American Geophysical Union*, 88, 301.
4698
- 4699 **Komar**, P.D., and J.C. Allan, 2007b: Increasing wave heights along the U.S. Atlantic
4700 coast due to the intensification of hurricanes. *Journal of Coastal Research*, in
4701 press.
4702
- 4703 **Kossin**, J. P., K. R. Knapp, D. J. Vimont, R. J. Murnane, and B. A. Harper, 2007a: A
4704 globally consistent reanalysis of hurricane variability and trends. *Geophys. Res.*
4705 *Lett.*, 34, L04815, doi:10.1029/2006GL028836.
4706
- 4707 **Kossin**, J. P., J. A. Knaff, H. I. Berger, D. C. Herndon, T. A. Cram, C. S. Velden, R. J.
4708 Murnane, and J. D. Hawkins, 2007b: Estimating hurricane wind structure in the
4709 absence of aircraft reconnaissance. *Wea. Forecasting*, 22, 89-101
4710
- 4711 **Kossin**, J. P., and D. J. Vimont, 2007: A more general framework for understanding
4712 Atlantic hurricane variability and trends. *Bull. Amer. Meteor. Soc.*, in press.
4713
- 4714 **Kunkel**, K.E., 2003: North American trends in extreme precipitation. *Natural Hazards*,
4715 **29**, 291-305.
4716
- 4717 **Kunkel**, K.E., S.A. Changnon, and J.R. Angel, 1994: Climatic aspects of the 1993 Upper
4718 Mississippi River basin flood. *Bull. Amer. Meteor. Soc.*, **75**, 811-822.
4719
- 4720 **Kunkel**, K. E., K. Andsager and D.R. Easterling, 1999: Long-term trends in extreme
4721 precipitation events over the conterminous United States and Canada. *Journal of*
4722 *Climate*, **12**, 2515-2527.
4723

- 4724 **Kunkel, K.E., N.E. Westcott, and D.A.R. Kristovich, 2002:** Assessment of potential
4725 effects of climate change on heavy lake-effect snowstorms near Lake Erie. *J.*
4726 *Great Lakes Res.*, **28**, 521-536.
4727
- 4728 **Kunkel, K. E., D. R. Easterling, K. Redmond and K. Hubbard, 2003:** Temporal
4729 variations of extreme precipitation events in the United States: 1895-2000.
4730 *Geophysical Research Letters*, **30**, 1900, 10.1029/2003GL018052.
4731
- 4732 **Kunkel, K.E., D.R. Easterling, K. Redmond, and K. Hubbard, 2004:** Temporal variations
4733 in frost-free season in the United States: 1895–2000, *Geophys. Res. Lett.*, **31**,
4734 L03201, doi:10.1029/2003GL018624.
4735
- 4736 **Kunkel, K.E., T.R. Karl, and D.R. Easterling, 2007a:** A Monte Carlo assessment of
4737 uncertainties in heavy precipitation frequency variations. *J. Hydrometeor.*, in
4738 press.
4739
- 4740 **Kunkel, K. E., R. A. Pielke, Jr. and S. A. Changnon, 1999:** Temporal fluctuations in
4741 weather and climate extremes that cause economic and human health impacts: A
4742 review. *Bulletin of the American Meteorological Society*, **80**, 1077-1098.
4743
- 4744 **Kunkel, K.E., K.E., M. Palecki, L. Ensor, D. Robinson, K.Hubbard, D. Easterling, and**
4745 **K. Redmond, 2007b:** Trends in 20th Century U.S. snowfall using a quality-
4746 controlled data set. Proceedings, 75th Annual Meeting, Western Snow Conference,
4747 in press.
4748
- 4749 **Landsea, C. W., et al, 2004:** The Atlantic hurricane database re-analysis project:
4750 Documentation for the 1851-1910 alterations and additions to the HURDAT
4751 database. In *Hurricanes and Typhoons: Past, Present and Future*, R. J. Murnane
4752 and K.-B. Liu, Eds., Columbia University Press.
4753
- 4754 **Landsea, C. W., 2005:** Hurricanes and global warming. *Nature*, **438**,
4755 doi:10.1038/nature04477.
4756
- 4757 **Landsea, C. (2007),** Counting Atlantic tropical cyclones back in time. *EOS*, 88(18), 197-
4758 203.
4759
- 4760 **Landsea, C.W., B.A. Harper, K. Hoarau and J.A. Knaff, 2006:** Can we detect trends in
4761 extreme tropical cyclones? *Science*. **313**, 452-454.
4762
- 4763 **Lemke, P., et al. 2007:** Observations: Changes in Snow, Ice and Frozen Ground., Chapter
4764 4, Report of Working Group I, Intergovernmental Panel on Climate Change,
4765 Fourth Assessment Report, in press.
4766
- 4767 **Lewis, P.J., 1987:** Severe storms over the Great Lakes: a catalogue summary for the
4768 period 1957–1985. Canadian Climate Center Report No. 87–13, Atmospheric
4769 Environment Service, Downsview, ON, Canada, 342 pp.

- 4770
4771 **Liu, K-b.**, 2004: Paleotempestology: Principles, methods, and examples from Gulf Coast
4772 lake sediments. In: *Hurricanes and Typhoons: Past, Present, and Future*, R.J.
4773 Murnane, R. J. and K-b. Liu, Eds., Columbia University Press, pp. 13-57.
4774
- 4775 **Liu, K-b.** and M. L. Fearn, 1993: Lake-sediment record of late holocene hurricane
4776 activities from coastal Alabama. *Geology*, **21**, 793-796.
4777
- 4778 **Liu, K-b.** and M. L. Fearn, 2000: Reconstruction of prehistoric landfall frequencies of
4779 catastrophic hurricanes in northwestern Florida from lake sediment records.
4780 *Quaternary Research*, **54**, 238-245.
4781
- 4782 **Liu, K-b.**, C. Shen, C. and K. S. Louie, 2001: A 1,000-year history of typhoon landfalls
4783 in Guangdong, southern China, reconstructed from Chinese historical
4784 documentary records. *Annals of the Association of American Geographers*, **91**,
4785 453-464.
4786
- 4787 **Louie, K.S.** and K.-b. Liu, 2003: Earliest historical records of typhoons in China. *Journal*
4788 *of Historical Geography*, **29**, 299-316.
4789
- 4790 **Louie, K.S.** and K.-b. Liu, 2004: Ancient records of typhoons in Chinese historical
4791 documents. In: *Hurricanes and Typhoons: Past, Present, and Future* , R.J.
4792 Murnane, R. J. and K-b. Liu, Eds., Columbia University Press, pp. 222-248.
4793
- 4794 **Ludlam, D.M.**, 1963: Early American hurricanes, 1492-1870. *American Meteorological*
4795 *Society*.
4796
- 4797 **Madden, R.** and P. Julian, 1971: Detection of a 40-50 day oscillation in the zonal wind in
4798 the tropical Pacific, *Journal of the Atmospheric Sciences*, **28**, 702-708.
4799
- 4800 **Madden, R.** and P. Julian, 1972: Description of global-scale circulation cells in the
4801 tropics with a 40-50 day period, *Journal of the Atmospheric Sciences*, **29**, 1109-
4802 1123.
4803
- 4804 **Magnuson, J. J.**, D.M. Robertson, B. J. Benson, R. H. Wynne, D.M. Livingston, T. Arai,
4805 R. A. Assel, R. G. Barry, V. Card, E. Kuusisto, N.G. Granin, T. D. Prowse, K. M.
4806 Stewart, and V. S. Vuglinski, 2000: Historical trends in lake and river ice cover in
4807 the Northern Hemisphere. *Science*, **289**, 1743–1746.
4808
- 4809 **Maloney, E. D.** and D.L. Hartmann, 2000a: Modulation of eastern North Pacific
4810 hurricanes by the Madden-Julian Oscillation, *Journal of Climate*, **13**, 1451-1460.
4811
- 4812 **Maloney, E. D.** and D.L. Hartmann, 2000b: Modulation of hurricane activity in the Gulf
4813 of Mexico by the Madden-Julian Oscillation, *Science*, **287**, 2002-2004.
4814

- 4815 **Maloney**, E. D. and D.L. Hartmann, 2001: The Madden-Julian Oscillation, barotropic
4816 dynamics, and North Pacific tropical cyclone formation. Part I: Observations,
4817 *Journal of the Atmospheric Sciences*, **58**, 2545-2558.
4818
- 4819 **Mann**, M. E. and K. Emanuel, 2006: Atlantic hurricane trends linked to climate change.
4820 *EOS*, **87**, 233-241.
4821
- 4822 **Mann**, M.E. and J. Park, 1994: Global-scale modes of surface temperature variability on
4823 interannual to century timescales, *Journal of Geophysical Research*, **99**, 25819-
4824 25833.
4825
- 4826 **Mann**, M.E., K.A. Emanuel, G.J. Holland and P.J. Webster, 2007: Atlantic tropical
4827 cyclones revisited. *EOS* (in press).
4828
- 4829 **Mann**, M.E., T.A. Sabbatelli and U. Neu, 2007: Evidence for a modest undercount bias
4830 in early historical Atlantic tropical cyclone counts. *Nature* (submitted).
4831
- 4832 **Manning**, D. M., and R. E. Hart, 2007: Evolution of North Atlantic ERA40 tropical
4833 cyclone representation. *Geophys. Res. Lett.*, **34**, L05705.
4834 doi:10.1029/2006GL028266.
4835
- 4836 **Mather**, J.R., R.T. Field, and G.A. Yoskioka (1967), Storm hazard damage along the
4837 East Coast of the U.S., *J. Appl. Meteor.*, **6**, 20-30.
4838
- 4839 **Maue**, R. N., and R. E. Hart, 2007: Comment on “Low frequency variability in globally
4840 integrated tropical cyclone power dissipation” by Ryan Sriver and Matthew
4841 Huber. *Geophys. Res. Lett.*, **34**, L05705. doi:10.1029/2006GL028266.
4842
- 4843 **McCabe**, G. J., M. P. Clark and M. C. Serreze, 2001: Trends in Northern Hemisphere
4844 surface cyclone frequency and intensity. *Journal of Climate*, **14**, 2763-2768.
4845
- 4846 **McCarthy**, D. W., J. T. Schaefer and R. Edwards, 2006: What are we doing with (or to)
4847 the F-xcale? *Preprints*, 23rd Conference on Severe Local Storms, St. Louis,
4848 Missouri, American Meteorological Society, Conference CD. (Available online at
4849 <http://ams.confex.com/ams/pdfpapers/115260.pdf>.)
4850
- 4851 **McKee**, T. B., N. J. Doesken and J. Kleist, 1993: Drought monitoring with multiple
4852 timescales. Preprints of the Eight Conference on Applied Climatology, Anaheim,
4853 California.
4854
- 4855 **Michaels**, P.J., P.C. Knappenberger, O.W. Frauenfeld, and R.E. Davis, 2004: Trends in
4856 precipitation on the wettest days of the year across the contiguous USA. *Int. J.*
4857 *Climatol.* **24**: 1873–1882.
4858
4859
4860

- 4861 **Millas, J.C.**, 1968: Hurricanes of the Caribbean and adjacent regions, 1492-1800.
4862 Academy of the Arts and Sciences of the Americas.
4863
- 4864 **Miller, A.J.**, Cayan, D., T. Barnett, N. Graham, and J. Oberhuber, 1994: The 1976-77
4865 climate shift of the Pacific Ocean, *OCEANOGRAPHY*, **1**, 21-26.
4866
- 4867 **Miller, D. L.**, Mora, C. I., Grissino-Mayer, H. D., Uhle, M. E. and Sharp, Z., 2006: Tree-
4868 ring isotope records of tropical cyclone activity. *Proc. Nat. Acad. Sci.*, **103**,
4869 14294-14297.
4870
- 4871 **Mo, K.C.** and R.E. Livezey, 1986: Tropical-extratropical geopotential height
4872 teleconnections during the northern hemisphere winter, *Mon. Wea. Rev.*, **114**,
4873 2488-2515, 1986.
4874
- 4875 **Mock, C.J.**, 2004: Tropical cyclone reconstructions from documentary records: examples
4876 for South Carolina, United States. In: *Hurricanes and Typhoons: Past, Present,*
4877 *and Future*, R.J. Murnane, R. J. and K-b. Liu, Eds., Columbia University Press, p.
4878 121-148.
4879
- 4880 **Moon, I.J.**, I. Ginis, T. Hara, H.L. Tolman, C.W. Wright, and E.J. Walsh (2003),
4881 Numerical simulation of sea surface directional wave spectra under hurricane
4882 wind forcing, *J. Phys. Ocean.*, **33**, 1680-1706.
4883
- 4884 **Mueller K.J.**, M. DeMaria, J. Knaff, et al., 2006: [Objective estimation of tropical cyclone](#)
4885 [wind structure from infrared satellite data](#). *Weather and Forecasting*, **21**, 990-
4886 1005.
4887
- 4888 **Nakamura, H.**, 1992: Midwinter suppression of baroclinic wave activity in the Pacific. *J.*
4889 *Atmos. Sci.*, **49**, 1629–1642.
4890
- 4891 **Neelin J.D.**, M. Munnich, H. Su, et al., 2006: [Tropical drying trends in global warming](#)
4892 [models and observations](#). *Proceedings of the National Academy of Sciences of the*
4893 *United States of America*, **103**, 6110-6115.
4894
- 4895 **Nicholas, R.** and D. S. Battisti, 2006. Drought recurrence and seasonal rainfall prediction
4896 in the Yaqui basin, Mexico. *Journal Applied Meteorology and*
4897 *Climatology*, accepted.
4898
- 4899 **Noel, J.**, and D. Changnon, 1998: A Pilot Study Examining U.S. Winter Cyclone
4900 Frequency Patterns Associated with Three ENSO Parameters. *J. Climate*, **11**,
4901 2152–2159.
4902
- 4903 **Nyberg, J.**, B. A. Malmgren, A. Winter, M. R. Jury, K. Halimeda Kilbourne, and T. M.
4904 Quinn, 2007: Low Atlantic hurricane activity in the 1970s and 1980s compared to
4905 the past 270 years. *Nature*, **447**, 698-702.
4906

- 4907 **Paciorek, C.J., J.S. Risbey, V. Ventura, and R.D. Rosen, 2002: Multiple indices of**
4908 **Northern Hemisphere cyclone activity, Winters 1949–99. *J. Climate*, **15**, 1573–**
4909 **1590.**
- 4910
- 4911 **Palmer, W. C. 1965. Meteorological drought. Research Paper No. 45, U.S. Department**
4912 **of Commerce Weather Bureau, Washington, D.C**
- 4913
- 4914 **Palmer, W.C. 1968. Keeping track of crop moisture conditions, nationwide: The new**
4915 **Crop Moisture Index. *Weatherwise* 21:156–161.**
- 4916
- 4917 **Pavia E.G. and A. Badan, 1998: [ENSO modulates rainfall in the Mediterranean](#)**
4918 **[Californias](#). *GEOPHYSICAL RESEARCH LETTERS*, 25, 3855-3858**
- 4919
- 4920 **Peterson, T. C. et al. 2002: Recent changes in the climate extremes in the Caribbean**
4921 **region. *Journal of Geophysical Research*, **107**, NO.D21, 4601,**
4922 **doi:10.1029/2002JD002251,2002.**
- 4923
- 4924 **Peterson, T. C., X. Zhang, M. Brunet India, J. L. Vázquez Aguirre, 2007: Changes in**
4925 **North American extremes derived from daily weather data. *Proceedings of the***
4926 ***National Academy of Science*, submitted.**
- 4927
- 4928 **Pickands, J. (1975), Statistical inference using extreme order statistics. *Annals of***
4929 ***Statistics* **3**, 119-131.**
- 4930
- 4931 **Pielke, R. A., Jr., 2005: Are there trends in hurricane destruction? *Nature*, **438**, E11.**
4932
- 4933 **Robeson, S. M., 2004: Trends in time-varying percentiles of daily minimum and**
4934 **maximum temperature over North America," *Geophysical Research Letters*, 31,**
4935 **L04203, doi:10.1029/2003GL019019.**
- 4936
- 4937 **Ropelewski, C., 1999: The great El Niño of 1997-1998: Impacts on precipitation and**
4938 **temperature. *Consequences*, **5 (2)**.**
- 4939
- 4940 **Robinson, D.A., K.F. Dewey, and R.R. Heim Jr., 1993: Global snow cover monitoring:**
4941 **an update. *Bull. Am. Meteorol. Soc.*, **74**, 1689–1696.**
- 4942
- 4943 **Sanders, F., and J.R. Gyakum, 1980: Synoptic-dynamic climatology of the “bomb”.**
4944 ***Mon. Wea. Rev.*, **108**, 1589–1606.**
- 4945
- 4946 **Schlesinger, M.E. and N. Ramankutty, 1994: An oscillation in the global climate system of**
4947 **period 65–70 years. *Nature*, 367, 723–726.**
- 4948
- 4949 **SEMARNAP, 2000: Programa nacional contra incendios forestales. Resultados 1995-**
4950 **2000. Mexico, 263 pp.**
- 4951

- 4952 **Semenov** VA, Bengtsson L, 2002: Secular trends in daily precipitation characteristics:
4953 greenhouse gas simulation with a coupled AOGCM. *CLIMATE DYNAMICS*, 19,
4954 123-140
4955
- 4956 **Serreze**, M. C., F. Arse, R. G. Barry and J. C. Rogers, 1997: Icelandic low cyclone
4957 activity. Climatological features, linkages with the NAO, and relationships with
4958 recent changes in the Northern Hemisphere circulation. *Journal of Climate*, **10**
4959 (3), 453-464.
4960
- 4961 **Seymour**, R. J., R. R. Strange, D. R. Cayan and R. A. Nathan, 1984: Influence of El
4962 Niños on California's wave climate. *Proceedings 19th International Conference*
4963 *on Coastal Engineering*, Amer. Soc. Civil Engrs., 577-592.
4964
- 4965 **Shabbar**, A. and W. Skinner, 2004: Summer drought patterns in Canada and the
4966 relationship to global sea surface temperatures. *J. Climate*, **17**, 2866–2880.
4967
- 4968 **Shein**, K. A., ed., 2006: State of the climate in 2005. *Bulletin of the American*
4969 *Meteorological Society*, **87**, 1-S102.
4970
- 4971 **Simmonds**, I., and K. Keay, 2000: Variability of Southern Hemisphere extra-tropical
4972 cyclone behavior, 1958–97. *J. Climate*, **13**, 550–561.
4973
- 4974 **Simmonds**, I. and K. Keay, 2002: Surface fluxes of momentum and mechanical energy
4975 over the North Pacific and North Atlantic Oceans. *Meteorology and Atmospheric*
4976 *Physics*, **80**, 1-18.
4977
- 4978 **Sims**, A. P., D. D. S. Niyogi and S. Raman, 2002: Adopting drought indices for
4979 estimating soil moisture: A North Carolina case study. *Geophysical Research*
4980 *Letters*, 29, 1183.
4981
- 4982 **Smith**, R.L., 2003: Statistics of extremes, with applications in environment, insurance
4983 and finance. Chapter 1 of *Extreme Values in Finance, Telecommunications and*
4984 *the Environment*, edited by B. Finkenstadt and H. Rootzen, Chapman and
4985 Hall/CRC Press, London, pp. 1-78.
4986
- 4987 **Smith**, R.L., C. Tebaldi, D. Nychka and L.O. Mearns, 2007: Bayesian modeling of
4988 uncertainty in ensembles of climate models. *Journal of the American Statistical*
4989 *Association*, under revision.
4990
- 4991 **Soja**, A.J., N. M. Tchebakova, N. H.F. French, M. D. Flannigan, H. H. Shugart, B. J.
4992 Stocks, A. I. Sukhinin, E.I. Parfenova, F. S. Chapin III and Jr., and P. W.
4993 Stackhouse, 2007: Climate-induced boreal forest change: Predictions versus
4994 current observations. *Global and Planetary Change*, in press.
4995
4996
4997

- 4998 **Sriver**, R. and M. Huber, 2006: Low frequency variability in globally integrated tropical
4999 cyclone power dissipation. *Geophysical Research Letters*, **33**, L11705,
5000 doi:10.1029/2006GL026167.
5001
- 5002 **Stahl**, K., R.D. Moore, I.G. McKendry, 2006: Climatology of winter cold spells in
5003 relation to mountain pine beetle mortality in British Columbia, Canada. *Climate*
5004 *Research*, **32**, 13-23.
5005
- 5006 **Stahle**, D. W., E. R. Cook, M. K. Cleaveland, M. D. Therrell, D. M. Meko, H. D.
5007 Grissino-Mayer, E. Watson, and B. H. Luckman, 2000: Tree-ring data document
5008 16th century megadrought over North America, *Eos Trans. AGU*, **81**, 121.
5009
- 5010 **Stone**, D.A., A.J. Weaver and F.W. Zwiers, 2000: Trends in Canadian precipitation
5011 intensity. *Atmosphere-Ocean*, **38**, 321-347
5012
- 5013 **Sun** B.M. and P.Y. Groisman, 2004: [Variations in low cloud cover over the United States](#)
5014 [during the second half of the twentieth century](#). *JOURNAL OF CLIMATE*, **17**,
5015 1883-1888.
5016
- 5017 **Therrell**, M. D., D. W. Stahle, M. K. Cleaveland, and J. Villanueva-Diaz, 2002: Warm
5018 season tree growth and precipitation in Mexico. *Journal of Geophysical Research*,
5019 **107 (D14)**, 4205.
5020
- 5021 **Tolman**, H.L., B. Balasubramanian, L.D. Burroughs, D. Chalikov, Y.Y. Chao, H.S.
5022 Chen, and V.M. Gerald (2002), Development and implementation of wind-
5023 generated ocean surface wave models at NCEP, *Wea. Forecasting*, **17**, 311-333.
5024
- 5025 **Trenberth**, K.E., 1990: Recent observed interdecadal climate changes in the Northern
5026 Hemisphere. *Bull. Amer. Meteor. Soc.*, **71**, 988-993.
5027
- 5028 **Trenberth**, K.E. and J.W. Hurrell, 1994: Decadal atmospheric-ocean variations in the
5029 Pacific. *Climate Dynamics*, **9**, 303-319
5030
- 5031 **Trenberth**, K.E. and D.J. Shea, 2006: Atlantic hurricanes and natural variability in 2005.
5032 *Geophysical Research Letters*, **33**, doi:10.1029/2006GL026894.
5033
- 5034 **Trenberth**, K.E., et al., 2002: The evolution of ENSO and global atmospheric
5035 temperatures. *J. Geophys. Res.*, **107**, 4065, doi:10.1029/2000JD000298.
5036
- 5037 **Uppala**, S.M., Kållberg, P.W., Simmons, A.J., Andrae, U., da Costa Bechtold, V.,
5038 Fiorino, M., Gibson, J.K., Haseler, J., Hernandez, A., Kelly, G.A., Li, X., Onogi,
5039 K., Saarinen, S., Sokka, N., Allan, R.P., Andersson, E., Arpe, K., Balsaseda,
5040 M.A., Beljaars, A.C.M., van de Berg, L., Bidlot, J., Bormann, N., Caires, S.,
5041 Chevallier, F., Dethof, A., Dragosavac, M., Fisher, M., Fuentes, M., Hagemann,
5042 S., Hólm, E., Hoskins, B.J., Isaksen, L., Janssen, P.A.E.M., Jenne, R., McNally,
5043 A.P., Mahfouf, J.-F., Morcrette, J.-J., Rayner, N.A., Saunders, R.W., Simon, P.,

- 5044 Sterl, A., Trenberth, K.E., Untch, A., Vasiljevic, D., Viterbo, P., and Woollen, J.
5045 2005: The ERA-40 re-analysis. *Quart. J. R. Meteorol. Soc.*, **131**, 2961-3012
5046 (doi:10.1256/qj.04.176).
5047
- 5048 **Vecchi**, G. A., and T. R. Knutson, 2007: On estimates of historical North Atlantic
5049 tropical cyclone activity. *J. Climate*, submitted.
5050
- 5051 **Verbout**, S. M., H.E. Brooks, L. M. Leslie, and D. M. Schultz, 2006: Evolution of the US
5052 tornado database: 1954-2003. *Weather and Forecasting*, **21**, 86-93.
5053
- 5054 **Vimont**, D. J., and J. P. Kossin, 2007: The Atlantic meridional mode and hurricane
5055 activity. *Geophysical Research Letters*, in press.
5056
- 5057 **Vincent**, L. A. and E. Mekis, 2006: Changes in daily and extreme temperature and
5058 precipitation indices for Canada over the 20th century. *Atmosphere-Ocean*, **44**, 177-
5059 193.
5060
- 5061 **Wang**, D. W., D. A. Mitchell, W. J. Teague, E. Jarosz and M.S. Hulbet, 2005: Extreme
5062 waves under Hurricane Ivan. *Science*, **309**, 896.
5063
- 5064 **Wang**, W. L. and V. R. Swail, 2001: Changes of extreme wave heights in Northern
5065 Hemisphere oceans and related atmospheric circulation regimes. *Journal of*
5066 *Climate*, **14**, 2201-2204.
5067
- 5068 **Wang**, X. L., V. R. Swail and F. W. Zwiers, 2006a: Climatology and changes of
5069 extratropical storm tracks and cyclone activity. Comparison of ERA-40 with
5070 NCEP/NCAR reanalysis for 1958-2001. *Journal of Climate*, **19**, 3145-3166.
5071
- 5072 **Wang**, X. L., H. Wan and V. R. Swail, 2006b: Observed changes in cyclone activity in
5073 Canada and their relationships to major circulation regimes. *Journal of Climate*,
5074 **19**, 895-916.
5075
- 5076 **Webster**, P. J., G. J. Holland, J. A. Curry and H.-R. Chang, 2005: Changes in tropical
5077 cyclone number, duration, and intensity in a warming environment. *Science*, **309**,
5078 1844-1846.
5079
- 5080 **Wehner**, M.F., Predicted 21st century changes in seasonal extreme precipitation events in
5081 the Parallel Climate Model, *J. Climate* **17** (2004) 4281-4290
5082
- 5083 **Wehner**, M., Changes in daily precipitation and surface air temperature extremes in the
5084 IPCC AR4 models. *US CLIVAR Variations*, **3**, (2005) pp 5-9. LBNL-61594
5085
- 5086 **Westerling**, A.L., H.G. Hidalgo, and D.R. Cayan, 2006. Warming and earlier spring
5087 increases in western U.S. forest wildfire activity. *Science* 313:940-943.
5088

- 5089 **Woodhouse**, C.A. and J. T. Overpeck, 1998: 2000 Years of Drought Variability in the
5090 Central United States. *Bulletin of the American Meteorological Society*, 79, 2693–
5091 2714.
- 5092
- 5093 **Wu**, L., B. Wang, and S. Geng, 2005: Growing typhoon influence on east Asia,
5094 *Geophysical Research Letters*, 32, L18703, doi:10.1029/2005GL022937.
- 5095
- 5096 **Wu**, C.C., K.H. Chou, Y.Q. Wang, et al., 2006: Tropical cyclone initialization and
5097 prediction based on four-dimensional variational data assimilation. *JOURNAL OF*
5098 *THE ATMOSPHERIC SCIENCES*, 63, 2383-2395.
- 5099
- 5100 **Xie**, L., L. J. Pietrafesa, J. M. Morrison, and T. Karl, 2005: Climatological and
5101 interannual variability of North Atlantic hurricane tracks. *Journal of Climate*, 18,
5102 5370-5381.
- 5103
- 5104 **Zhang**, R., T. L. Delworth, and I. M. Held, 2007: Can the Atlantic Ocean drive the
5105 observed multidecadal variability in Northern Hemisphere mean temperature?
5106 *Geophysical Research Letters*, **34**, L02709, doi:10.1029/2006GL028683.
- 5107
- 5108 **Zhang**, X., W. D. Hogg, and E. Mekis, 2001: Spatial and temporal characteristics of
5109 heavy precipitation events over Canada. *Journal of Climate*, 14, 1923-1936.
- 5110
- 5111 **Zhang**, X., J. E. Walsh, J. Zhang, U. S. Bhatt and M. Ikeda, 2004: Climatology and inter-
5112 annual variability of Arctic cyclone activity. 1948-2002. *Journal of Climate*, **17**,
5113 2300-2317.
- 5114
- 5115 **Zwiers**, F. W., and V. V. Kharin, 1998: Changes in the extremes of the climate simulated
5116 by CCC GCM2 under CO₂ doubling. *Journal of Climate*, **11**, 2200-2222

5117 **Table 2.1 Regressions for the decadal trends of increasing wave heights measured off the**
 5118 **Washington coast (NDBC buoy #46005). [after Allan and Komar (2006)]**

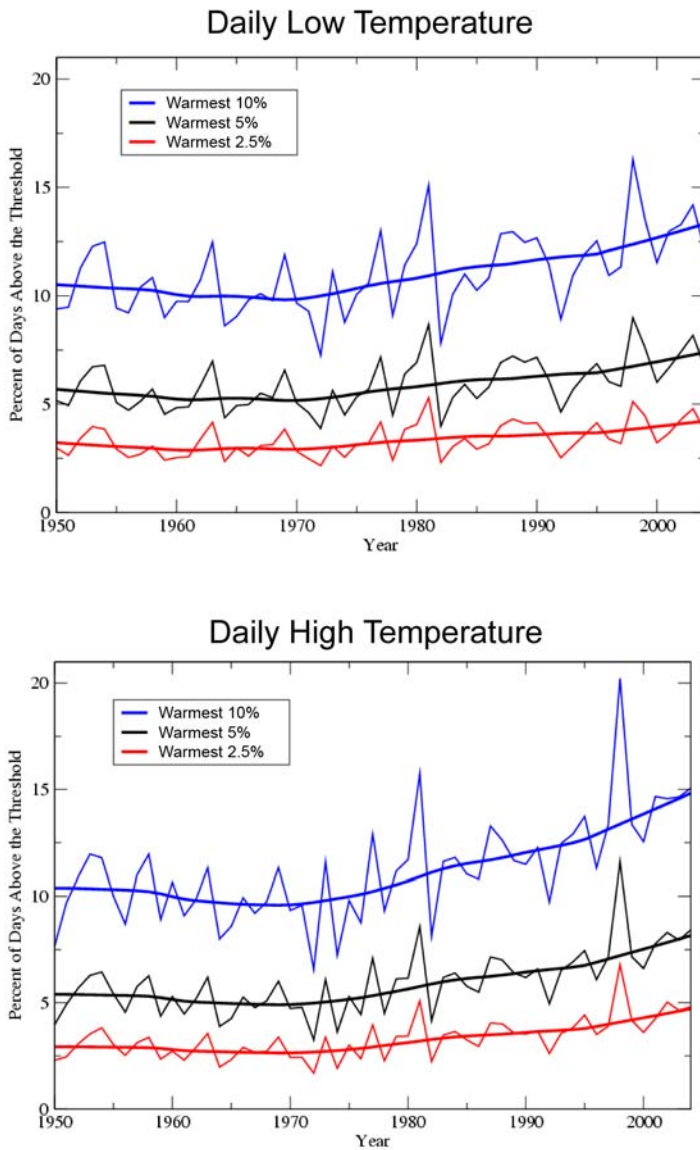
5119

5120	Wave Heights	Rate	Ratio of Rate to	Statistical
5121		(m/yr)	Annual Average	Significance*
5122				
5123	Annual Average	0.024	1.0	SS
5124	Winter Average	0.032	1.3	SS
5125	Five Largest	0.095	4.0	SS
5126	Three Largest	0.103	4.3	NSS
5127	Maximum	0.108	4.5	NSS
5128	100-yr Projection	≈0.13	≈5.5	estimate

5129

5130 SS = statistically significant at the 0.05 level; NSS = not statistically significant.

5131



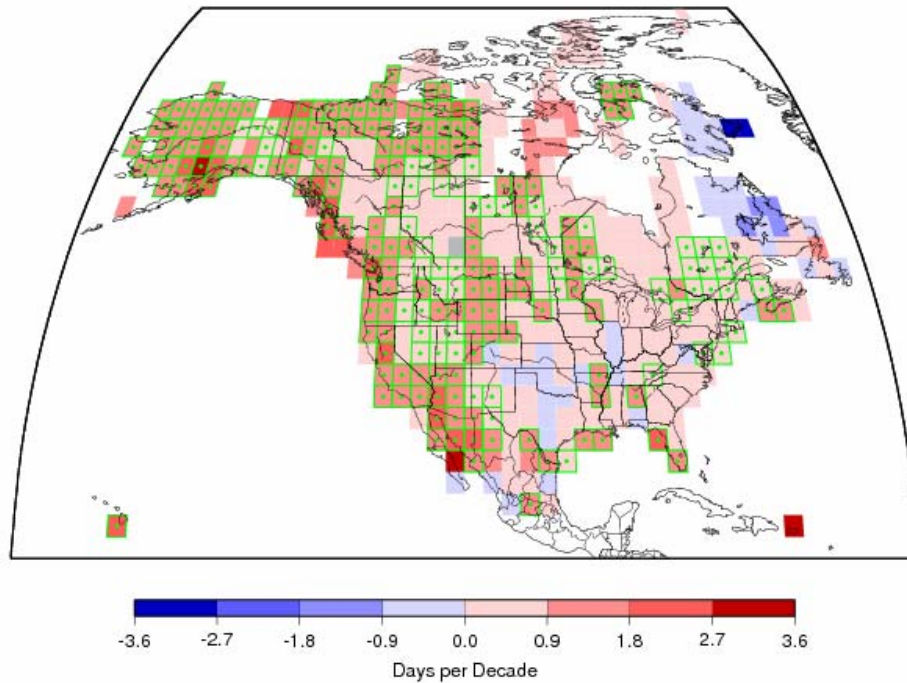
5132

5133

5134 **Figure 2.1** Changes in the percent of days in a year above three thresholds for North
 5135 America for daily high temperature (top) and daily low temperature (bottom) from
 5136 Peterson et al. (2007).

5137
5138

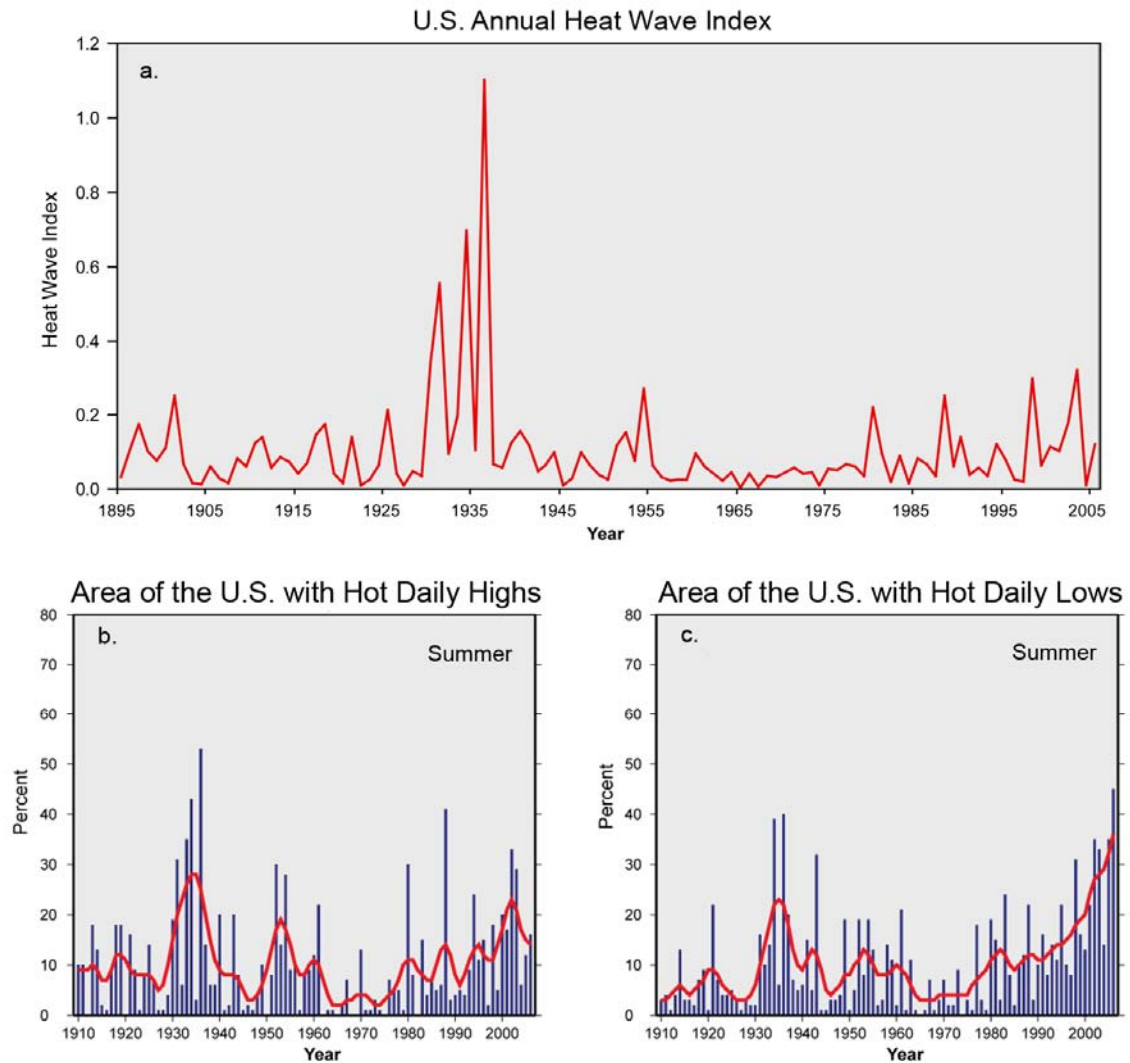
Trends in Number of Days With Unusually Warm Daily Low Temperature



5139
5140

5141 **Figure 2.2** Trends in the number of days in a year when the daily low is unusually warm
5142 (ie. In the top 10% of warm nights for the 1950-2004 period). Grid boxes with green
5143 squares are statistically significant at the $p=0.05$ level, (from Peterson et al. 2007). A
5144 trend of 1.8 days/decade translates to a trend of 9.9 days over the entire 55-year (1950-
5145 2004) period, meaning that 10 days more a year will have unusually warm nights.

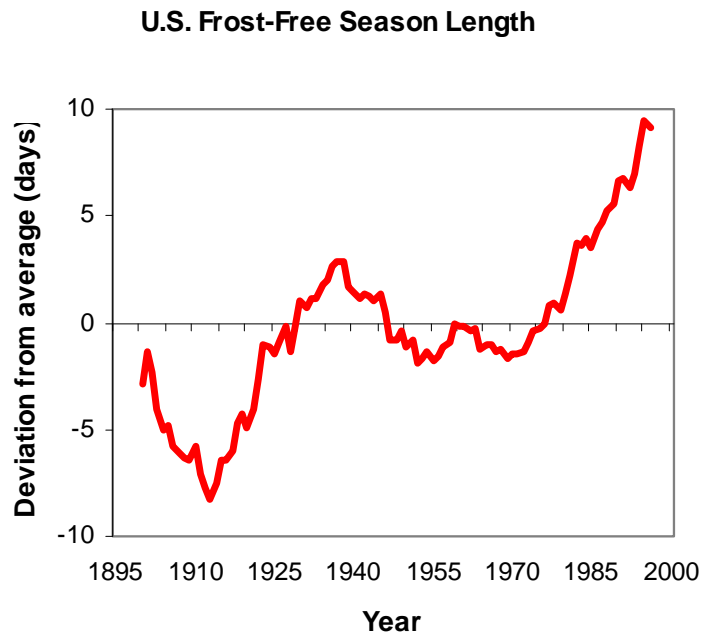
5146



5147

5148

5149 **Figure 2.3** Time series of (a) annual values of a U.S. national average “heat wave”
 5150 index. Heat waves are defined as warm spells of 4 days in duration with mean
 5151 temperature exceeding the threshold for a 1 in 10 year event. (updated from Kunkel et al.
 5152 1999); (b)Area of the U.S. (in percent) with much above normal daily high temperatures
 5153 in summer; (c) Area of the U.S. (in percent) with much above normal daily low
 5154 temperatures in summer. Blue vertical bars give values for individual seasons while red
 5155 lines are smoothed (9-yr running) averages.



5156

5157

5158 **Figure 2.4** Change in the length of the frost free season averaged over the U.S. (from
5159 Kunkel et al. 2003). The frost-free season is at least 10 days longer on average than the
5160 long-term average.

Changes in the Daily Range of Temperature for Mexico

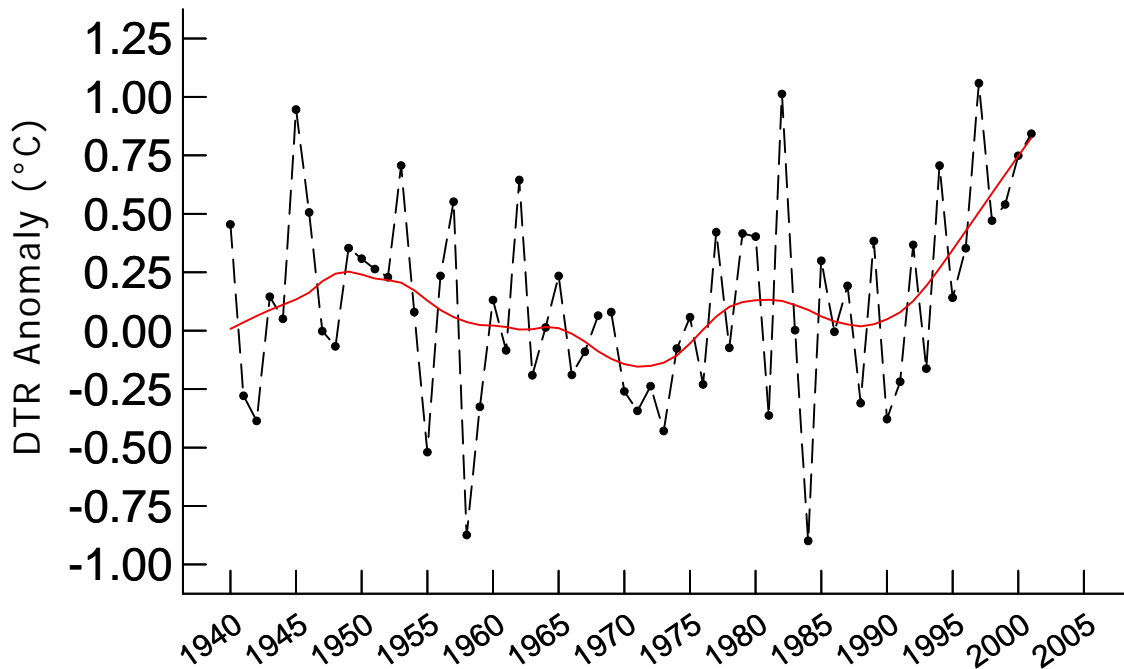
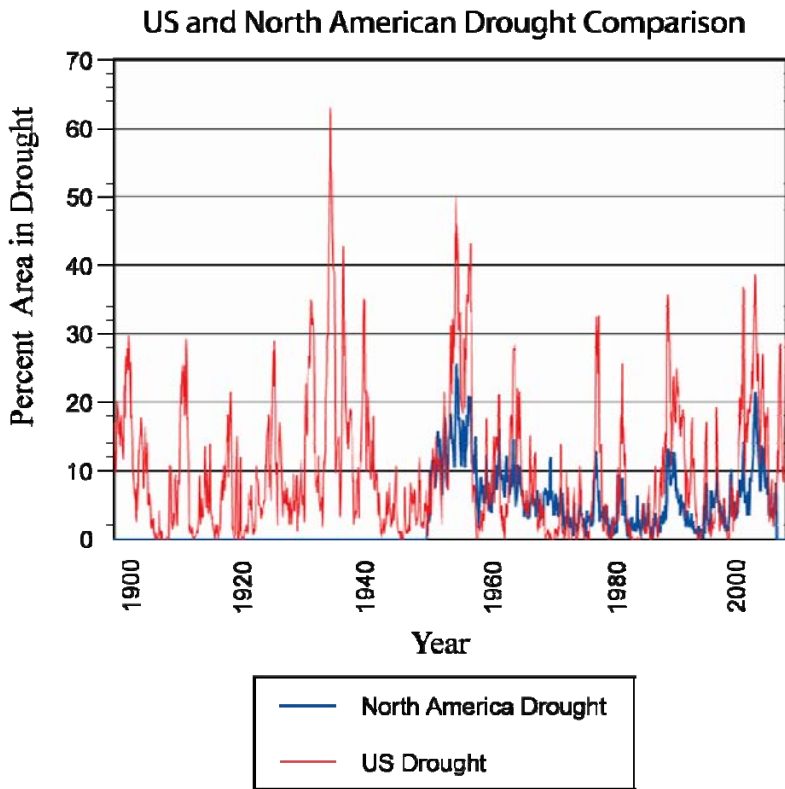


Figure 2.5 Change in the daily range of temperature (difference between the daily low and the daily high temperature) during the warm Season (June-Sept) for Mexico. This difference is known as a Diurnal Temperature Range (DTR). The recent rise in the daily temperature range reflects hotter daily summer highs. The time series represents the average DTR taken over the four temperature regions of Mexico as defined in Englehart and Douglas, 2004. Trend line (red) based on LOWESS smoothing ($n=30$).



5192

5193

5194 **Figure 2.6** the area (in percent) of area in severe to extreme drought as measured by the
 5195 Palmer Drought Severity Index for the U.S. (red) from 1900 to present and for North
 5196 America (blue) from 1950 to present.

5197
5198
5199
5200
5201
5202
5203
5204
5205
5206
5207
5208
5209
5210
5211
5212
5213
5214
5215
5216
5217
5218
5219
5220
5221
5222

Western U.S. Drought Area for the last 1200 years

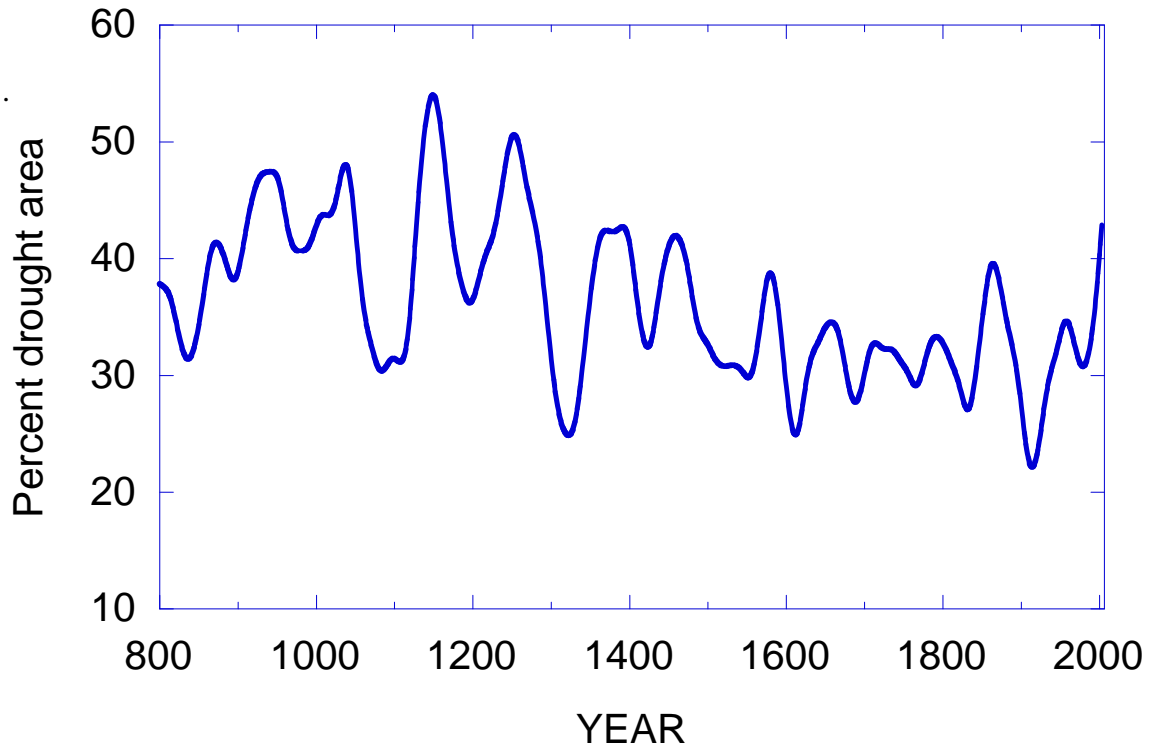
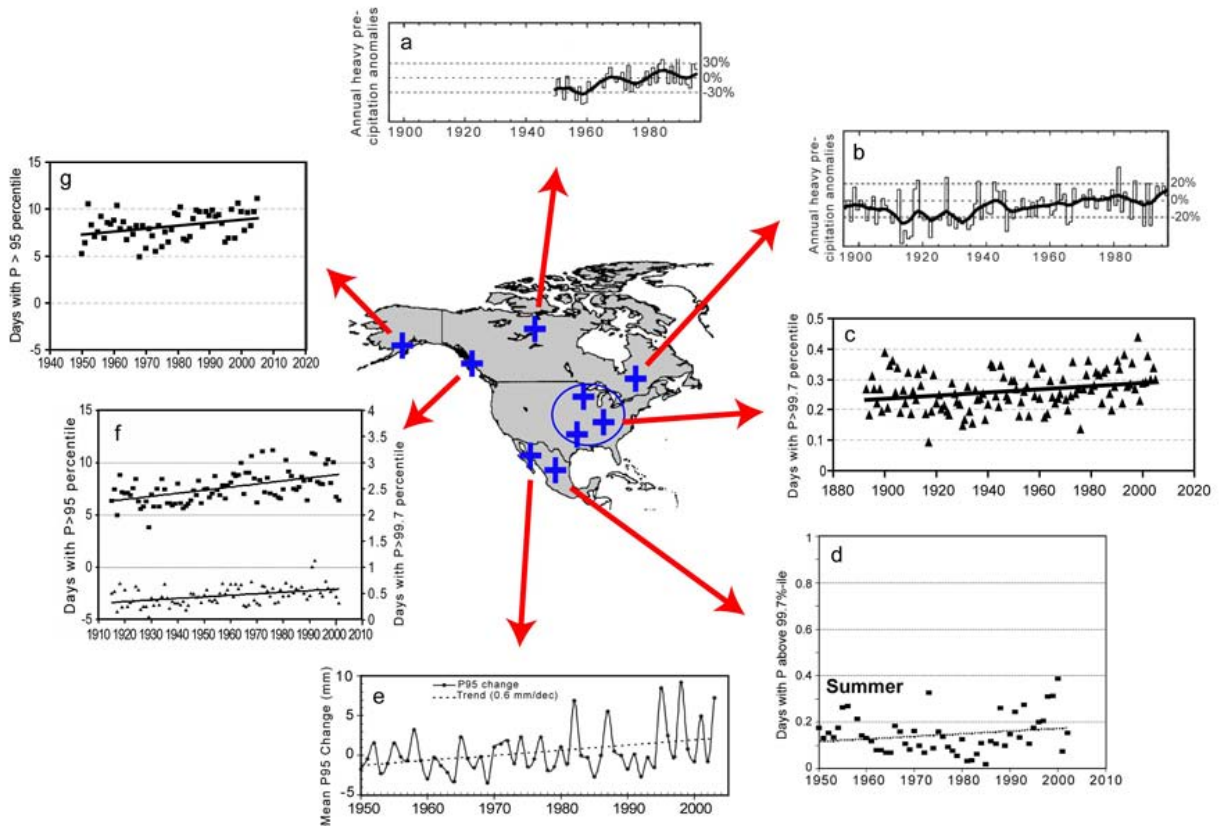


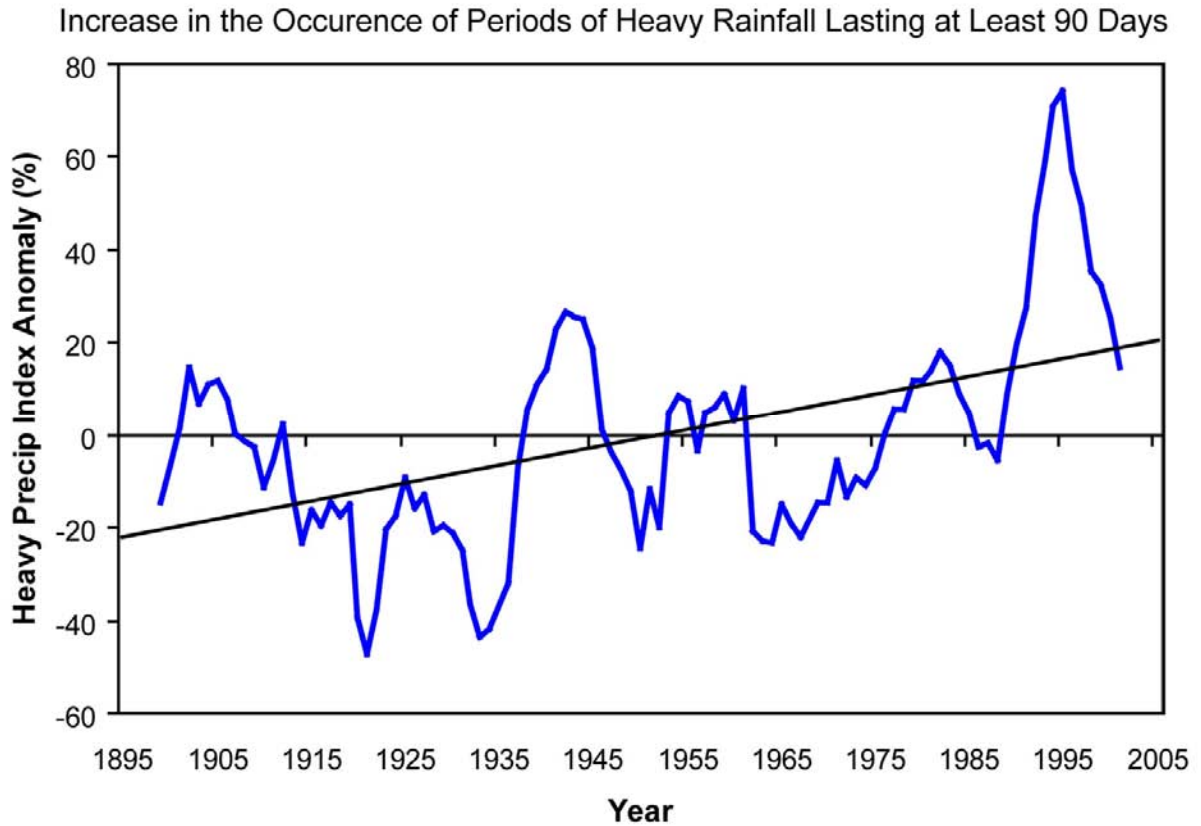
Figure 2.7 Area of drought in the western U.S. as reconstructed from tree rings (Cook et al. 2004).

Regions of N. America where Heavy and Very Heavy Precipitation has Increased



5223
5224

5225 **Figure 2.8** Regions where disproportionate increases in heavy and very heavy
5226 precipitation during the past decades were documented compared to the change in the
5227 annual and/or seasonal precipitation. Because these results come from different studies,
5228 the definitions of extreme precipitation vary. (a) annual anomalies (% departures) of
5229 heavy precipitation for northern Canada. (b) as (a), but for southeastern Canada. (c) the
5230 top 0.3% of daily rain events over the central United States and the trend (22%/113 yrs)
5231 (updated from Groisman et al. 2005). (d) as for (c), but for southern Mexico. (e) change
5232 of intensity of the upper 5% of daily rain events in the core monsoon region of Mexico,
5233 relative to the 1961-1990 base period. (Cavazos et al., 2007) (f) upper 5%, top points, and
5234 upper 0.3%, bottom points, of daily precipitation events and linear trends for British
5235 Columbia south of 55°N. (g) upper 5% of daily precipitation events and linear trend for
5236 Alaska south of 62°N.



5237
5238

5239 **Figure 2.9** Frequency (expressed as a percentage anomaly from the period of record
5240 average) of excessive precipitation periods of 90 day duration exceeding a 1-in-20-year
5241 event threshold for the U.S. Annual values have been smoothed with a 9-yr running
5242 average filter. The black line shows the trend (a linear fit) for the annual values.

5243

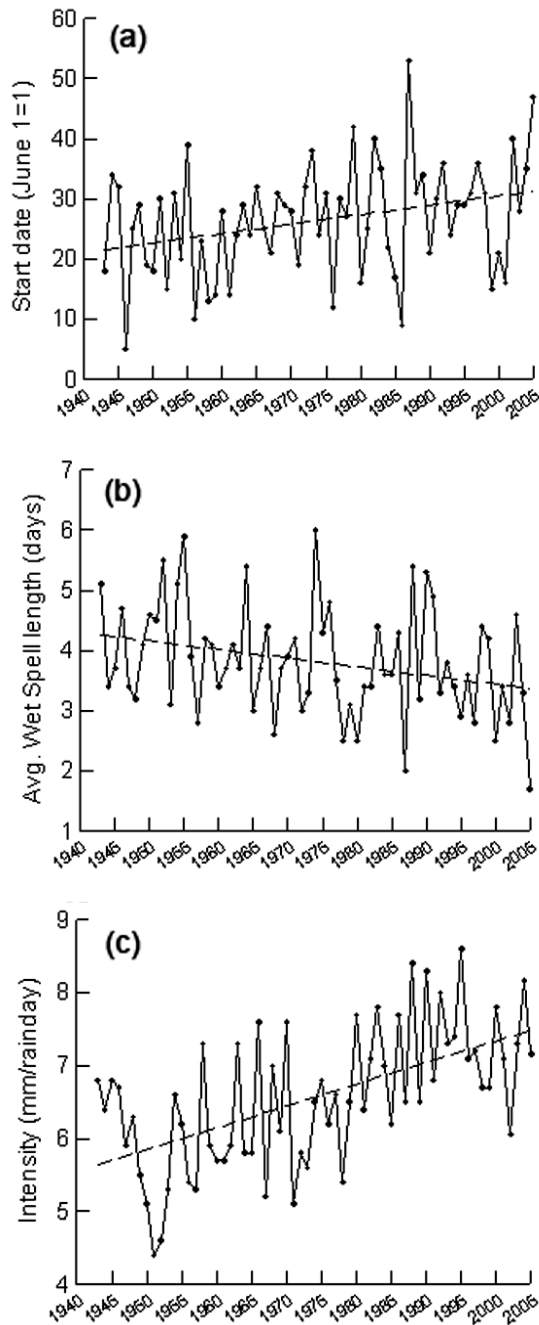
Percentage of Rainfall from Hurricanes/Tropical Storms



5244
5245

5246 **Figure 2.10** Average (median) percentage of warm season rainfall (May-November)
5247 from Hurricanes and tropical storms affecting Mexico and the Gulf Coast of the United
5248 States. Figure updated from Englehart and Douglas 2001.

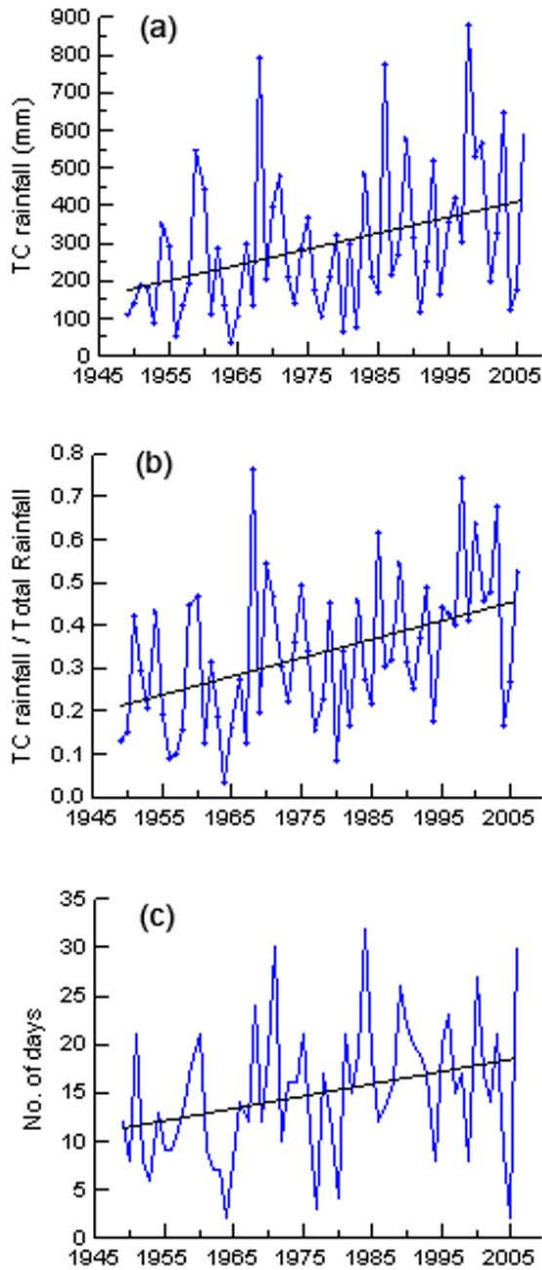
Changes in Monsoon Rainfall for Mexico



5249
5250

5251 **Figure 2.11** Variations and linear trend in various characteristics of the summer
 5252 monsoon in southern Sonora, Mexico, including (a) the mean start date June 1 = Day 1
 5253 on the graph; (b) the mean wet spell length defined as the mean number of consecutive
 5254 days with mean regional precipitation ≥ 1 mm; and (c) the mean daily rainfall intensity for
 5255 wet days defined as the regional average rainfall for all days with rainfall ≥ 1 mm.

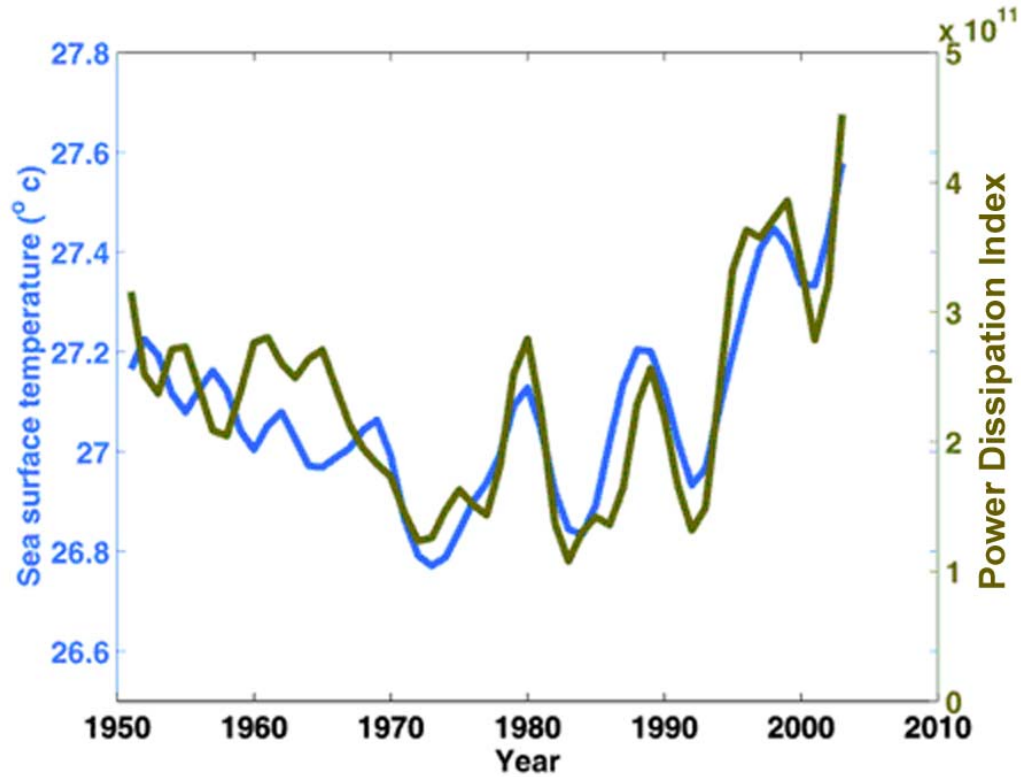
Hurricane/Tropical Storm Rainfall
for Manzanillo, Mexico



5256
5257

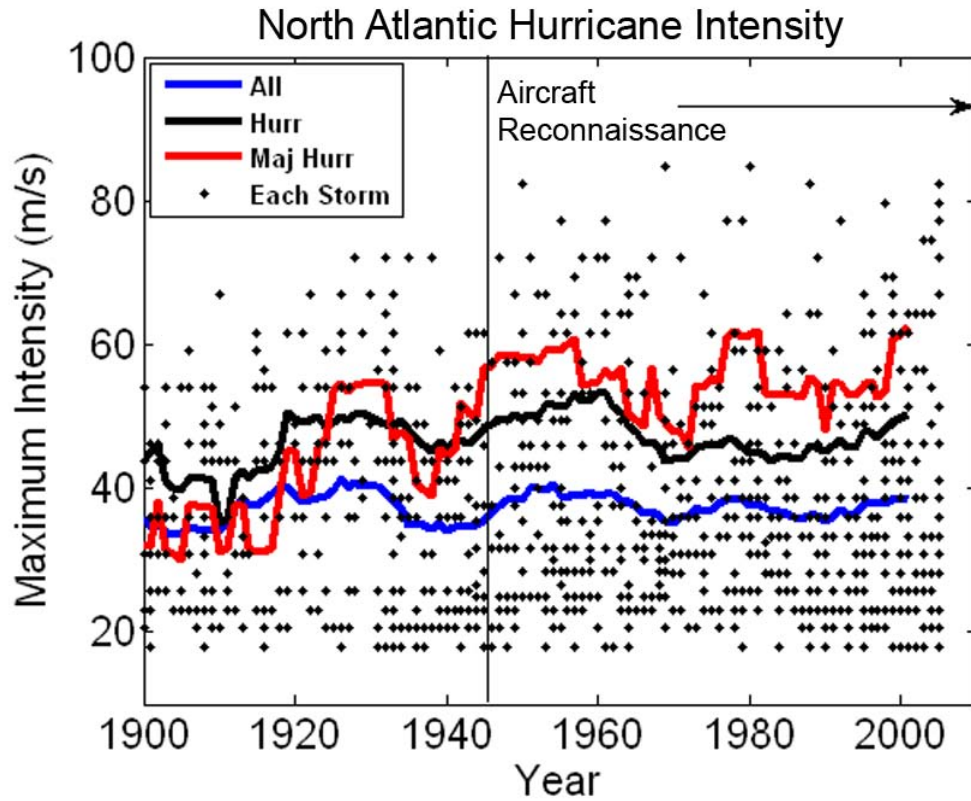
5258 **Figure 2.12** Trends in hurricane/tropical storm rainfall statistics at Manzanillo, Mexico,
5259 including (a) the total warm season rainfall from hurricanes/tropical storms; (b) the ratio
5260 of hurricane/tropical storm rainfall to total summer rainfall; and (c) the number of days
5261 each summer with a hurricane or tropical storm within 550km of the stations

Relationship Between Sea Surface Temperatures and Hurricane Power in the North Atlantic Ocean



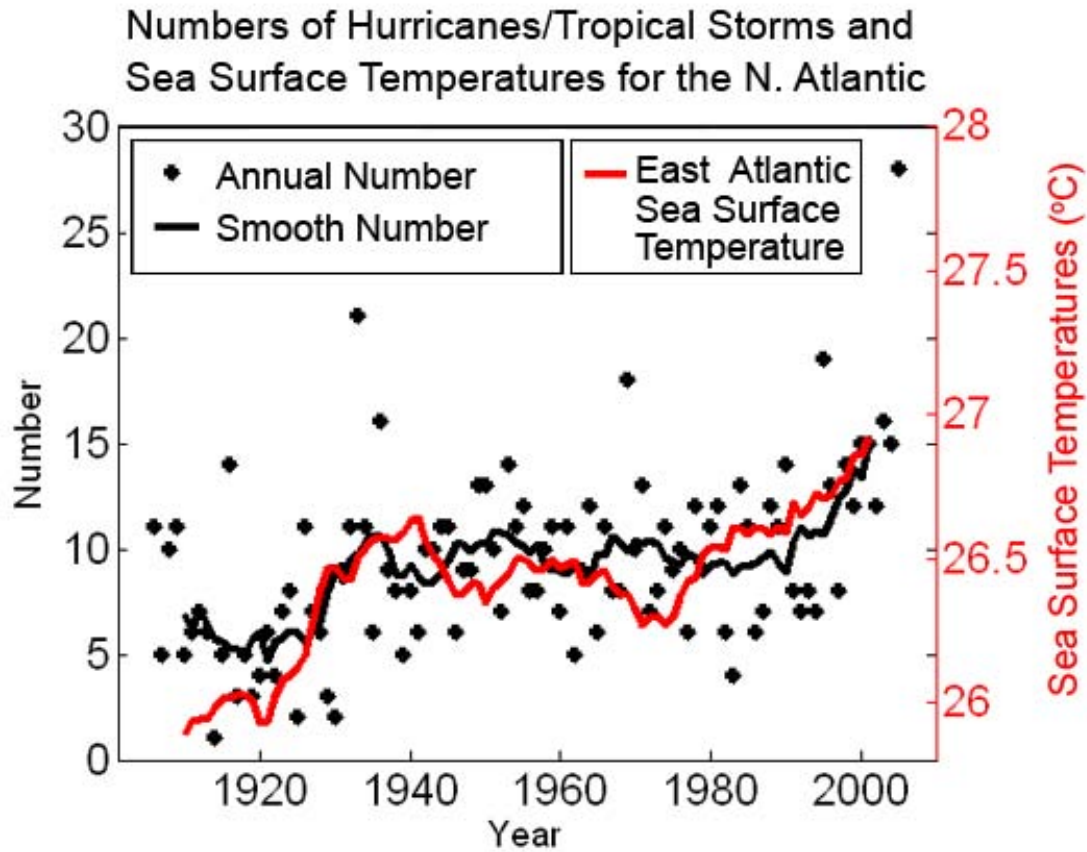
5262
5263

5264 **Figure 2.13** Sea surface temperatures (blue) correlated with the Power Dissipation Index
5265 for North Atlantic hurricanes (Emanuel, 2007). Sea Surface Temperature is from the
5266 Hadley Centre dataset and is for the Main Development Region for tropical cyclones in
5267 the Atlantic, defined as 6-18°N, 20-60°W. The time series have been smoothed using a 1-
5268 3-4-3-1 filter to reduce the effect of interannual variability and highlight fluctuations on
5269 time scales of 3 years and longer.



5270
5271

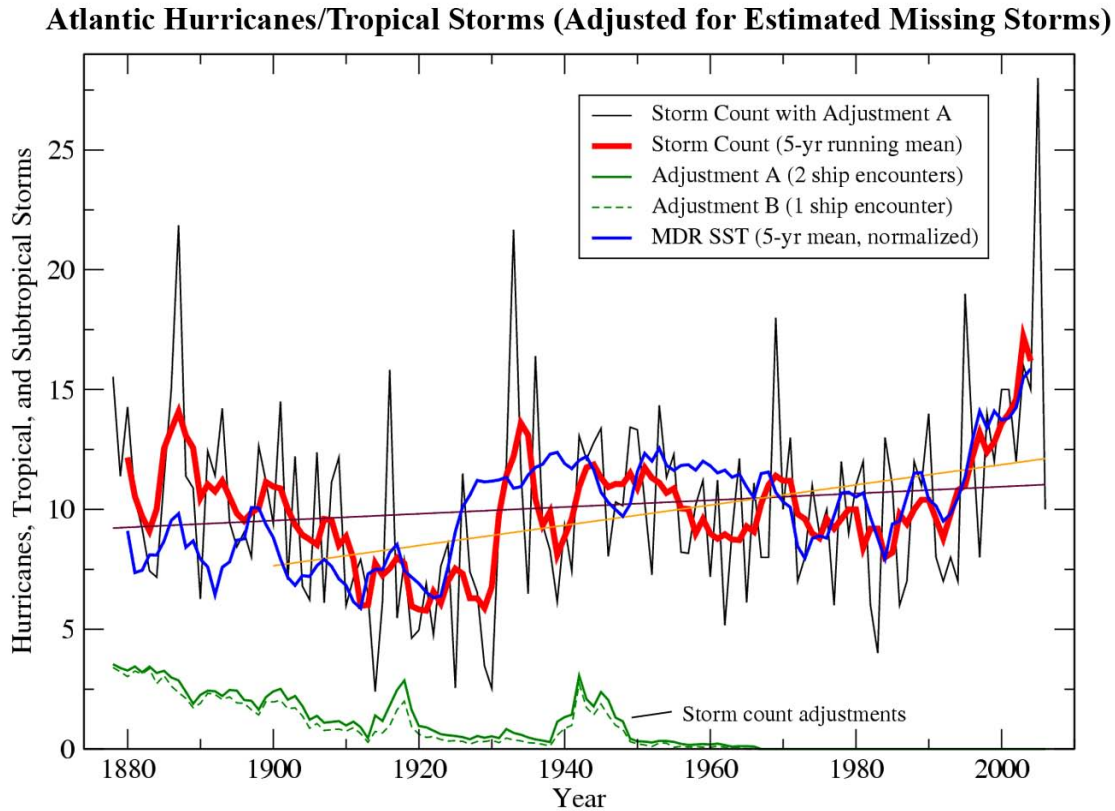
5272 **Figure 2.14** Century changes in the intensity of North Atlantic tropical cyclones,
5273 hurricanes and major hurricanes. Also shown are all individual tropical cyclone
5274 intensities. (From Holland and Webster 2007).



5275

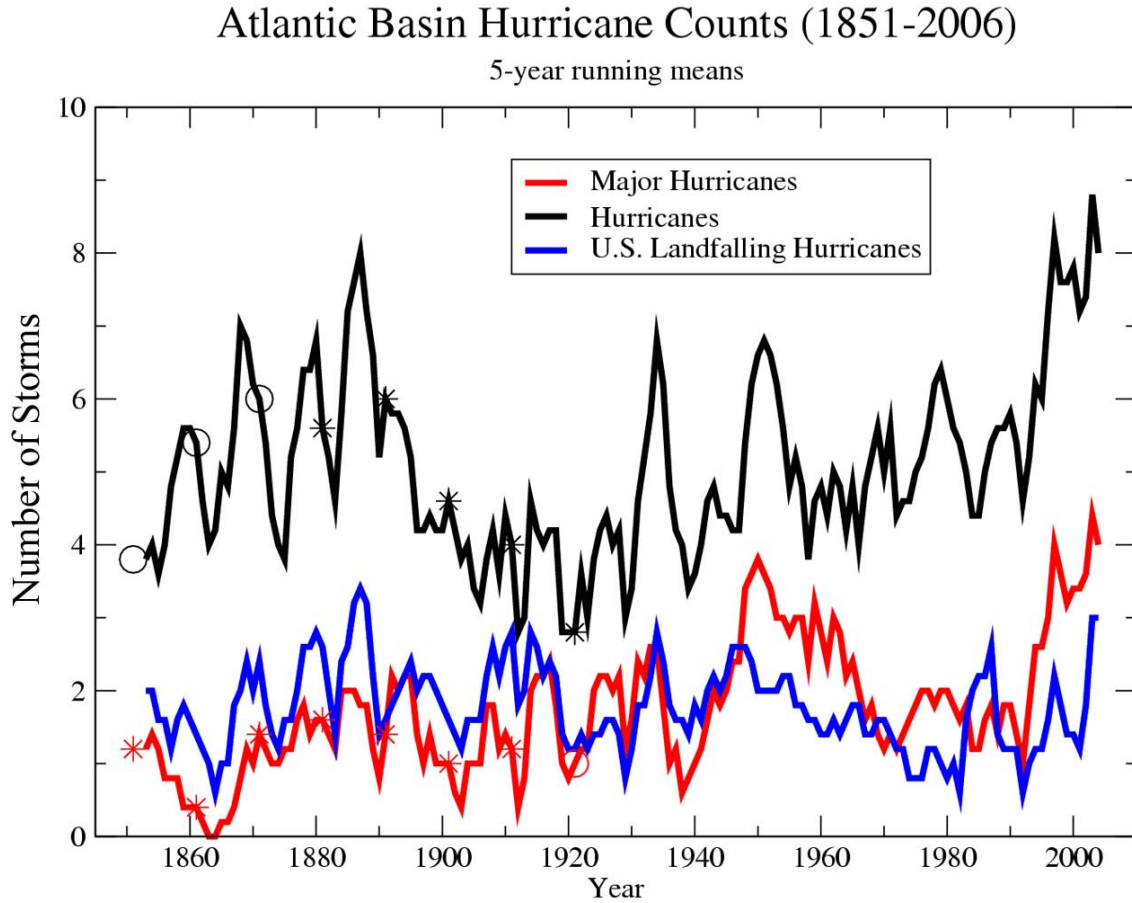
5276

5277 **Figure 2.15** Combined annual numbers of hurricanes and tropical storms for the North
 5278 Atlantic (black dots), together with a 9-year running mean filter (black line) and the 9-
 5279 year smoothed sea surface temperature in the eastern North Atlantic (red line). Adapted
 5280 from Holland and Webster (2007).



5281
5282

5283 **Figure 2.16** Atlantic hurricanes and tropical storms for 1878-2006, using the adjustment
 5284 method A for missing storms described in the text. Black curve is the adjusted annual
 5285 storm count, red is the 5-yr running mean, and solid blue curve is a normalized (same
 5286 mean and variance) 5-yr running mean sea surface temperature index for the Main
 5287 Development Region of the tropical Atlantic (HadISST, 80-20W, 10-20N; Aug.-Oct.).
 5288 Green curves show the adjustment that has been added for missing storms to obtain the
 5289 black curve, assuming two simulated ship-storm “encounters” are required for a modern-
 5290 day storm to be “detected” by a historical ship traffic for a given year. Dashed green
 5291 curve is an alternative adjustment sensitivity test requiring just one ship-storm simulated
 5292 encounter for detection. Straight lines are least squares trend lines for the adjusted storm
 5293 counts. (Adapted from Vecchi and Knutson, 2007).

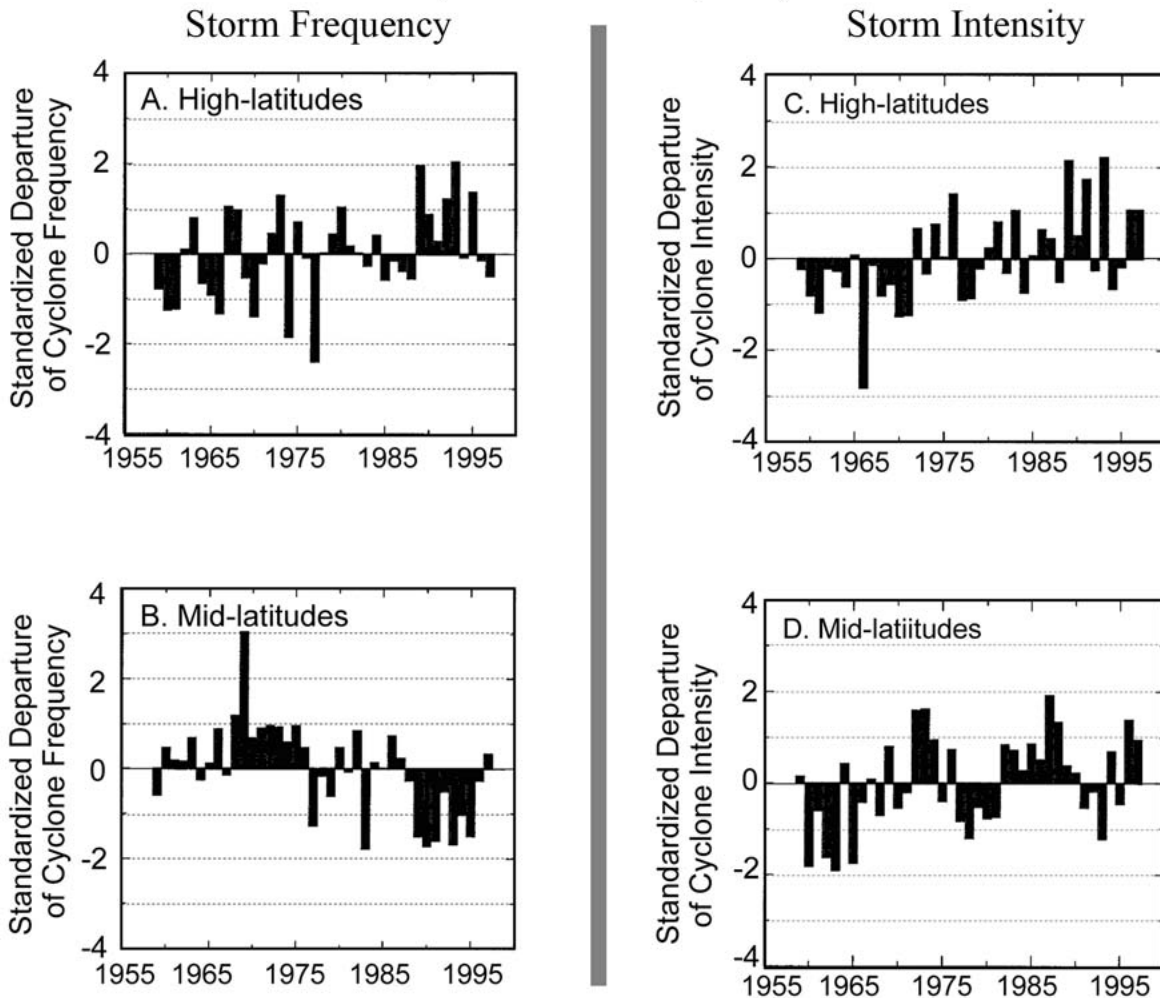


5294

5295

5296 **Figure 2.17** Counts of total North Atlantic basin hurricanes (black), major hurricanes
 5297 (red) and U.S. landfalling hurricanes (blue) based on annual data from 1851 to 2006 and
 5298 smoothed (using a 5-year running mean). Asterisks on the time series indicate years
 5299 where trends beginning in that year and extending through 2005 are statistically
 5300 significant ($p=0.05$) based on annual data; circles indicate non-significant trend results.

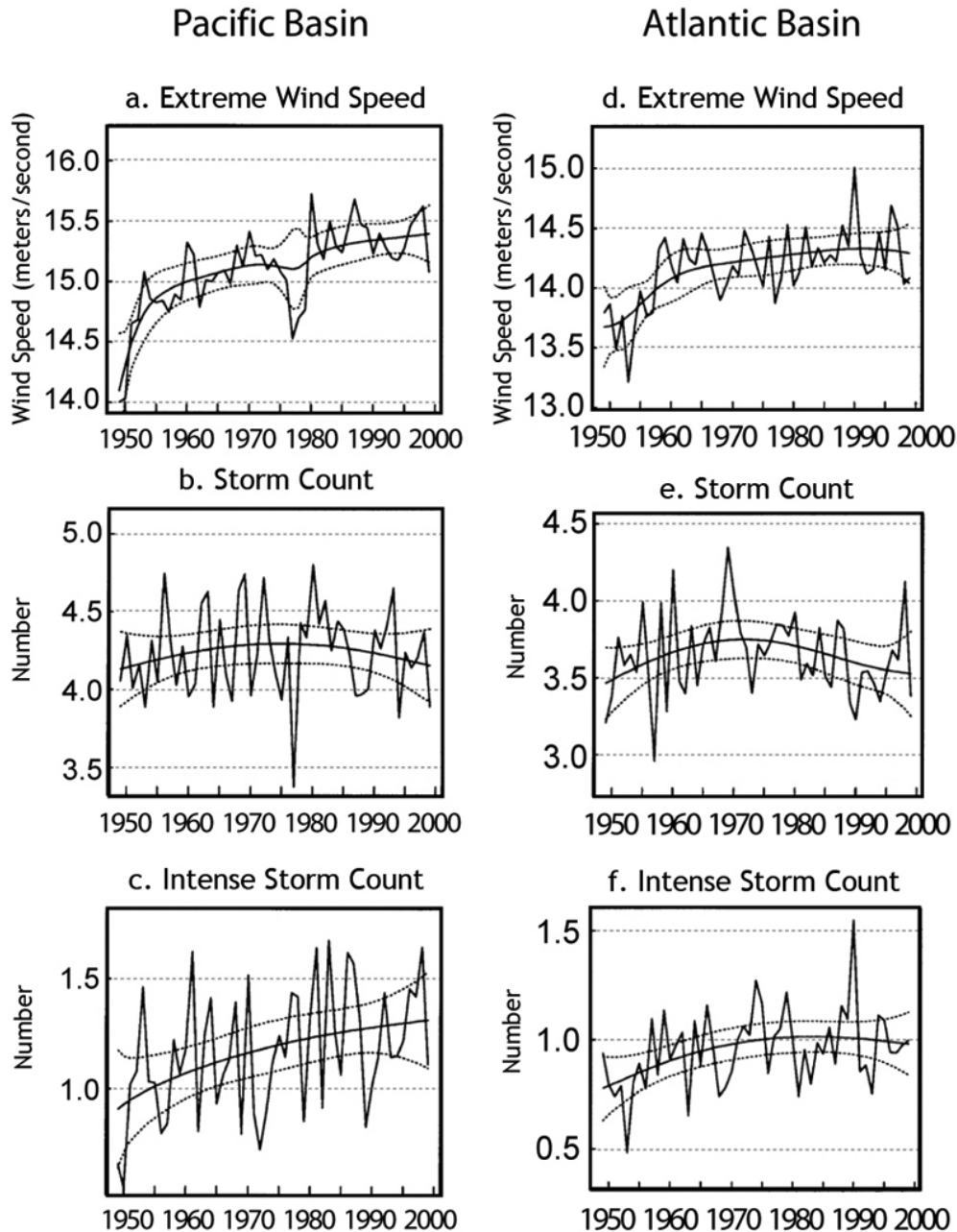
Changes in Frequency and Intensity of Winter Storms (Northern Hemisphere)



5301
5302

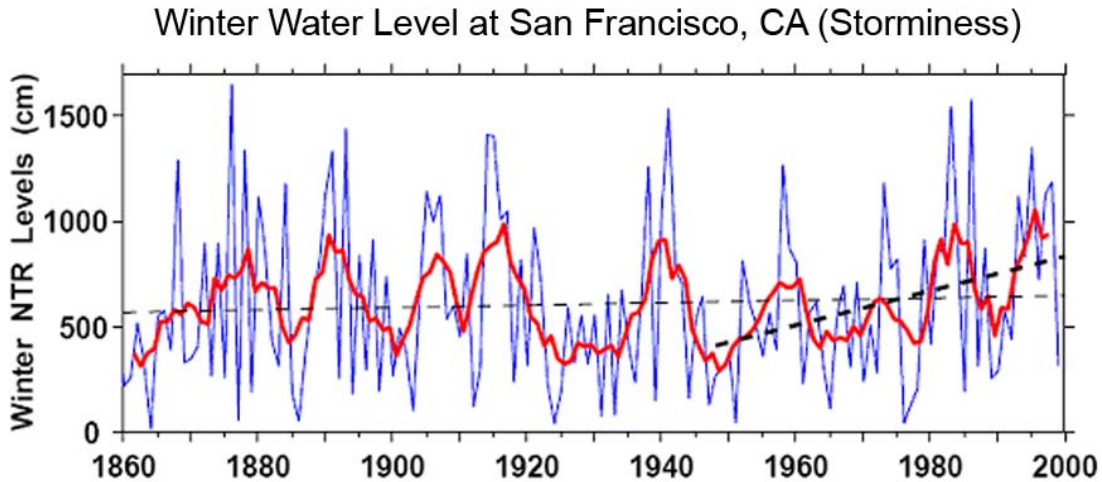
5303 **Figure 2.18** Changes from average (1959-1997) in the number of winter (Nov-Mar)
5304 storms each year in the Northern Hemisphere for (a) high latitudes (60°-90°N), and (b)
5305 mid-latitudes (30°-60°N), and the change from average of winter storm intensity in the
5306 Northern Hemisphere each year for (c) high latitudes (60°-90°N), and (d) mid-latitudes
5307 (30°-60°N). [Adapted from McCabe et al. 2001].

Winter Storm Characteristics for the Pacific and Atlantic



5308
5309

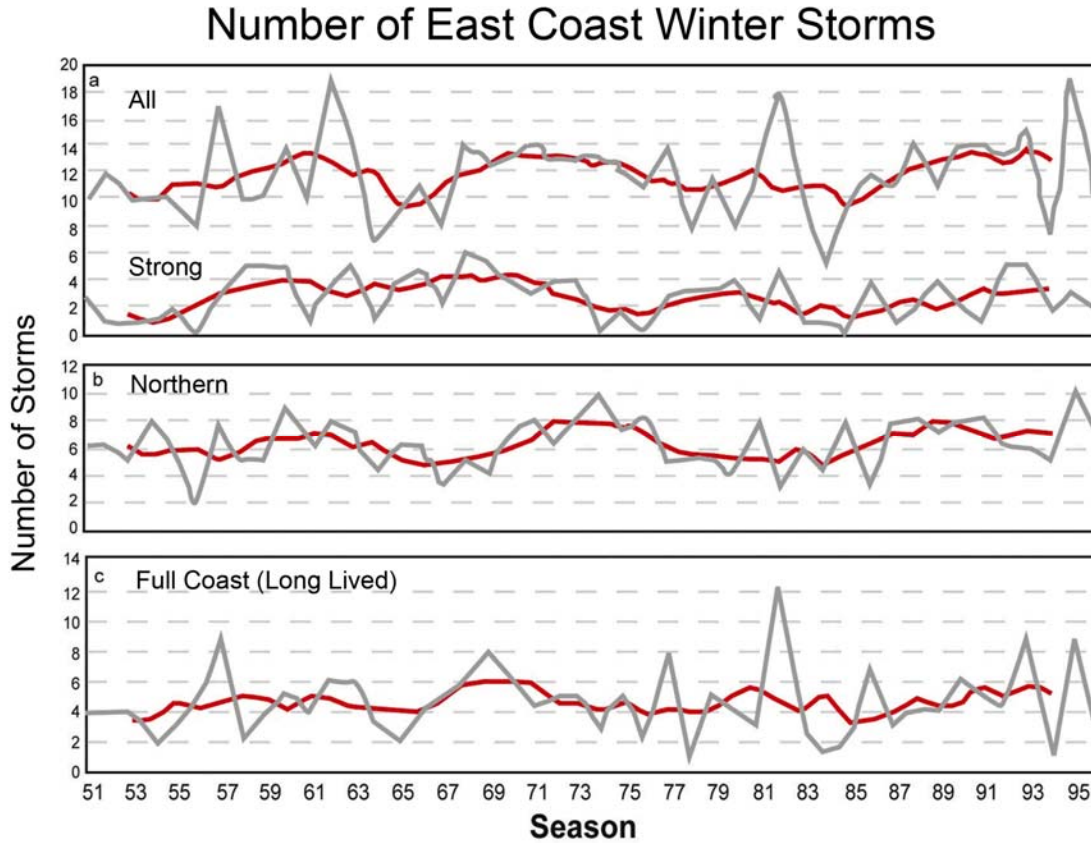
5310 **Fig. 2.19** Extreme wind speed (meters per second), number of winter storms, and number
5311 of intense (≤ 980 hPa) winter storms for the Pacific region (20° - 70° N, 130° E- 112.5° W;
5312 panels a-b-c) and the Atlantic region (20° - 70° N, 7.5° E- 110° W; panels d-e-f). The thick
5313 smooth lines are the trends determined using a Bayesian spline model, and the thin
5314 dashed lines denote the 95% confidence intervals. [Adapted from Paciorek et al. 2002].



5315

5316

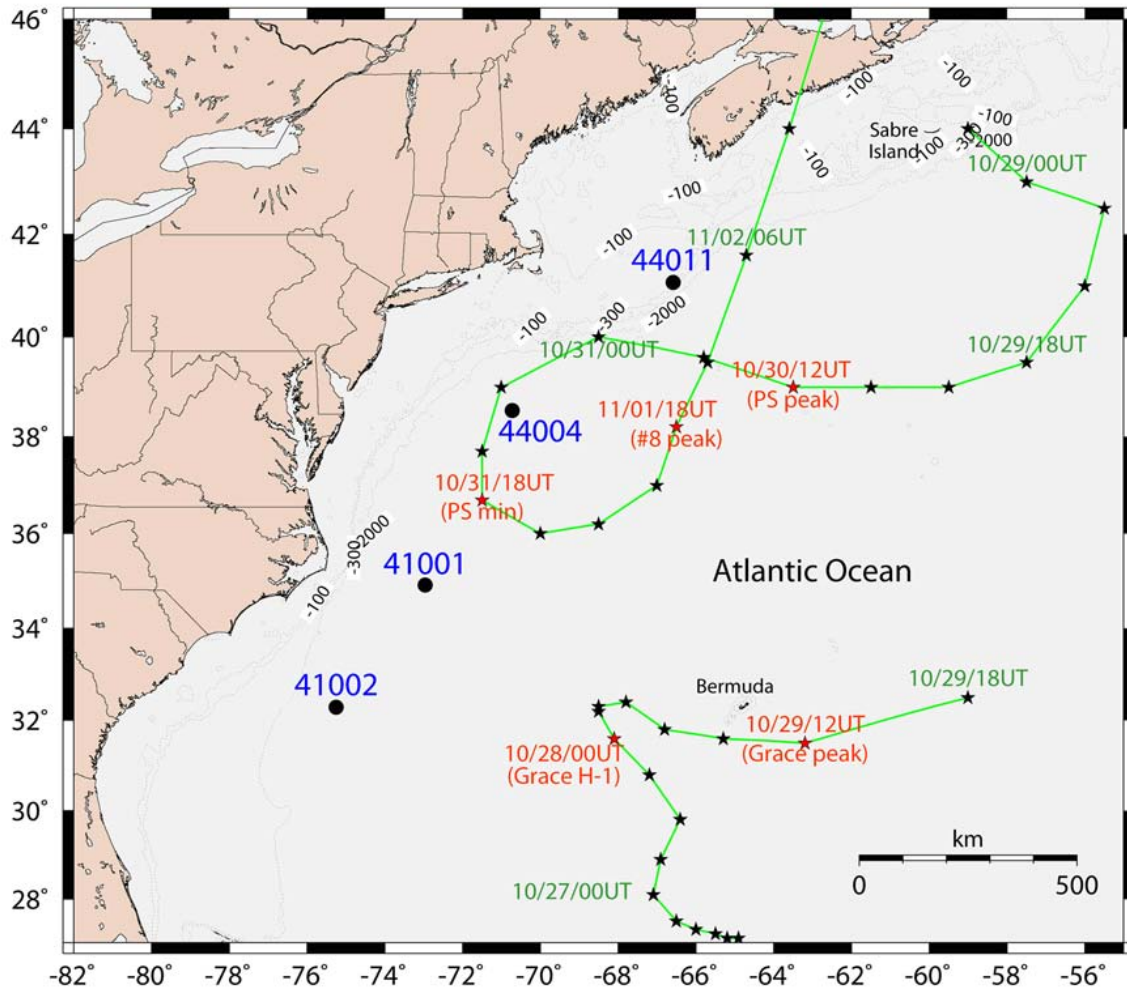
5317 **Figure 2.20** Cumulative extreme Non-Tide Residuals (NTR) (water level) exceeding the
5318 98th percentile level of hourly NTR levels at San Francisco, during winter months (Dec-
5319 Mar), with the 5-yr running mean (red line). Least squares trend estimates for the entire
5320 winter record (light dashed line) and since 1948 (bold dashed line), the period covered by
5321 NCEP reanalysis and ERA-40 data used in most ETC studies. [Adapted from Bromirski
5322 et al. 2003].



5323
5324

5325 **Figure 2.21** Seasonal totals (gray line) covering the period of 1951-1997 for (a) all East
5326 Coast Winter Storms (ECWS; top curve) and strong ECWS (bottom curve), (b) northern
5327 ECWS (>35°N), and (c) those ECWS tracking along the full coast. Data points along the
5328 5-yr moving average (black) correspond to the middle year. [Adapted from Hirsch et al.
5329 2001].

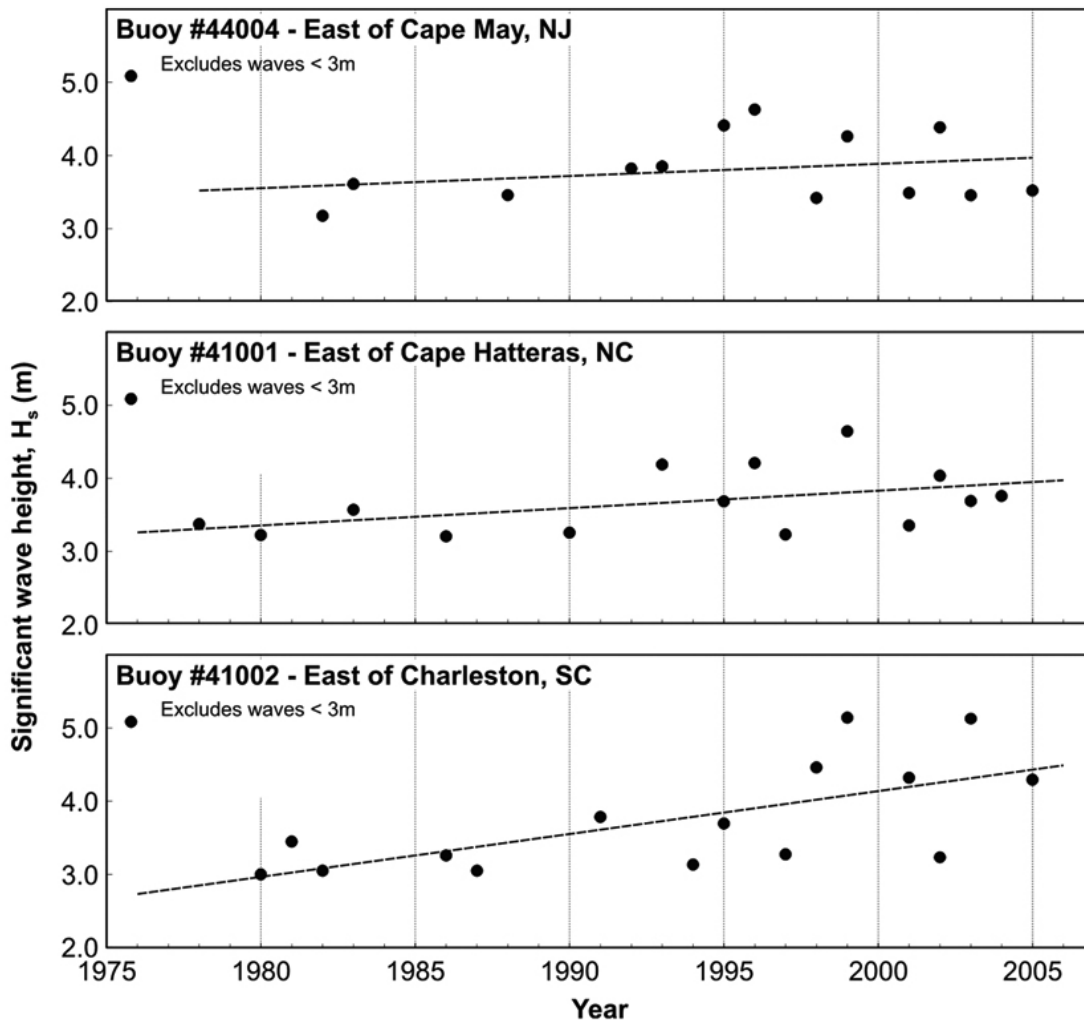
The Track of the 1991 “Perfect Storm”



5330
 5331
 5332
 5333
 5334
 5335
 5336
 5337
 5338
 5339

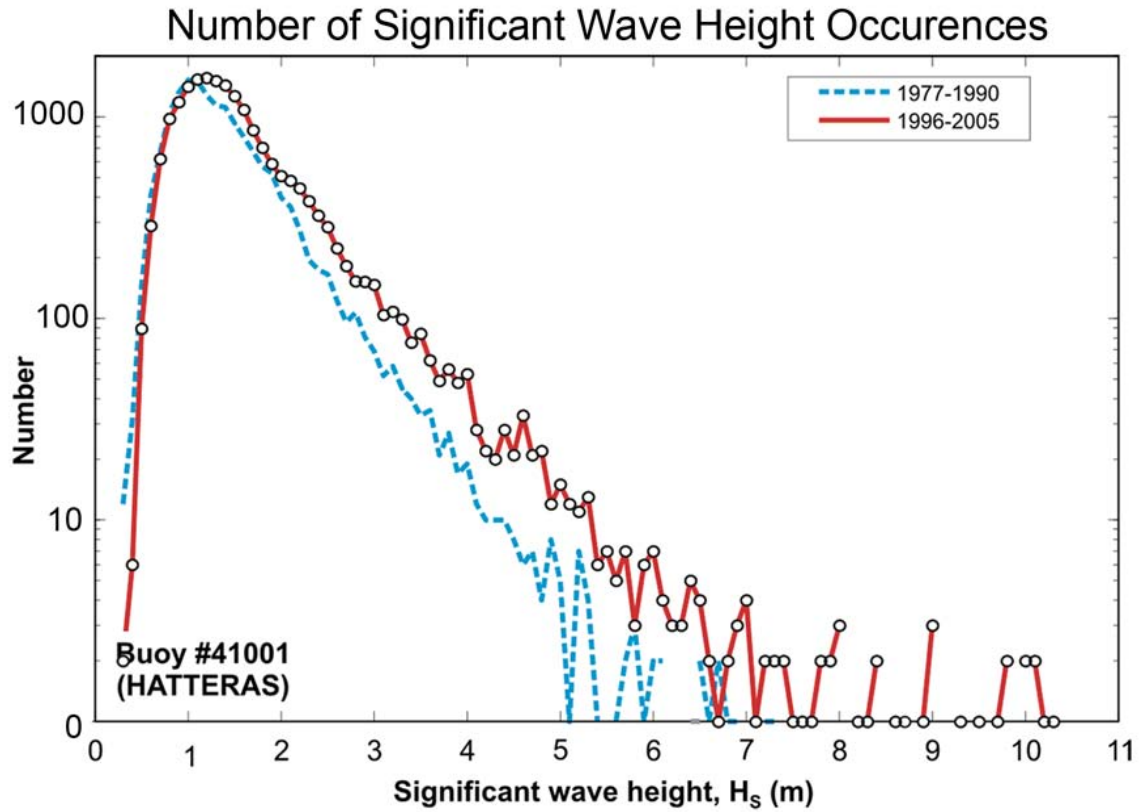
Figure 2.22 Track of the October 1991 “Perfect Storm” (PS) center showing the east-to-west retrograde propagation of a non-typical Nor’easter. The massive ETC was reenergized as it moved southward by absorbing northward propagating remnants of Hurricane Grace, becoming unnamed Hurricane #8 and giving rise to the name “Perfect Storm” for this composite storm. Storm center locations with date/hr time stamps at 6-hr intervals are indicated by stars. Also shown are locations of open ocean NOAA buoys that measured the extreme waves generated by these storms. [Adapted from Bromirski 2001].

Increase in Hurricane Generated Wave Heights



5340
 5341
 5342
 5343

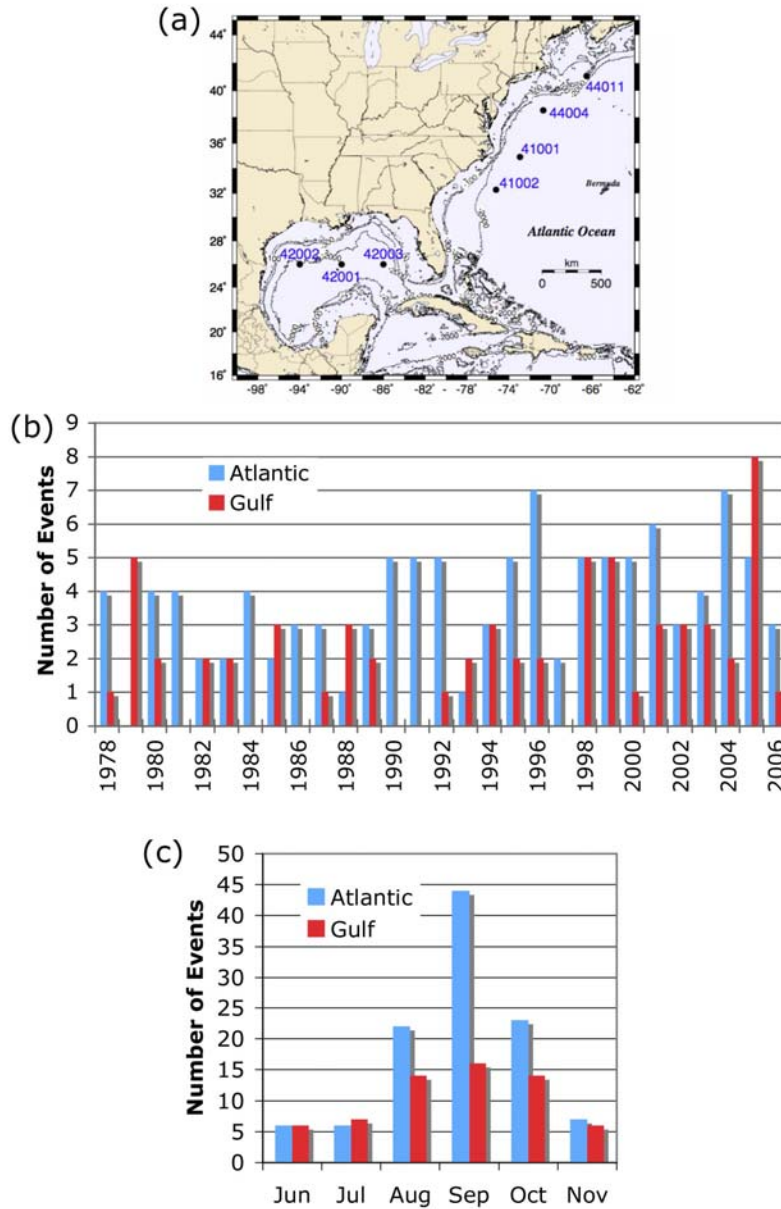
Figure 2.23 Increases in the summer, hurricane-generated wave heights of 3 meters and higher significant wave heights (from Komar and Allan 2007, and in review).



5344
5345

5346 **Figure 2.24** Number of significant wave heights measured by the Cape Hatteras buoy
5347 during the July-September season, early in its record 1976-1991 and during the recent
5348 decade, 1996-2005 (from Komar and Allan 2007a,b).

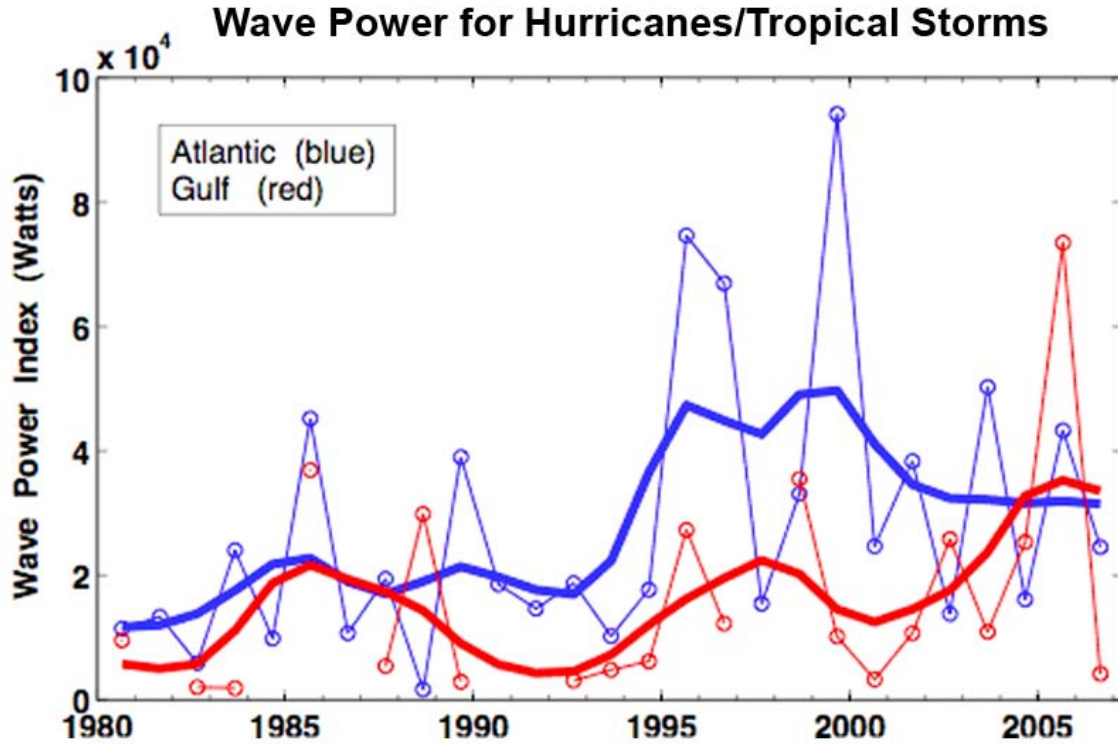
Number of Significant Wave Events During the Atlantic Hurricane Season



5349
5350

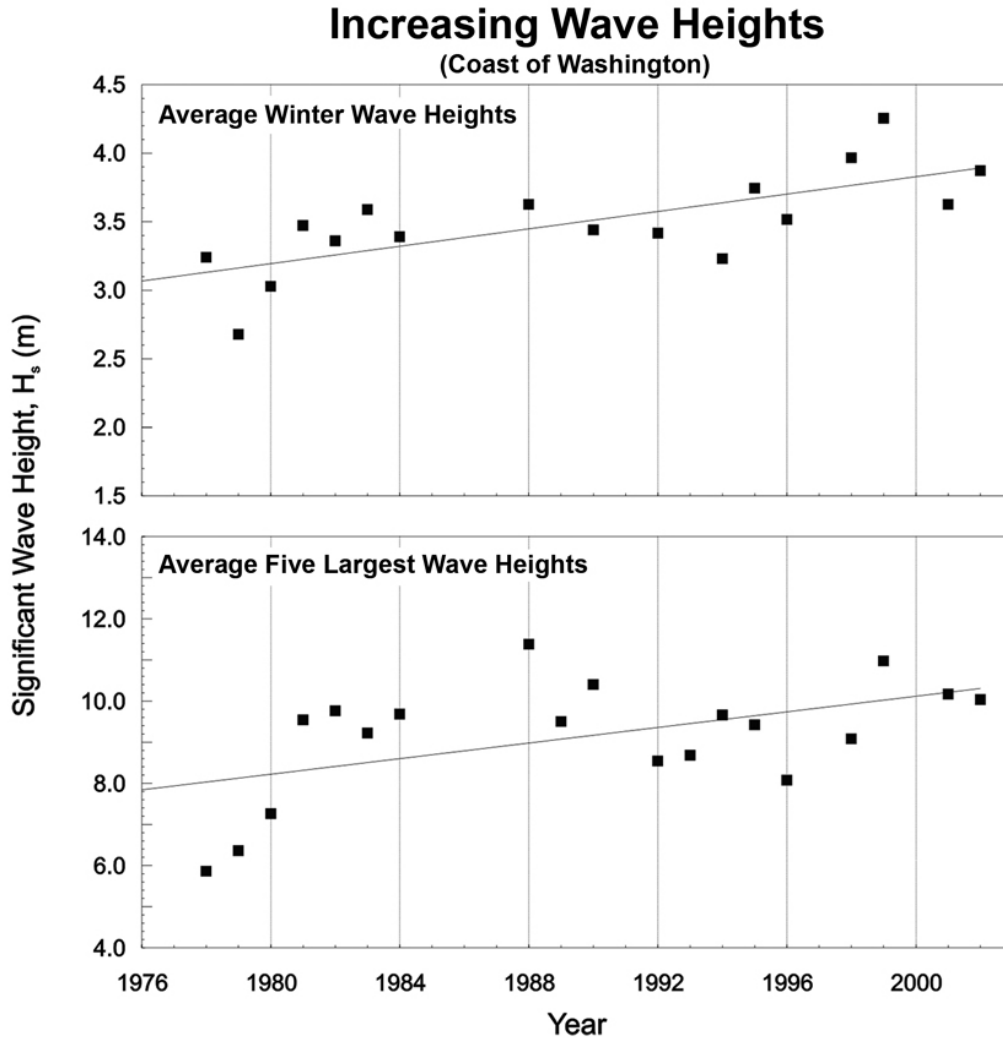
5351 **Figure 2.25** (a) Location of the NOAA Atlantic and Gulf buoys discussed. Bathymetric
5352 contours identify the continental shelf boundary. (b) Total number of significant wave
5353 events per hurricane season. (c) Total number of wave events identified during each
5354 month of the June-November hurricane season for all buoy data available from NOAA's
5355 National Ocean Data Center (NODC) from 1978-2006. Panels (b) and (c) show the

5356 number of wave events associated with hurricanes/tropical storms with wave heights that
5357 exceeded 3 m at a minimum of one of the buoys in each group. Each event was counted
5358 only once, even if observed at multiple buoys in a group. No data were available from
5359 NODC for any of the Atlantic buoys during the 1979 hurricane season. [Adapted from
5360 Bromirski, 2007b]



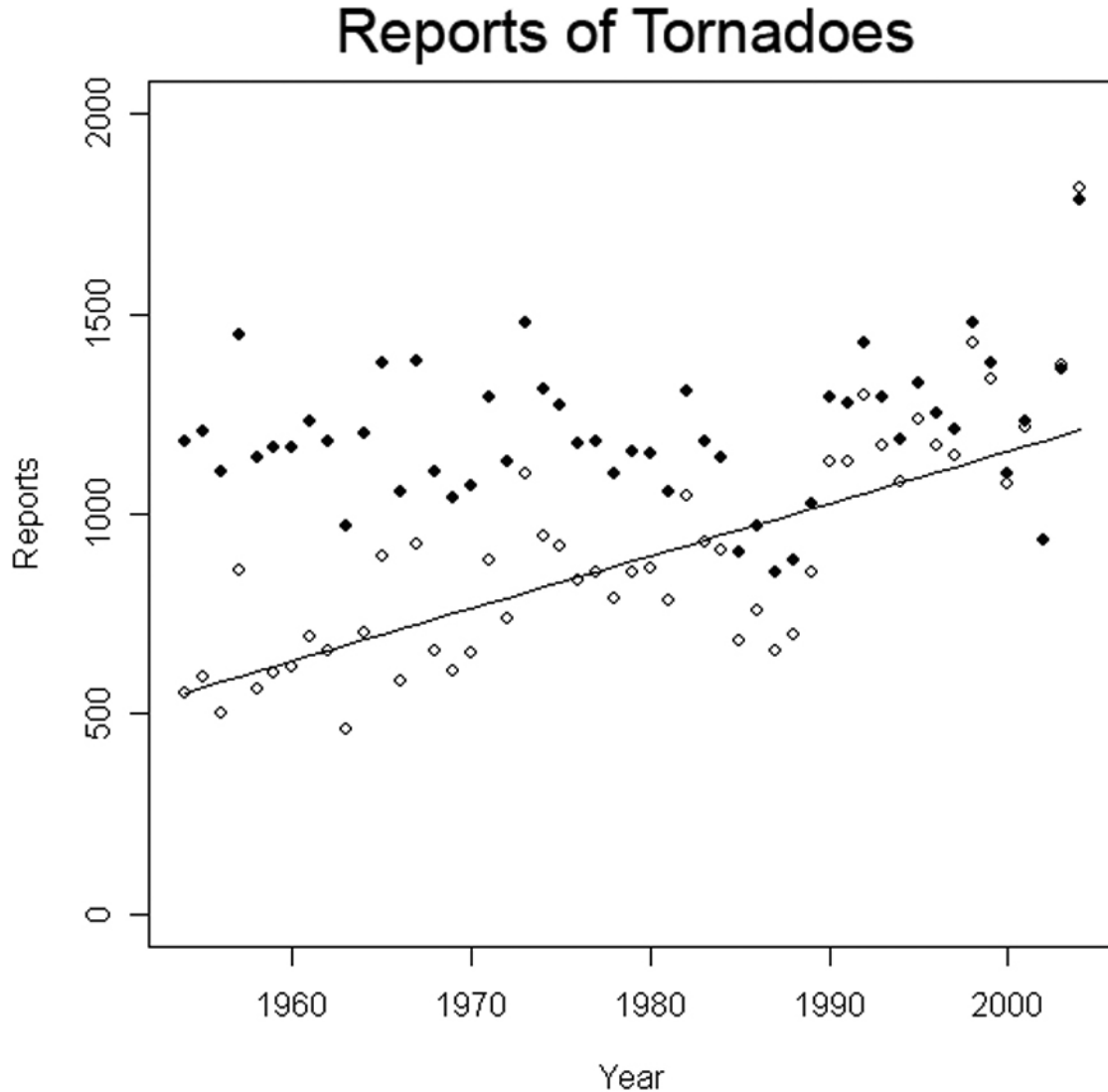
5361
 5362
 5363
 5364
 5365
 5366
 5367

Figure 2.26 A measure of the total annual tropical cyclone wave power in the western North Atlantic and Gulf regions obtained as the mean of the available annual deep water wave power (the wave power index, WPI). Longer period variability is emphasized by lowpass filtering the annual data with three iterations of a 1-2-1 smoothing operator, giving the Atlantic and Gulf region WPI (thick lines). [Adapted from Bromirski, 2007b]



5368
5369

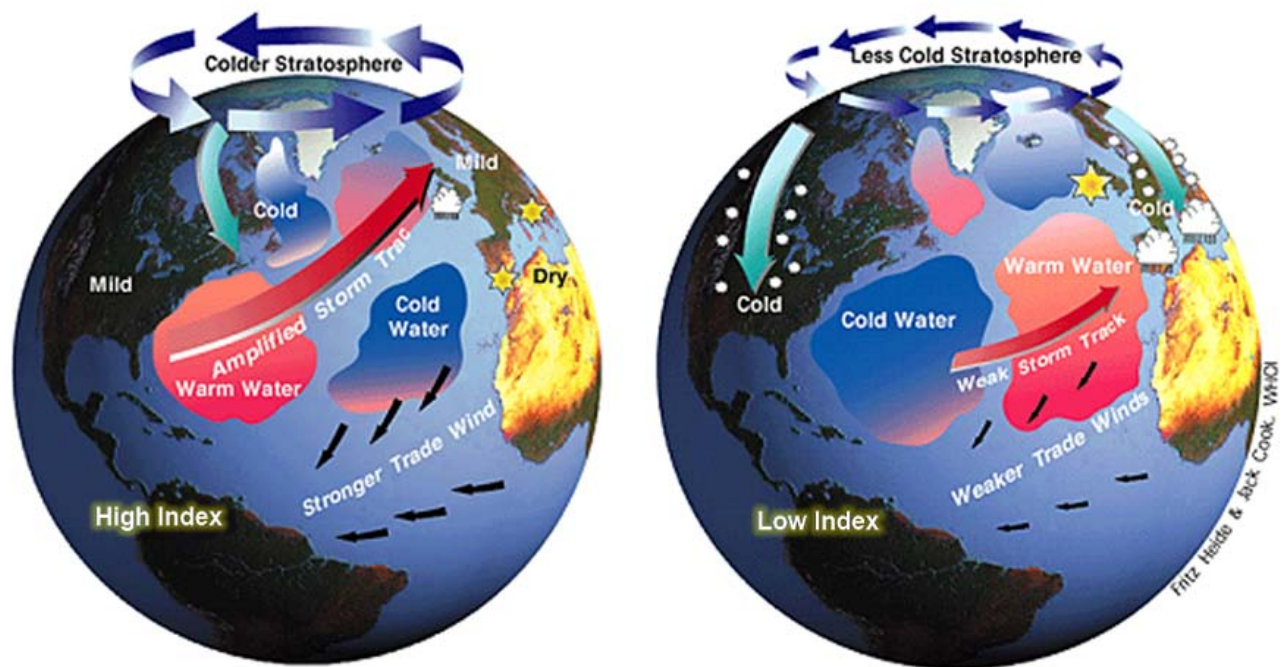
5370 **Figure 2.27** The trends of increasing wave heights measured by NOAA’s National Data
5371 Buoy Center (NDBC) buoy #46005 off the coast of Washington [after Allan and Komar
5372 (2006)]



5373
5374

5375 **Figure 2.28** Tornado reports in official database in USA from 1954-2004. Open circles
5376 are raw reports, solid line (linear regression) is the trend for raw reports, solid circles are
5377 reports adjusted to 2002 reporting system. The adjusted data show little or no trend in
5378 reported tornadoes. The trend in raw reports reflects an increasing density of population
5379 in tornado-prone areas, and therefore more opportunity for sightings, rather than a real
5380 increase in the occurrences of tornadoes.

The North Atlantic Oscillation



5381

5382

5383

Figure 2.29 Schematic of the North Atlantic Oscillation (NAO) showing its effect on

5384

extremes. Illustrations by Fritz Heidi and Jack Cook, Woods Hole Oceanographic

5385

Institution.